UNIVERSITY OF THE WITWATERSRAND, JOHANNESBURG
SCHOOL OF MECHANICAL, INDUSTRIAL AND AERONAUTICAL ENGINEERING

VERIFICATION OF THE UNIVERSAL THERMODYNAMIC MODEL FOR COOLING SYSTEMS ON TWO WATER CHILLERS IN THE FIELD

Ryan Patrick Leong

A research report submitted to the Faculty of Engineering and the Built Environment, University of the Witwatersrand, in fulfilment of the requirements for the degree of Master of Science in Engineering

Johannesburg 2012

I declare that this project is my own, unaided work. It is being submitted towards the degree of Master of Science in Engineering in the University of the Witwatersrand, Johannesburg. It has not been submitted before for any degree or examination at any other University.

_____

(Ryan Patrick Leong)

_5th___ day of __March____ (year) __2012_____

ABSTRACT

An analysis and verification study was conducted into the Universal Thermodynamic Model for cooling systems, which claims to accurately assess the performance of all refrigerating machines from only a few, non-intrusive measurements. The model and its derivation were studied to confirm its applicability to vapour-compression water chillers and its accuracy was practically investigated via tests on two such chillers serving the air-conditioning system of an office building. The two chillers used employ reciprocating and centrifugal compressors, respectively.

The experimental method entailed recording a number of measurements under normal, or fault-free, conditions and, for each set of data, calculating the COP obtained directly from measurement and that predicted by the model. Comparisons between the two values for each data set were used as an indication of accuracy. The predicted COP for the reciprocating machine was shown to be very accurate with a 2.97% maximum difference between COP values, while that for the centrifugal chiller was even more precise, yielding a maximum difference of 1.14%.

An additional test was conducted on the centrifugal chiller that simulated an operational fault – excessive fouling in its condenser – and the model showed the presence, though not the nature, of this simulated fault. Comparisons between key constants and graphs obtained under normal and throttled conditions allowed for some fault diagnosis. The predicted and measured COP values under the faulty conditions were also calculated and shown to correspond within 2.45%.

The Universal Thermodynamic Model proved to be an accurate and reliable performance assessment tool for the two chillers. In every case the difference between predicted and measured COP was less than the experimental uncertainty of the latter. It was also shown that the model could be used for limited fault diagnosis through simulation of a practical operation defect and analysing certain parameters. Practical recommendations for similar future work are provided based on experimental shortcomings of this study.

ACKNOWLEDGEMENTS

The following are noted for their assistance and support:

- Dr Michael Bailey-McEwan, project supervisor
- Mr Glenn Drew, maintenance engineer at Investec, Sandton
- Mr Patrick Leong, Managing Director of Enviroware Construction

CONTENTS

List of Figures

List of Tables

1. INTRODUCTION

1.1 Refrigeration Machines

Refrigeration, or cooling, machines have found their way into the life of almost every person in every industry on the planet. From preserving perishable goods in storage to ensuring that the air supply in an office space is ideally suited to high levels of worker productivity and even to maintaining the temperature in a laboratory at a level conducive to certain chemical reactions, such machines can be considered as indispensable to society. In fact, Gordon and Ng [(1)] p. 1, are of the opinion that *chillers*, as they often term refrigeration machines, 'permeate our daily lives' even on a domestic level, evidenced by the vast number of regular household refrigerators in service around the world.

In South Africa, mining has traditionally been one of the largest industrial sectors and according to the South African Chamber of Mines [(2)] the local mining industry employed over 515 000 people in underground mines as of the beginning of 2009. Working conditions far below the earth's surface become increasingly difficult with depth, owing to the combination of excessively high ambient temperatures and large amounts of dust and pollutants in the air. Thus, cooling systems are particularly imperative in deep, hot mines since they are chiefly responsible for making the environment bearable and ensuring that the health of the workers is not placed under risk.

Since refrigeration systems are so widely utilised in a number of different scenarios, it is merely a matter of consequence that their reliability and performance efficiencies have become topics of much consideration to designers, manufacturers, users and academics alike. Many textbooks, technical papers, postgraduate dissertations and theses are devoted to devising different means and procedures by which refrigeration machine performance can be monitored and optimised. For example, Moran and Shapiro [(3)] devote their tenth chapter to the fundamentals and operation of

refrigeration cycles and the works of Phelan, Brandemuehl and Krarti [12], Grimmelius et al. [4] and Lee [18] are all chiefly devoted towards accurately monitoring the operating performance of chillers.

Publications, such as the *International Journal of Heat and Mass Transfer* and the *International Journal of Refrigeration*, regularly document research conducted in the field of heating, ventilation and cooling (HVAC) and bear testament to the strong interest in these spheres. The paper submitted by Gordon and Ng [5] is typical of the type of work that appears in such a publication.

Owners and operators of cooling devices in industrial applications also concern themselves with the efficiency and operation of their machines since both these factors have a direct bearing on running costs and certain other expenses. Apart from maintenance operations, the cost of running a refrigeration machine is largely dominated by the amount of electrical power it requires to function according to specification. Improving its efficiency thus means reducing the amount of this input power.

Aside from the reduced cost of consuming fewer kilowatt-hours of power, utility providers also encourage more efficient use of the machines by offering some sort of additional incentive to high-demand users who cut down on their consumption. The Demand-Side Management (DSM) program implemented by ESKOM [7] is a good example of such a scheme since users have a range of options that will benefit them financially if they participate in the scheme.

However, as stressed by Bailey-McEwan [8] pp. 1-3, operating costs for cooling devices are relatively insignificant when compared to the penalties that result from unsatisfactory machine performance or unavailability brought about by a breakdown. Such penalties are particularly severe in underground mines where the health and safety of workers is prejudiced when the cooling systems operate in an inadequate way or when the entire operation must be suspended in the event of a machine breakdown. To varying extents, both of the above scenarios also affect productivity of the mine either through decreased worker output resulting from poor working

conditions or via a complete shutdown of the site if it is deemed necessary for worker safety. Stewart [9] states that various forms of heat illness can occur when people are exposed to high amounts of heat stress and that these illnesses may result in death if not treated correctly.

Thus, the obvious conclusion can be drawn that investigations into means of ascertaining and interpreting the operating performance of a refrigerating machine will prove highly beneficial to anyone maintaining, operating or utilising it. Improved efficiencies mean lower costs for the owners of the machine and a smaller risk of a breakdown by minimising the need for using more power than necessary to meet the cooling demand. This is beneficial, both economically and socially. The large number of different applications in which cooling machines operate makes such investigations potentially very beneficial.

1.2 Introductory Concepts

In order to correctly diagnose and analyse the actual performance of a refrigeration machine it is necessary to obtain its current levels of performance and compare the findings with some sort of benchmark or yardstick. Logically, this yardstick should be in the form of the machine's corresponding normal or optimum performance. Bailey-McEwan [8] p. 120 emphasises this same point by stating: "actual performance cannot be properly assessed without a yardstick to compare it with; this yardstick being at least the corresponding normal performance."

However, before the above concept can be fully appreciated it is first necessary to define what is meant by certain key terms. The definitions of the terms that follow on pages 4 to 6 are adopted from Bailey-McEwan [8] pp. 119-125 and are used consistently throughout subsequent sections.

For diagnostic purposes any refrigeration device can broadly be considered as a generic process that converts inputs into outputs via some internal means, as given by Figure 1.1, which has been taken from Isermann [10]. The means by which the device performs this transformation is determined to a large extent by its particular *process parameters* and *state variables* and the final output is influenced to some degree by external disturbances, or *noise*.

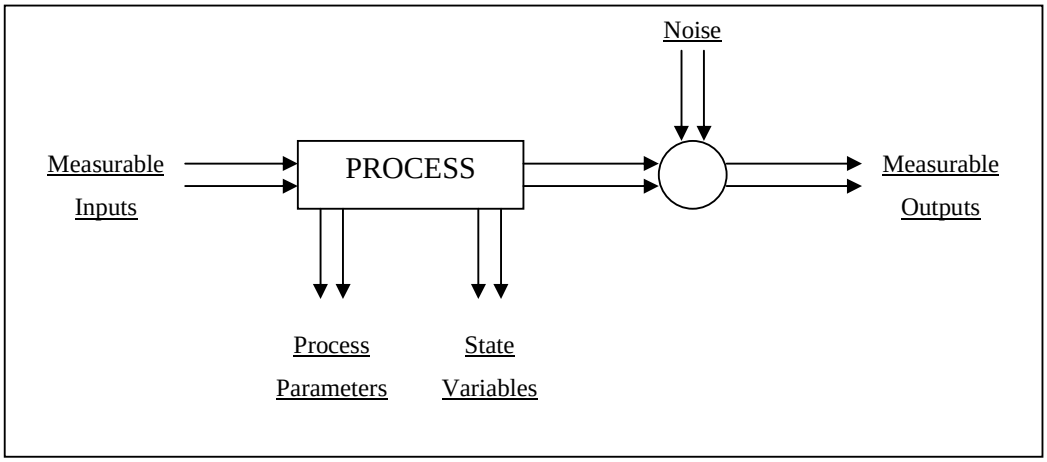

Figure 1.1: Process and Definitions, (Isermann [10])

A process parameter is, loosely, a physical attribute of the machine and its components, that is either constant over time or changes very gradually with time. Examples of such parameters in chillers are the inside diameters of the pipes through which refrigerant flows and the effective surface area that facilitates heat transfer in the heat exchangers. State variables, on the other hand, are internal states that vary with time in a much more significant and rapid way, and a machine operator usually controls their quantities directly or indirectly according to specifications. The refrigerant content by mass of a component at any one time is typical of a state variable.

Once process parameters and state variables are clearly defined it becomes possible to distinguish between *normal*, *design*, *optimum* and *satisfactory* performance of cooling devices. All four modes of operation assume static conditions when the machine operates at steady state and transient effects associated with starting up are neglected.

Normal performance is defined as static performance when all of the machine's state variables and process parameters are at their specified design values, regardless of its user-defined inputs. Such a scenario is indicative of a machine that has recently undergone preventive and remedial maintenance and thus has no operational faults. It is important to note that normal performance is also a function of process inputs and that actual performance can only be compared to it if the inputs correspond to one another, hence the term *corresponding normal performance*.

Design performance is defined as normal performance when the operating regime, which constitutes both the externally imposed inputs and the control philosophy (user-specified set points) are at design specification. Since design performance is thus for fixed inputs and control philosophy, it is often of very little use when assessing actual performance, as elaborated upon in section 1.3.

Optimum performance is static performance when all the measures of effectiveness and quality of performance, both of which are discussed below, satisfy some pre-determined criteria for optimality. Process parameters and state variables need not be at design values for optimality, since certain off-design combinations may allow the machine to operate optimally.

Finally, Bailey McEwan [8] p. 124 states that satisfactory performance of a refrigerating machine is static performance in which: 1) measures of effectiveness of actual performance correspond to required measures within certain pre-agreed tolerances or approach such values as closely as the machine's specifications and its process parameters permit; and 2) measures of quality of actual performance either correspond to, within pre-agreed tolerances, or are better than the values obtained under corresponding normal performance.

In order to compare actual performance to corresponding normal or optimum values and deem whether it is satisfactory or not, Bailey-McEwan [8] pp. 124-125 points out that the *effectiveness* and *quality* of the former must first be determined either via direct measurement or through derivations based thereon. Measures of effectiveness of refrigeration machine performance gauge whether the machine is providing the

right amount of cooling. Examples of such measures are the chilled water flow rate and the cooling load that indicates whether the device is extracting the required amount of heat from the space being cooled. Conversely, measures of quality of performance are either measured values of inputs required by the machine to perform the cooling or derived values that illustrate how efficiently the machine is cooling, taking into account the relation between certain key inputs and outputs. Such measures include the amount of input power required by the machine and its corresponding coefficient of performance (COP).

Bailey-McEwan [8] pp. 124-125 also notes that once the distinction is made between different modes of operation it becomes possible to assess whether the actual performance is satisfactory based on accurate measurements and comparisons. In order to draw valid conclusions, however, the following criteria have to be fulfilled: 1) The actual operating performance of the machine must first be ascertained with acceptable accuracy so that uncertainties in the measurements are small enough for it to be meaningfully compared with the corresponding normal or optimum performance; and 2) The normal or optimum performance must be known in advance or predicted with sufficient accuracy so that comparisons drawn from the actual performance measures are meaningful and can be used with confidence.

Table 1.1 below summarises the key definitions introduced above for easy reference since subsequent sections adopt consistent use of them. The importance of a clear distinction between modes of operation will be illuminated in the following section that identifies current problems with ascertaining and assessing refrigeration machine performance.

Table 1.1: Key Definitions, Bailey-McEwan [8] pp. 119-125

TERM	DEFINITION
Process Parameter	Machine attribute approximately constant with time
State Variable	Internal state that varies significantly, but not instantaneously, with time
Operating Regime	The set of inputs and control philosophy
Normal Performance	State variables and process parameters at design specification, regardless of inputs
Design Performance	Normal performance with operating regime at design specification
Optimum Performance	Measures of effectiveness and quality of performance that satisfy pre-specified criteria for optimality
Satisfactory Performance	1) Measures of effectiveness of performance that satisfy or approach criteria for satisfactory performance as closely as the machine's process parameters and specifications permit 2) Measures of quality of performance that satisfy or are better than corresponding normal values

1.3 Measuring Corresponding Normal Performance

As mentioned in section 1.1 above, a means of easily measuring and assessing actual performance with high accuracy will prove beneficial to the many people who maintain, operate or utilise refrigeration machines. Efficiency will consequently be maintained at higher levels and the risk of breakdowns will be minimised by a combination of more efficient operation and appropriate reactions to early warning signals that indicate unsatisfactory performance. As has already been noted, correct assessment of actual performance requires a priori knowledge of corresponding normal or optimum values that can be used as a benchmark to be compared against.

Numerous attempts have been made to devise methods that predict corresponding normal or optimum performance. These methods range from the highly complex to the fairly simple and some employ the use of accurately recorded historical data, whereas others require only a few characteristic measurements to be taken. Certain of

the more common procedures will be introduced and critically discussed in this section.

However, before an analysis of the various diagnostic tools is begun, it is necessary to stress a point briefly touched upon in the preceding section and emphasised by Bailey-McEwan [8] pp. 119-121. The importance of using the *corresponding* normal or optimum performance as the yardstick against which actual performance is compared cannot be over-emphasised. Using corresponding performance means that the inputs and control philosophy, which together constitute the *operating regime*, must be the same for the actual performance being diagnosed and for either the normal or optimum measures that are used as benchmarks. If comparisons are attempted where the operating regimes differ, incorrect conclusions will be drawn since the actual performance is strongly influenced by the type and value of inputs and by the control philosophy.

No matter how accurate and practical the means of diagnosis is, comparisons must be drawn between data sets that relate to the same operating regime or else a fault may either go undetected or be incorrectly diagnosed. In refrigerating machine installations that operate at part duties to compensate for seasonal fluctuations in required cooling load such mistakes may be made more often since operating at part duty requires an operating regime different to full duty.

Since measures of design performance are based on a specified set of inputs and control philosophy they may be highly unreliable as the benchmark to use in comparison with actual performance. In many circumstances, particularly in mining applications where conditions are often unique and unpredictable, the operating regime for actual performance is very different to that which the machine was designed for. This necessarily means that comparisons drawn against design performance are likely to be inadequately meaningful or even invalid.

With this point clear and understood, the main thrust of this section remains to identify different means that have been adopted to predict corresponding normal or

optimum performance. According to Bailey-McEwan [8] p. 159, current practice broadly follows one of four main paths:

1) Using information already available from manufacturers that lists normal performance for a range of anticipated off-design conditions

2) Predicting normal performance via an extensive set of accurate operating data recorded over time

3) Predicting normal or optimum performance through detailed and comprehensive fundamental mathematical modelling

4) Predicting performance via simpler fundamental modelling and a limited set of key operating data

These main methods are discussed and critically analysed below in terms of their respective shortcomings. Where possible, ways of overcoming their weaknesses are suggested.

Using manufacturers' quoted data

In some situations manufacturers of cooling devices will supply users with information of performance characteristics under design conditions and also for a limited set of user-specified, off-duty conditions anticipated when operating at part duties.

Bailey-McEwan [8] p. 159 points out that for applications that encounter constant diurnal and slowly varying seasonal fluctuations in duty, such data may prove very useful. However, in more common instances where the diurnal duty of the machine is not so constant and varies to a wide degree, a limited data set will be insufficient in trying to predict corresponding normal performance for the considerable range of conditions encountered. It may be argued then that a more comprehensive data set be requested from the manufacturers that covers all expected off-design conditions, but

this is infeasible and amounts to an unrealistic expectation. Compiling an extensive data set requires a considerable amount of extra work on the part of the manufacturers, as they would have to run large numbers of tests on each machine that they produce. Furthermore, Bailey McEwan [8] p. 159 indicates that releasing such complete information on the performance characteristics of their devices amounts to releasing proprietary information and manufacturers are, understandably, reluctant to divulge such data.

Bailey-McEwan [8] p. 160 also states that in mining applications in particular, the duties of refrigeration machines for cooling the workings are subject to substantial and permanent changes as a consequence of the unpredictable nature of mining. Since these changes are highly irregular, it is also very unlikely that manufacturers or users will be able to predict the corresponding operating regimes that will prevail, so even if they were willing to release a more substantial set of data it is probable that these would not encompass some of the prevailing operating regimes.

Therefore, although some manufacturers of refrigerating machines do offer users a set of normal performance measures for certain off-design conditions, only a limited number of applications can enjoy this benefit. For industries in which the operating conditions are irregular and not easily predicted, another, more versatile technique is necessary.

Using historical data

A method sometimes used that is unique to a particular machine and its environment is to build up an accurate and extensive set of historical data under a range of fault-free conditions. This set is then used to develop a regression model that will predict normal performance for the range of conditions recorded.

However, according to Bailey-McEwan [8] pp. 160-161, predicting corresponding performance measures in this way is not practical for a number of reasons, particularly in a mining environment where significant seasonal variations occur. Firstly, ensuring that the data is recorded under fault-free conditions means that a high

standard of instrument and machine maintenance must be consistently maintained, which is both a costly and time-consuming requirement. Secondly, the benefit of such a model can only be realised if it encompasses the entire range of off-design conditions that will be encountered. Obviously this is a very tedious task and requires a large amount of additional work that may be infeasible in many situations. Thirdly, in applications that encounter significant seasonal variations, building up a data set capable of predicting corresponding performance for all conditions may take several years to fully develop. Obviously, investing in a method that is so slow to deliver the benefits is undesirable.

In addition to the direct inconveniences encountered on site there are also drawbacks associated with constructing the corresponding regression model from the acquired data and these disadvantages are pointed out by Bailey-McEwan [8] p. 161. If conditions are encountered that are outside the range of the data base the regression model will be invalid as a predictive tool. Thus, even if many years have been devoted to collecting data it is possible that unique conditions may be encountered in the future that are not catered for. Furthermore, regression models inherently only consider input and output variables of the process and do not yield the values of important, non-measurable process parameters and state variables that are vital for correct fault identification. To estimate these quantities, mathematical models need to be employed.

Using comprehensive fundamental mathematical models

One technique that is both highly versatile and not overly time consuming once the model itself has been constructed and verified is to predict corresponding performance values via comprehensive mathematical models derived from fundamental principles. As a consequence of its fundamentally based nature, this method has a broad range of applicability and is easy to use once fully developed.

One of the most striking benefits of this method is pointed out by Bailey-McEwan [8] pp. 161-162 as its ability to predict normal or optimum performance for any given combination of inputs and control philosophy. These values are merely variables in

the developed equations and can be adjusted at will to suit the operating regime. Also, both normal and optimum performance can be predicted by adjusting the process parameters and state variables in the model accordingly.

Bailey-McEwan [8] p. 162 remarks that mathematical models can also be used for in-depth fault diagnosis since they can, in principle, estimate the actual values of certain important, non-measurable process parameters and state variables, on the basis of measurable quantities. Comparisons between these quantities under actual and corresponding normal or optimum performance identify the type and location of certain faults. Once a model is developed for a particular machine it can be applied to similar machines with different specifications and of different makes by simply adjusting variable quantities as discussed above.

However, the task of developing a model is by no means simple and requires a large amount of dedication and validation to ensure that it is reliable and accurate. If a completely new refrigeration device is adopted for an existing application, then a corresponding entirely new model must be developed and the old model becomes inapplicable. Using such models also requires that a relatively large number of measurements be recorded so that unknown process parameters and state variables that characterise machine performance can be solved for. Also, comprehensively modelling certain machine components requires proprietary information. Thus, although this method has numerous advantages, it has certain impracticalities that take away from its appeal.

Using a Simpler, Empirically Tuned Model

To a certain extent, the impracticalities encountered when using fundamental mathematical modelling to ascertain corresponding performance can be overcome by using simpler modelling techniques. As for the detailed method described in the preceding section, these types of models are also derived from basic physical principles, but are not developed to the point of being specific to a particular type of machine.

One such technique that has attracted significant attention of late is the *Universal Thermodynamic Model* developed by Gordon and Ng [1], who use the First and Second Laws of Thermodynamics to derive their formula for performance evaluation. In short, the formula assesses the quality of machine performance with relatively few measurements and is fundamentally derived so that it is, in theory, globally applicable to all machine types. Taking a limited number of measurements under fault free conditions over the machine's entire operating range and then using these measurements in a regression analysis to set certain constants in the model enables prediction of corresponding normal performance. The developers of the model call this technique *tuning*. Although a detailed review of this method is reserved for a subsequent section, its main advantages and disadvantages are outlined below.

The main advantage of employing the Universal Thermodynamic Model is the ease with which valuable performance quantities with high economic value can be predicted. Far fewer measurements are required in order to accurately predict corresponding normal performance than if a detailed model was used. Work performed by Thomas [11], Gordon and Ng [5] and Phelan, Brandemuehl and Krarti [12] are all testaments to the practicality of the model.

However, as can be expected, this technique is not without its drawbacks, which are outlined by Bailey-McEwan [8] p. 165. The data recorded when tuning the model must also be independently verified as representing fault-free operating conditions so that the corresponding benchmarks can be used with confidence and the global nature of the model makes it difficult to easily identify the type and isolate the location of detected faults.

Nevertheless, the versatility and practicality of Gordon and Ng's method still make it an attractive method of performance prediction for complex machines where detailed mathematical models are unavailable. In addition, certain of its disadvantages can be reasoned to be of negligible consequence, while others have been overcome to an extent, as discussed in Section 3 and Section 6 below. One of the objectives of this study, as mentioned in the next section, is to evaluate the model's fault diagnosis

capabilities and Section 6.3 shows how a low level of fault diagnosis can be achieved via the Universal Thermodynamic Model.

Although conditions may arise which lie outside the range of fault-free conditions for which measurements have been recorded, the ease with which a check can be conducted make it a simple matter to gather a new set of data for an unforeseen operating regime. This amounts to doing a performance check on the machine and testing under these desirable conditions. Previous work done on verifying the model by Thomas [11] employed this very technique of recording values after maintenance operations as a way of obtaining normal performance. Ng, Chua et al [13] also developed techniques that enable the model to predict optimum performance and a brief survey of their work is carried out in Chapter 2. The poor ability of the model to identify and isolate faults can be argued as being a minor drawback. In most situations, the time spent finding the location of a known fault is insignificant compared to the penalties that would result if its presence was not detected in the first place. Although fault isolation is necessary, it does not have to be done by the model. Nevertheless, it will be attempted to show that a very limited and low level of fault diagnosis is possible through inspection of the model's outputs.

Thus, the question that arises is the extent of applicability of the Universal Thermodynamic Model to large-capacity, complex machines found frequently in industry. Valid conclusions from this question will further enhance the attractiveness of the model as a quick and effective performance analysis tool.

1.4 Objectives of the Study

In this chapter the clear need for a quick and accurate performance measurement and assessment tool for refrigeration machines has been reviewed in light of the economical and practical advantages that will result. It is necessary to predict corresponding normal or optimum performance and use these as a yardstick against which actual performance is compared.

Various techniques that have been adopted to predict corresponding normal performance have been introduced and briefly reviewed, with particular attention paid to the advantages and disadvantages of each. It appears that Gordon and Ng's Universal Thermodynamic Model has the potential to become more widely used in industry if it can be verified for large-capacity, complex machines employing complicated refrigeration cycles.

The importance of comparing actual performance with normal or optimum values under the same operating regime has been emphasised. Neglect of this requirement risks leading to invalid conclusions and incorrect decisions based on operating performance. In extreme cases, such a mistake may be just as detrimental as having no performance assessment tool at all.

The objectives of this study are as follows:

1. Understand and critically analyse the assumptions made by Gordon and Ng in deriving their Universal Thermodynamic Model.

2. Examine the extent to which the predictive power of the Universal Thermodynamic Model can be satisfactorily extended to large-capacity refrigeration machines using complicated refrigeration cycles.

3. For at least one representative, complex machine in the field, evaluate the effectiveness of the Universal Thermodynamic Model in detecting under-performance and possible faults.

4. For the machine(s) which are used to assess the effectiveness of the Universal Thermodynamic Model, evaluate the model's fault-diagnosis capabilities.

2. LITERATURE REVIEW

Consistent with the objectives just defined, the literature review is focused on the following issues: presentation and critical analysis of different methods adopted for predicting corresponding normal performance of refrigeration machines; the need for accurately and efficiently assessing performance of large machines employing complex refrigeration cycles; outlining the history and development of Gordon and Ng's Universal Thermodynamic Model with particular reference to validating tests performed by them; and attention to any reference noting the importance of matching operating regimes when drawing comparisons between actual and desirable performance. Each paper in the review is analysed according to its respective contributions to these concepts.

2.1 Diagnosing Faults from Actual Machine Performance

Bailey-McEwan [8] pp. 294-303 describes and analyses the work of selected authors who aimed to assess and diagnose refrigeration machine performance directly from measurements taken over time. In addition to the disadvantages put forward in chapter 1 with adopting this method of performance assessment, each attempt described also encountered some unique obstacles of its own.

Gluckman [14] attempted to link some common faults to their primary symptoms based on data obtained over years of operation and performance monitoring. From his data, he constructed a table that listed some common faults and their most prominent, observable symptoms and intended that it be used as a diagnostic tool to determine probable causes of faults. An operator could diagnose a fault simply by locating any irregular set of symptoms on the table and selecting the type of fault whose symptoms matched them most closely. Table 2.1 shows one of Gluckman's tables as it appears in Bailey-McEwan [8] p. 294.

Table 2.1: Lookup Table for Primary Faults, (Gluckman [14])

Fault	Primary Symptoms
Condenser air blanketing (non-condensable gas in condenser)	High condensing pressure, apparent liquid subcooling
Liquid flooding in condenser	High condensing pressure, apparent liquid subcooling
Condenser water-side fouling	High condensing pressure, no liquid subcooling, high water pressure drop
Low condenser water flow	High condensing pressure, no liquid subcooling, low water pressure drop
Oil in refrigerant in evaporator	Low evaporating temperature
Insufficient refrigerant charge	Low evaporating pressure

Despite the potential practical and economic benefits of simply using a lookup table to diagnose faults, this method poses a unique potential problem that is pointed out by Bailey-McEwan [8] pp. 294-295. Gluckman [14] distinguishes between symptoms by referring to their 'high' or 'low' values for certain parameters, which implicitly requires that the interpretation of and distinction between 'high' and 'low' be made with respect to normal values. However, in most on-site cases such comparisons are usually made with respect to design values and, as has already been explained, actual and design performance are not directly comparable unless the operating regimes are identical for both. If these are not identical, operators using design performance as their benchmark are then likely to incorrectly diagnose faults since many parameters are subject to large variations based on the operating regime of the device. Of course, this illustrates the concept stressed in the first chapter of the necessity of using correct corresponding performance as a comparative benchmark.

Bailey-McEwan [8] pp. 295-296 also surveys work performed by Hall and Unsted [15], and later by Hemp et al. [16] that lightly addresses the problem of off-design operating regimes misleadingly suggesting unsatisfactory performance. Their programs, as indicated by Bailey-McEwan [8] p. 295, "draw the user's attention to off-design inputs" by instructing them to first check the machine's input quantities relative to design specification. Although not explicit and exhaustive in their treatment of the issue, they at least give some attention to the possibility of misdiagnosing faults due to off-design operating regimes. Table 2.2 is taken from Bailey-McEwan [8] p. 295

and summarises the deviations in certain state variables that each set of authors considers as suggesting an off-design operating regime.

Table 2.2: Deviations Reported by Programs of Hall and Unsted [15] and Hemp et al. [16]

	DEVIATION IN MEASURED QUANTITY	Hall and Unsted	Hemp et. al.
	EVAPORATOR AND CONDENSER		
1	Water flow rate < 80% of design value	√	
2	Inlet water temperature > 3˚C above or below design value	√	
3	Refrigerant pressure > 5% above or below design value	√	
4	Water pressure drop too low or too high		√
5	Difference between temperature of condensing/evaporating refrigerant, and saturation temperature at refrigerant pressure, too high		√
	CONDENSER		
6	Outlet refrigerant temperature > saturation temperature at condensing pressure, or more than 1˚ below this	√	
	COMPRESSOR		
7	Excessive superheat at compressor inlet		√
8	Outlet superheat > 2˚C above or below design value	√	

Grimmelius et al. [4] attempted fault diagnosis from direct measurement in a conventional way. Of particular importance is that they draw comparisons between measured values and corresponding normal quantities. Twenty diagnostic variables were monitored from a custom-built machine for any noticeable deviations from normal values to identify the presence of faults. The normal quantities were obtained via linear regression, which in turn was based on 8000 separate sets of measured data recorded under fault-free conditions. Based on measurements taken, 37 “failure modes”, or sets of deviations deemed to represent faults, were identified and their respective effect on the diagnostic variables was determined. From this a *failure mode symptom matrix* was constructed that could be used in a similar way to Gluckman’s table to suggest a fault, based on typical symptoms that characterise it. Table 2.3 is an extract from a failure mode symptom matrix of Grimmelius et al. [4], as it appears in Bailey-McEwan [8] p. 298.

Table 2.3: Extract from a failure mode symptom matrix, (Grimmelius et al. [4])

	Compressor				Evaporator			Condenser	
Failure Mode	Inlet Pressure	Electrical Power	Super-Heat	(other measurements)	Outlet Pressure	Chilled water temperature change	(other measurements)	Sub-cooling at outlet	(other measurements)
1a	<	<	>		>	<			
1b	>		>		>	<			
2		>						<	
3		<	>			<			
4	>	>	<		>	>			
5	<	<	>		<	>			

<: decreased value due to fault >: Increased value due to fault

1a: Compressor, suction side, increase in flow resistance
1b: Compressor, discharge side, increase in flow resistance
2: Condenser, water side, increase in flow resistance
3: Refrigerant liquid line from condenser, increase in flow resistance
4: Thermostatic expansion valve, control unit: power element loose from pipe
5: Evaporator, chilled water side, increase in flow resistance

Although Grimmelius et al. [4] were correct in using corresponding normal performance as their benchmark their method contains some inherent shortcomings, which are identified by Bailey-McEwan [8] pp. 298-299. Unanticipated faults, which may arise under irregular or untested operating conditions, may produce symptoms that cannot be interpreted by their model. In other situations, different faults may produce the same primary symptoms and thus become indistinguishable from one another. Where multiple faults exist in one machine their respective symptoms are likely to interfere with each other and significantly reduce the probability of a correct diagnosis. Finally and most obviously, obtaining such an extensive data set is simply too time-consuming and tedious to gain widespread popularity in industry.

In reviewing the works of Gluckman [14], Hall and Unsted [15], Hemp et al. [16], and Grimmelius et al. [4] discussed above, Bailey-McEwan [8] pp. 294-303 emphasises the importance of detecting off-design inputs or control philosophy, which may contribute significantly to unsatisfactory performance. All of the papers attempt fault diagnosis from measurements only and one useful benefit of this is detection of off-design inputs. However, not all operating faults can be detected from measurements alone and so these methods might not be sufficiently reliable as performance monitoring tools.

In reaction to the shortcomings of fault diagnosis by measurement alone, Bailey-McEwan [8] pp. 303-321 reverts to process modelling techniques, which derive important measures of performance based on measurements or estimates of important process parameters or state variables, as the most desirable method of performance assessment. This procedure is justified by its ability to reveal faults that are either not detectable by measurements alone or are highly unanticipated.

Reference is made to Isermann [10] who indicated that fault diagnosis via process modelling requires three separate models:

- A model of the actual, or observed, process
- A model of the normal process
- A model of the faulty process

Isermann [10] also goes on to state that mere detection of faults is not enough and that correct diagnosis is also of high importance. In order to achieve effective diagnosis, however, the model must use the fundamental laws that govern the process.

2.2 Universal Thermodynamic Model

The Universal Thermodynamic Model, which is the primary focus of this study, attempts to precisely predict the COP of a machine based on relatively few experimental measurements, some of these being water-circuit quantities. Although several papers have been submitted on this method, analysing three publications that outline its main aspects can effectively track its evolution. A full review of the model is reserved for the following chapter, so a brief outline of its development is presented below.

Gordon and Ng [5] review and further develop their method that was first introduced in Gordon and Ng [6]. They point out that their method, the Universal Thermodynamic Model, pertains to all types of refrigeration machines and that it is simple enough to yield analytic formulae for key performance characteristics. They state that their model captures the essential physics of the refrigeration mechanism by analysing how irreversibilities affect the performance of a specific machine. A brief justification of their work is given by referring to existing methods of performance analysis as being case-specific and therefore not widely applicable to all machine types.

Gordon and Ng [5] then discuss how refrigeration machines can be characterised by curves of 1/COP versus 1/ (Cooling Rate), as shown in Chapter 3. From these curves it is shown that there is an intermediate range of cooling capacities for which COP is a maximum and that, for different rates of cooling, different types of irreversibilities dominate over others. The essential elements and assumptions of the curves are discussed and these are used to arrive at a general formula, which is given by Equation 3.1 or Equation 3.2 in the next chapter.

This formula is then shown to apply to reciprocating, centrifugal, absorption, thermo-acoustic and thermoelectric chilling devices. Of particular interest are the results obtained for reciprocating and centrifugal chillers, since they constitute a major proportion of the types of devices used in industry.

For reciprocating machines, the predictive power of the model was shown to be highly accurate. Tests were conducted on a nominal 63kW cooling capacity air-cooled device and experimental values were obtained from the manufacturer's catalogue for COP values between 1.5 and 3.5 and for cooling capacities of 37-65kW. Curves of predicted COP versus measured COP were obtained and Gordon and Ng [5] show that the predicted values have a RMS error of 4% relative to the measured values.

The tests performed by Gordon and Ng [5] on the centrifugal chillers were aimed more at illustrating the diagnostic capabilities of the model. In this study the impact that heat exchanger fouling has on the performance of a refrigerating machine was explored by taking measurements and predicting the COP before and after maintenance operations, in which the heat exchanger tubes were cleaned, were performed. It was shown that the performance of the machine improved by about 36% on average for similar operating regimes.

Ng, Chua et al [13] provide further justification on the development of the Universal Thermodynamic Model by stating that it can be used for analysis of an installed, operating reciprocating machine by taking only a few vital measurements instead of performing a large number of time-consuming experiments. They further develop their interpretation of the characteristic curve to be in line with an adapted version of the Universal Thermodynamic Model. They argue that the previous version of the formula characterised machine performance in terms of three lumped empirical parameters whose physical significance is not clearly defined since they constitute the combined effects of a number of different irreversibilities.

The alternative model submitted still uses three parameters to illustrate machine performance, but the physical significance of these parameters is clearer. The parameters in the new version specifically quantify the total entropy production, the heat exchanger thermal resistance and the equivalent heat leak of the machine. The new method, according to Ng, Chua et al. [13], allows for more powerful fault diagnosis than before since it becomes easier to identify where performance degradation occurs once the parameters are well defined and understood.

Another key objective fulfilled by Ng, Chua et al [13] is their illustration of how the Universal Thermodynamic Model can be adapted to determine optimal machine operating conditions and how the potential improvement in COP can be realised from minor machine modifications. Determination of optimum performance via the formula is achieved by taking the derivative of COP with respect to heat lost at the evaporator and with respect to the evaporator's effective thermal conductance. These derivatives are both set equal to zero for optimisation and solved simultaneously. Once experimental values are found for key parameters, values for the heat transfer rate and the thermal conductance that maximise COP can be determined.

In a later presentation, Ng, Gordon and Chua [17] further demonstrate the diagnostic, optimisation and predictive capabilities of the adapted version of their Universal Thermodynamic Model and also qualitatively illustrate the shortcomings of adopting an endoreversible model to predict performance. Endoreversible models assume that the refrigeration cycles are internally reversible and that the only losses that occur are external to the system. Through experiments performed on different chillers, which are discussed below, it was shown that internal irreversibilities do have a significant effect on performance.

The predictive capabilities of the model were illustrated by Ng, Gordon and Chua [17] for a variety of chillers through experimentation. For a reciprocating device, it was proven that values for key parameters obtained via the model are in close agreement with the same values obtained through rigorous measurement. The analysis adopted for a centrifugal machine involved taking key measurements before and after maintenance operations and comparing how the model predicts the corresponding performance characteristics. It was shown that, as expected, the model accurately identified that the heat exchanger tubes had been cleaned. The internal irreversibilities of the chiller, which are, in many cases, not affected by heat exchanger cleaning, remained unchanged but the conductance term in the model did vary, which is indicative of the cleaning operations that were carried out on the heat exchanger tubes. Tests were also conducted on an absorption device and on thermoacoustic and thermoelectric chillers, which confirmed the universal applicability of the model.

Lee [18] extended the Universal Thermodynamic Model to predict the performance of screw liquid chillers under various operating conditions by conducting a number of experiments that validate its accuracy and applicability. His experiments involved taking water side measurements of cooling water inlet temperature, chilled water inlet or outlet temperature, and cooling capacity. He opts for the older version of the Universal Thermodynamic Model, which utilises lumped parameters instead of more physically meaningful ones. Thirty-six sets of experiments were performed to cover all combinations of testing conditions for a nominally rated 211kW liquid chiller using a semi-hermetic twin-screw compressor. Lee [18] goes on to prove that his experiments yield a high degree of correspondence between measured performance quantities and predicted ones. Plots of 1/COP versus 1/ (Cooling Rate) for a variety of operating conditions illustrate that the experimental data points obtained lie very close to the straight-line curve predicted by the Universal Thermodynamic Model and the RMS error between measured and predicted COP obtained by Lee is about 1.43%.

Phelan, Brandemuehl and Krarti [12] propose methods of conducting in-situ, or non-intrusive, performance tests on chillers. They point out that using manufacturers' data or laboratory measurements is often risky when trying to assess performance since, as was mentioned previously in section 2.1, the installed device in actual operation often operates in a considerably different way to what was initially thought. This then prompts the need for in-situ field measurements, which can be taken without significantly disrupting the machine's desired operation.

At the time of publishing their article, Phelan, Brandemuehl and Krarti [12] observed that there were no widely accepted equipment-specific protocols that outline how to conduct in-situ tests on refrigeration machines. Conventional methods all involved the development of custom measurement plans and analytical procedures for each installation. In addition to being time-consuming, such methods will also often result in inconsistent performance measurements and increased evaluation costs.

The testing procedure proposed by Phelan, Brandemuehl and Krarti [12] makes use of the earlier version of the Universal Thermodynamic Model, since the alternate version had not been developed at that stage. However, the model was still selected over

other existing methods since it only requires a limited number of parameters, which makes it attractive for practical field-testing. Ways in which both temperature-dependent and temperature-independent versions of the model, which are introduced in Section 3.1, can be used to predict performance from a few key measurements are discussed. They developed five methods for performing in-situ tests. These methods encompass scenarios that depend either on manufacturers' data or measured values for both the temperature-dependent and independent models under imposed loads or over short durations of time. Validation of the proposed methods was conducted on two chillers at a high school in Victoria, Texas and the results obtained were considered in conjunction with the expected experimental uncertainty. It was found that the deviations between measured and predicted COP were smaller than the inherent experimental error, thus indicating that the Universal Thermodynamic Model was acceptably accurate.

The experiments conducted by Phelan, Brendemuehl and Krarti [12] also illustrated that part-load operation was the most significant factor affecting operating efficiency, and that evaporator and condenser water temperatures have only a secondary impact. It was also concluded that the temperature-independent and, to a lesser extent, the temperature-dependent models are valid and attractive for field tests. The simpler, temperature-independent model is easier to implement and compute and so it was deemed the most desirable option. Although the temperature-dependent model is slightly more complex, it was shown to be accurate for calculating energy consumption, which also determines COP. In addition, a limited data set was proven to be sufficient when adopting the temperature-dependent model, which enhances its attractiveness.

Thomas [11] undertook to verify the Universal Thermodynamic Model through experimentation on a 10.5MW(R) [A] chiller used in conjunction with four other identical chillers on a gold mine. Both the old and new models, respectively referred to as the *graphical method* and the *magnification constants method* by Thomas [11], were used and evaluated in terms of their accuracy with respect to measured performance quantities. The conclusion reached was that the two models could not be separated in terms of accuracy and reliability, but the graphical method was deemed

[A]: MW(R) denotes Megawatts of refrigeration capacity

superior in terms of diagnostic capability. This is a result of the requirement that, when using the older model a number of plots need to be generated before the final curve can be obtained. These intermediate graphs provide a number of additional tools that facilitate easier identification of faults, or in the words of Thomas [11]: they "allow the user a number of extra tools to allow for better pin-pointing of possible problems." Figures 5.1, 5.2, 5.5 and 5.6 in Section 5 show the graphs that were generated for the centrifugal chiller in this study. Analysis of their slope and intersections with the x and y-axes can offer insight into possible causes of faults.

Thomas' opinion here differs from that of Ng, Chua et al [13]. He suggests that the older version of the model is more effective at identifying and diagnosing faults whereas Ng, Chua et al. [13] developed the alternative version as a means to facilitate easier fault diagnosis. The older version of the model will be used in the remainder of this study for the following reasons:

. The study can be aligned with other verification studies on the Universal Thermodynamic Model, such as Lee's [18] investigation of a chiller with a screw compressor.

. The literature surveyed- such as Gordon and Ng [5], Lee [18] and Phelan, Brandemuehl and Krarti [12] - provides detailed information on the application of and practical precautions with the older version, which becomes useful when the experimental data of this report is to be manipulated for interpretation.

2.4 Review of Chapter

Different attempts to devise quick and practicable methods of performance analysis have been discussed. One mistake often encountered when assessing performance is to compare actual performance with design performance, which is likely to lead to incorrect conclusions about the former if the operating regimes differ. The literature has revealed that some authors, such as Grimmelius et al. [4], avoid this mistake by correctly using corresponding normal performance as the benchmark, but few have explicitly stressed its paramount importance.

The Universal Thermodynamic Model, which claims to accurately predict normal performance, has been introduced and its development has been outlined. Attention has been given to instances where its creators have verified its accuracy through experimentation for a broad range of different cooling devices. It has also been noted how the model has evolved from an earlier lumped parameter formula into a version that clearly identifies the physical significance of each category of irreversibility. Investigations undertaken by authors who elected to use the earlier version have been presented in an attempt to distinguish its advantageous aspects and a review of Thomas' [11] investigation in particular serves to justify the adoption of the older version in the remainder of this study.

3. ANALYSIS

3.1 Review of the Universal Thermodynamic Model

Gordon and Ng [1] pp. 6-7 offer some important introductory concepts on their Universal Thermodynamic Model and its early developments that confirm the physical possibility of a universally applicable model for all chillers. They propose that all chillers can be characterised by how their Coefficient of Performance (COP) changes with respect to cooling rate and that a plot of 1/COP versus 1/ (Cooling Rate), taken from Gordon and Ng [1] p. 6 and given in Figure 3.1 below, is instructive in illustrating the universal aspects of all real, or non-idealised, devices.

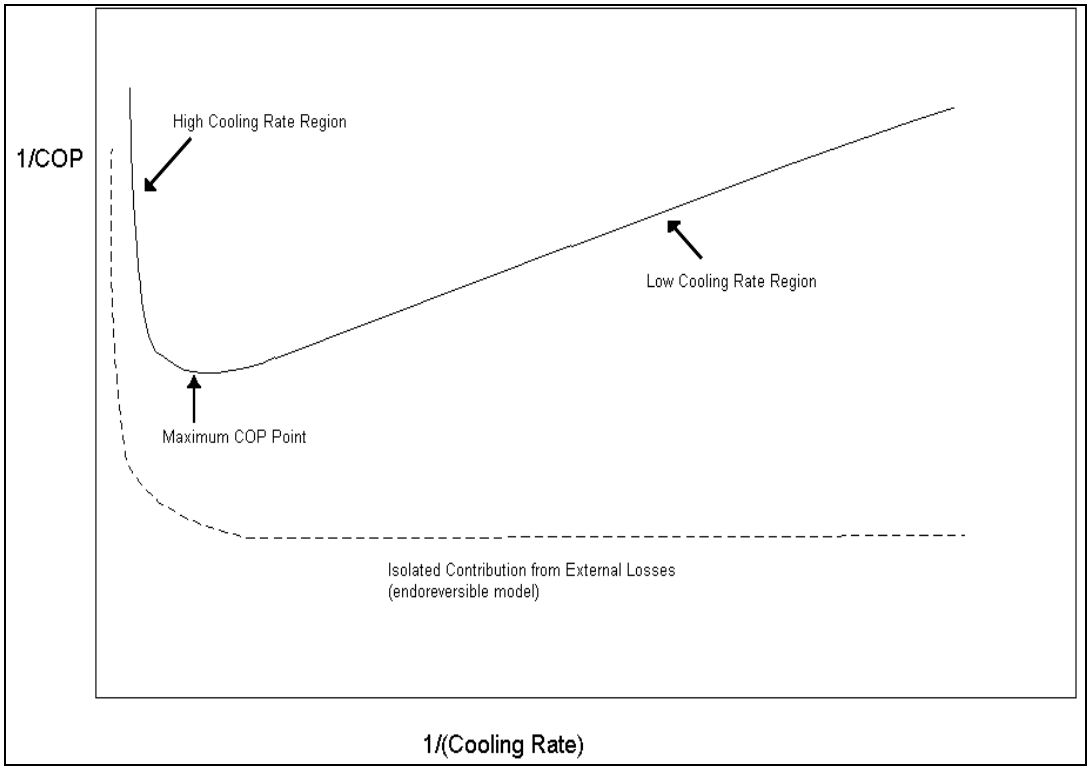

Figure 3.1: 1/COP versus 1/ (Cooling Rate), (Gordon and Ng [1] p. 6)

All real chillers have irreversibilities that act to impair their operating performance at both high and low cooling rates. In the case of mechanical chillers, the bottleneck of finite-rate heat transfer in the heat exchangers limits the machine's performance at high cooling capacities. Such an irreversibility is termed *external* since it is a consequence of the machine's thermal communication with its reservoirs (the warm and cool environments that heat is, respectively, rejected into and removed from). The region of high cooling capacity is shown in the figure and it can be observed that as the cooling rate increases to a limiting value of infinity, the COP rapidly approaches zero.

At low cooling rates, internal irreversibilities dominate performance. This comes about since external irreversibilities, such as heat transfer to the surroundings, are diminished at low cooling rates but internal losses are affected to a lesser degree. Therefore, the internal irreversibilities contribute a greater portion of the overall irreversibility. Internal irreversibility mechanisms include dissipation from fluid and mechanical friction, and throttling, and all of these losses occur within the machine itself. This region is also shown on the figure and it can be seen that the COP drops off, although not as drastically as before, as the cooling rate decreases.

Thus, since different types of irreversibilities dominate at high and low cooling rates, Gordon and Ng [(1)] pp. 6-7 note that there must be some intermediate range in which COP reaches or approaches a maximum value, as shown on the figure where 1/COP is at a minimum. Logically, designers and manufacturers of refrigerating machines aim to have this maximum COP point occur near the point of the most frequent operating regime. This is chiefly due to the idea that frequent operation at high efficiency will result in cost savings. Thus, determination of the point of maximum COP becomes an important goal for both manufacturers and users alike.

The figure also reveals that, for the majority of attainable cooling capacities, plotting the reciprocals of COP and cooling rate yields a straight line. In fact, non-linearity only exists for a small portion of excessively high cooling rates that approach infinity and for which the COP rapidly approaches zero. It is most likely that manufacturers avoid designing their devices in this region since a large majority of the power drawn

to achieve the high cooling capacities will be dissipated wastefully. The conclusion can therefore be drawn that a linear relationship between 1/COP and 1/ (Cooling Rate) can be safely assumed provided the cooling rate is not exceedingly high.

As an aside remark, the figure also indicates the isolated contribution of external losses on the COP of refrigerating machines, shown by the broken line below the main curve. Considering only external losses as being significant means that internal irreversibilities are considered negligible and the machine is correspondingly seen as being internally reversible or *endoreversible.* It can be seen that under an endoreversible assumption, COP reaches a maximum value at the limit of zero cooling rate. Although a detailed discussion of the inadequacies of the endoreversible model is not attempted here, it is sufficient to say that it does not model real machines with a high level of accuracy and that a fundamentally sound mathematical model that considers all loss mechanisms is preferable.

Although the above argument was made with respect to mechanical chillers and their specific loss mechanisms, Gordon and Ng [1] pp. 6-7 point out that there are always irreversibilities that disfavour both very high and low cooling rates no matter the type of machine. Thus, in theory, their formula should be valid for all types of chillers. In some of the papers reviewed in Section 2, such as Gordon and Ng [5], Thomas [11] and Lee [18], the model is verified for a number of different machines employing different principles of refrigeration.

Once it is understood that the operating performance of all refrigeration devices can be characterised by both their internal and external losses it becomes appropriate to enter into a more detailed analysis and review of the Universal Thermodynamic Model. What follows is an introduction to the mathematics behind the model and a brief description as to how it should be used practically. The formulae are presented in more detail in Appendix A and Appendix B.

It is important to note that, as was mentioned in chapter 2, only the early version of the model is presented. This version quantifies machine irreversibilities as three lumped parameters instead of three clearer, more physically meaningful quantities.

The model considers a basic vapour-compression refrigerating device, as shown in Figure 3.2 below, which has been adapted from Moran and Shapiro [3] p. 450. The machine comprises a compressor, condenser, expanding device and evaporator. Heat is removed from a cool environment by the evaporator and rejected into a warm environment by the condenser to achieve the refrigerating effect.

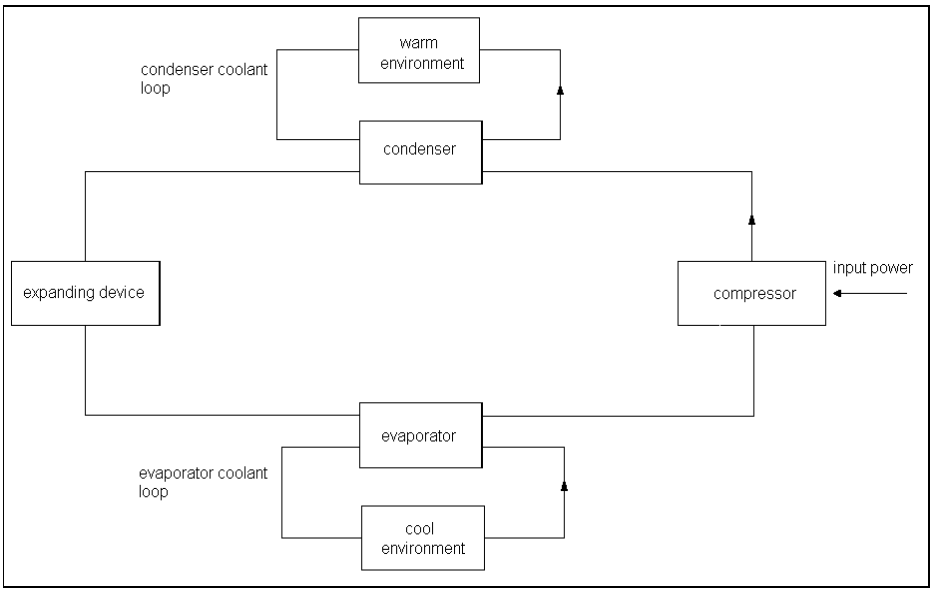

Figure 3.2: Vapour-Compression Device (altered from Moran and Shapiro [3] p. 450)

By invoking both the First and Second Laws of Thermodynamics, the Universal Thermodynamic Model equates to the following two forms, as given by Bailey-McEwan [8] p. 349. His work re-presents a detailed derivation of the model based primarily on Gordon and Ng [5], Gordon, Ng and Chua [19] and Gordon and Ng [20]. It is important to note that these formulae assume that the dominant loss mechanisms in the machine are internal irreversibilities, this being generally so for manufacturer's intended operating ranges in commercially available vapour-compression chillers.

$$\frac{1}{COP} = -1 + \frac{T_{Ci}}{T_{Eo}} + \frac{1}{Q_E} \cdot \left[q_{lp.side} \cdot \frac{T_{Ci}}{T_{Eo}} + q_{hp.side} \right] \qquad [3.1]$$

$$\frac{1}{COP} = -1 + \frac{T_{Ci}}{T_{Eo}} + \frac{1}{Q_E} \cdot \left[q_{lp.side} \cdot \frac{T_{Ci}}{T_{Eo}} + q_{hp.side} \right] + \Theta_{E,C} \qquad [3.2]$$

T_{Ci} and T_{Eo} respectively denote the absolute coolant water temperatures at the condenser inlet and evaporator outlet. $q_{hp.side}$ and $q_{lp.side}$ are measures of the "losses" due to irreversibilities at the condenser and evaporator, respectively, and Q_E is the heat transfer at the evaporator. The term $\Theta_{E,C}$ represents the effect of fouling in the condenser and evaporator.

Equation [3.1] is used when no significant heat exchanger fouling exists in the machine, while Equation [3.2] does not make this assumption and takes possible fouling into account. Gordon, Ng and Chua [19] express the additional term in Equation [3.2] in measurable variables as follows:

$$\Theta_{E,C} = \frac{q_{lp.side} \cdot \left[\frac{T_{Ci}}{T_{Eo} \cdot F_C} + \frac{T_{Ci}}{T_{Eo}} \cdot \left(\frac{1}{F_C} + \frac{1}{F_E} \right) \right] + \frac{q_{hp.side}}{F_C}}{T_{Eo}} \qquad [3.3]$$

The terms F_C and F_E are heat exchanger factors for the condenser and evaporator, respectively, according to Gordon, Ng and Chua [19].

Cengel and Turner [21] describe the mechanism of heat exchanger fouling. They point out that it occurs over time as deposits accumulate on the heat transfer surfaces, providing additional resistance to heat transfer and impeding the rate of transfer in the heat exchanger. The most common type of fouling stems from the precipitation of solid deposits or deposition of suspended solids in a fluid on the heat transfer surfaces; an everyday example of this phenomenon is shown by the layer of calcium-based deposits that forms on the inside of a household kettle after prolonged use. During maintenance operations on a cooling machine, if the heat exchanger surfaces are cleaned thoroughly the effect of fouling becomes negligible.

As related by Bailey-McEwan [8] pp. 349-351, Gordon, Ng and Chua [19] point out that application of Equations [3.1] and [3.2] to practical scenarios requires a key distinction to be made about the nature of the heat-carrying fluid temperatures, T_{Ci} and T_{Eo}. If the experimental values obtained for these two temperatures are relatively constant, then the following *temperature-independent* version of the model should be

used, which predicts the following straight-line relationship between 1/COP and 1/ (Cooling Rate):

$$\frac{1}{COP} = C_0 + \frac{C_1}{Q_E} \qquad [3.4]$$

The value of C_1, the slope of the straight line, depends on the internal losses $q_{lp.side}$ and $q_{hp.side}$. C_0 is the intercept of the line with the vertical axis and, in the event of significant heat exchanger fouling, depends on the heat exchanger factors F_C and F_E and on the same internal irreversibilities as C_1: $q_{lp.side}$ and $q_{hp.side}$.

For situations with appreciable variations in T_{Ci} and T_{Eo}, the *temperature-dependent* model is adopted. This version of the Universal Thermodynamic Model assumes that the internal irreversibilities of throttling through the expansion device, non-isentropic compression and fluid friction are not excessive and that the heat leaks follow a linear heat transfer law. This model is re-presented by Bailey-McEwan [8] p. 351 via Gordon, Ng and Chua [19] as:

$$\frac{1}{COP} = -1 + \frac{T_{Ci}}{T_{Eo}} + \frac{-C_0 + C_1 \cdot T_{Ci} - C_2 \cdot \frac{T_{Ci}}{T_{Eo}}}{Q_E} \qquad [3.5]$$

The constants C_0, C_1 and C_2 indicate the influence of the machine's internal irreversibilities. A brief comparison of Equation [3.5] and Equation [3.2] shows that, for a fixed condenser inlet water temperature T_{Ci}, the constants C_0 and C_1 can be considered to loosely represent the term $q_{hp.side}$, which accounts for irreversibilities in the condenser and C_2 represents $q_{lp.side}$, or the irreversibilities in the evaporator.

Both the temperature-dependent and temperature-independent models are attuned to a particular machine by determining the values of the constants. This entails obtaining accurate values of the water-circuit temperatures T_{Ci}, T_{Eo}, the load on the evaporator Q_E and the COP over the machine's operating range. The constants are then approximately determined via linear regression since, in general, the relationship between 1/COP and 1/ (Cooling Rate) has been proven to be a straight line.

Thereafter, the attuned model can be used to predict the machine's COP for a number of operating conditions. Limited fault diagnosis can be achieved by interpreting how the values of the constants change from corresponding normal predictions. This involves observing how the curves change in terms of their shape and position relative to the axes.

Aside from its simplicity and practicality, a key advantage of the model is its ability to predict corresponding normal performance, the importance of which has been stressed in chapters 1 and 2 above. This merely amounts to performing initial tests under specified normal conditions for a range of probable inputs and using the outcomes as performance benchmarks. Of course, this requires that the operating data for normal performance must be verified as being acceptably accurate by supplementary, confirming measurements.

3.2 Experimental Analysis

Before testing can be conducted to try and verify the Universal Thermodynamic Model for complicated industrial refrigeration machines, it is important to clarify certain aspects of the proposed experiment.

3.2.1 Required Measurements

Inspection of Equations [3.4] and [3.5] reveals what quantities need to be measured in order to verify and later apply the Universal Thermodynamic Model to the machine to be tested. Assuming that the fluid inlet and outlet temperatures will not prove constant across the measurements, the following variables will need to be recorded for a range of operating conditions to attune the temperature-dependent version of the model:

- T_{Ci} and T_{Eo}, the condenser inlet and evaporator outlet water temperatures. In some installations, thermometers are permanently positioned to constantly monitor these variables and can be used to determine the experimental values. Obviously, this will require some sort of validation check on the instrument's accuracy to determine the level of confidence with which it can be used. If no such devices exist on the machine, or if they are deemed insufficiently accurate, then temperature sensors obtained externally can be used, the accuracy of which must be assured. This will amount to placing the new sensors on or into the corresponding pipes at the condenser inlet or evaporator outlet and as close to the actual heat exchanger as possible to try and obtain accurate readings.

- Q_E, the evaporator load, which measures the rate of heat removal at the evaporator. The following expression is given by Cengel and Turner [21] for evaporator heat transfer in terms of measurable quantities:

$$Q_E = m_{flE} \cdot C_E \cdot \Delta T_E \qquad [3.6]$$

The quantity m_{flE} is the mass flow rate of chilled water through the evaporator in kilograms per second. C_E is the specific heat of the fluid and it should strictly correspond to the log mean temperature of the water through the evaporator, the determination of which is described by Cengel and Turner [21].

Obtaining the log mean temperature requires the values of two other key evaporator temperatures, the refrigerant inlet and outlet temperatures T_{ERi} and T_{ERo}. However, Moran and Shapiro [3], pp. 85-86, state that, over limited temperature intervals, specific heat of an incompressible substance like liquid water 'can be treated as constant without a serious loss of accuracy'. Thus, the specific heat at the average chilled water temperature across the evaporator can be used to simplify the determination of Q_E. The change in temperature across the evaporator, ΔT_E, is obtained from the measurements of water temperatures described earlier.

- The COP of the machine. This requires utilisation of Equation [3.7], which states that the COP is equivalent to the cooling load on the evaporator divided by the power input to the device. The cooling load will be obtained as described in the point above whereas the power input can be determined by measuring the power drawn by the compressor and other machine components and multiplying this by a measurable power factor. Equation [3.8] is adapted from McPartland and Novak [22] p. 86 for measuring power of typical three phase machines:

$$COP = Q_E / P \qquad [3.7]$$

$$P = \sqrt{3}.V.I.\cos\Phi \qquad [3.8]$$

The cos(φ) term is the power factor, and can be directly obtained by measurement. It is the ratio of the actual power flowing to the load over the apparent or measurable power in the circuit. Both the voltage V and current I can also be ascertained by measurement via a voltmeter and ammeter respectively. It must also be confirmed beforehand that the chiller is, in fact, a three-phase device. If it is not then the above formula will simply read P = V.I.cos (φ).

Although the above points describe ways of manually deriving the required quantities, some installations are equipped with automated systems that display these values directly. Obviously, in such scenarios, the accuracy of these readings must be determined before they can be utilised with any confidence.

3.2.2 Model Validation

In addition to those measurements that are explicitly required by the Universal Thermodynamic Model, certain other quantities also need to be obtained as a means of confirming the accuracy of such measurements. These quantities can then be used in an energy balance to ascertain whether the actual performance measurements are sufficiently accurate. The balance will take into account all measurable energy transfers at the main system components and give an indication of the validity of the recorded values.

Heat transfers other than those at the heat exchangers and the compressor are likely to occur due to machine losses, such as heating of oil in the bearings and then the oil having to be cooled, and due to heat lost to the surroundings at the evaporator. Nevertheless, such quantities should be very small when compared to those at the main system components and the balance should sum closely to zero if the measuring equipment is sufficiently accurate. The required measurements for the energy balance are as follows:

- Water temperatures at the condenser outlet and evaporator inlet, T_{Co} and T_{Ei} respectively, need to be measured in addition to those at the condenser inlet and evaporator outlet defined above.

- Mass flow rate of heat-removing water through the condenser, m_{flC}.

An effective way of validating the predictive accuracy of the Universal Thermodynamic Model is to compare the predicted COP obtained from the model with the actual, or indicated, COP under the same operating conditions. The procedure will also require an uncertainty analysis on the instruments yielding the measurements to estimate the overall uncertainty in indicated COP and other measured quantities. The deviations between measured and predicted performance can then be determined and it can be ascertained whether these variations are smaller than the expected experimental uncertainty, which would then suggest acceptable accuracy in the experimental outcomes.

3.2.3 Fault Simulation

Once it is decided that the model predicts performance with acceptable accuracy under normal conditions, supplementary tests can be performed to try and illustrate its diagnostic capability. This will require simulating real, faulty conditions and monitoring how the COP changes.

A faulty condition often encountered in field installations is that of heat exchanger fouling, which has been introduced above. Prolonged use of the machine results in deposits building up on the water sides of the heat exchanger surfaces that ultimately act to impede the heat transfer. The version of the Universal Thermodynamic Model that will be employed allows for the effects of fouling when they become noticeable, as mentioned in section 3.1.

For example, fouling in a machine's condenser adds to the resistance to heat transfer between the hot and cold fluids since it introduces another resistive layer for the heat to pass through and thus reduces the COP. The machine, in turn, will try to compensate for this increased resistance and maintain a fairly consistent cooling effect by increasing the condensing pressure and temperature of the refrigerant. However, raising the pressure and temperature of condensation means that the compressor must do more work and draw more electrical power to cope with the increased load.

One way of simulating the effects of fouling is to restrict the flow of water through the heat exchangers so that heat transfer is impaired. As for the case of actual fouling, the machine will try to maintain the heat transfer rate by increasing the log mean temperature difference to compensate for the greater resistance to heat transfer due to this lower flow. It achieves this by increasing the condensing temperature and hence pressure, thus forcing the compressor to do more work.

Many installations facilitate the variation of water flow rate by an adjustable valve that acts as a water shut-off point if maintenance operations are required on the heat exchanger and also to assist with water-balancing through the component. A number of measurements can then be taken at a number of different water flow rates to

determine how the COP changes accordingly. This number of different water flow rates must be sufficiently large to comprehensively illustrate the predictive power of the universal model, but must not be so large as to be impractical.

3.2.4 Practical Constraints

However, before the above tests can be performed there are a number of practical aspects of the experimental procedure that need to be addressed. These are chiefly preliminary considerations that depend on the installation and are listed below.

- The degree to which the machine's operating regime can be adjusted. This depends on how severely alterations to the machine's operating regime affect the building that it serves and might also depend on the time of day selected to perform tests. More drastic variations will probably be allowed when there are very few occupants inside the building than when it is full.

- How long the machine takes to reach steady state after its operating regime has been adjusted. Maintenance personnel should be able to give an approximate estimate for this time. The time frame will depend on the attributes of the installation itself, in particular the length of water piping throughout the system, which will directly affect the volume of chilled water in the building.

- The impact that variant thermal load of the building and varying external ambient conditions will have on the readings obtained. Ideally, both should be as constant as possible to achieve optimal testing conditions. This will also depend on the time of day selected for the tests.

The considerations discussed above are merely guidelines that aim to assist the testing process by identifying constraints that will typically be encountered. Upon inspection and analysis of the selected test site a more detailed experimental procedure can be drawn up that outlines precisely what is to be performed in a step-wise manner.

3.3 Review of Chapter

The Universal Thermodynamic Model has been introduced with emphasis placed on the linear relationship between the reciprocals of COP and cooling rate within the manufacturers' intended operating ranges of vapour-compression refrigeration machines, and on the effect that internal and external irreversibilities have on operating performance. Within the manufacturers' intended operating ranges, internal irreversibilities dominate, while the external irreversibilities of heat transfer across finite temperature differences start to dominate as cooling rates increase towards the manufacturers' design maximum. This places a maximum on attainable COP.

Both the temperature-independent and temperature-dependent versions of the model indicate that the performance of any mechanical chiller can be characterized by its internal irreversibilities, which, in turn, can be characterized by 'lumped' parameters, or constants. These constants can be determined via accurate measurement of outlet chilled water temperature T_{Eo}, inlet condenser water temperature T_{Ci}, water chilling load Q_E and COP over the chiller's operating range. For any operating regime within this range, the appropriate version of the model can be used to predict the chiller's corresponding normal performance, which enables its actual performance to be meaningfully assessed.

Certain irreversibilities, notably external ones due to water-side fouling in heat exchangers, become more prominent over time if the chiller is left to operate without appropriate maintenance being carried out on it. The model enables limited fault diagnosis in such cases through interpreting changes in its 'lumped' parameters from their normal values.

Finally, methods to obtain the key quantities recorded by the model, to validate the accuracy of the measured quantities and to simulate the fault of excessive water-side fouling are given as bases of the experimental procedure described in Chapter 5 for the chillers described in Chapter 4.

4. EXPERIMENTAL FACILITY

4.1 Site Description

The Investec building in Sandton, Johannesburg, utilizes eight dedicated, water-cooled refrigeration machines in their HVAC (Heating, Ventilation and Air-Conditioning) system. The chillers are all housed in the building's basement so that they do not interfere with operations at ground level and so that the machines are accessible to maintenance personnel and engineers. Of the eight chillers, seven employ reciprocating compressors whereas one uses a centrifugal compressor. The reciprocating chillers are similar York units and all employ two identical compressors in parallel. The centrifugal machine is manufactured by Carrier and uses a single compression stage.

The entire HVAC system, including its measurement and display devices, was installed and is maintained by the contracted company, Enviroware Construction. The site information that follows has been obtained from them.

With respect to the points raised in the practical constraints of section 3.2.4, a high degree of freedom is available for testing since the other seven chillers will compensate for any induced changes in operating regime on one machine via the Building Management System, or BMS. This system is made up of a series of sensors and actuators that monitor the cooling or heating requirements of the building and control the air-conditioning system accordingly. Thus, manually reducing the cooling capacity of one of the devices will cause the other seven to slightly increase their capacities so that the building's internal environment is maintained. Of course, this is only achievable if maximum cooling is not being called for and there is some available capacity in the refrigeration system.

However, if a machine is adjusted so that the required pressure difference across the compressor to achieve the desired cooling gets too large an automatic safety mechanism is activated and the whole machine shuts down. This precautionary measure ensures that the compressor is not made to operate beyond its capacity since it may have permanently damaging effects. If, for example, the condenser inlet water reaches a very high temperature thus limiting the amount of heat rejection from the refrigerant, the machine may be in danger of tripping out since the increased water temperature ultimately means a corresponding increase in condensing pressure, and hence pressure rise that the compressor must achieve in order to meet the cooling demand.

Cooling towers on the roof of the building house the heat-rejecting, or coolant, water that is cooled down before being re-circulated back to the condensers. Four cooling fans that can be operated automatically or manually regulate the temperature of the water in the towers by controlling the amount of induced air flow over the water. The fans draw atmospheric air through the cooling towers so changes in the ambient wet-bulb temperature will affect the temperature of the water entering the condenser.

The decision whether to test the centrifugal or a reciprocating machine largely depended on the ease with which the experiments could be conducted. Factors that could facilitate easy testing include the time taken for the device to reach steady state after changes are induced, the ease of obtaining readings and their accuracy and the presence of adequate measuring points on the machine if external instruments have to be employed.

However, due to favourable time constraints and the willingness of the maintenance personnel at Investec, tests were performed on both types of machine. Verification of the Universal Thermodynamic Model on two different devices obviously proved more valuable than validation on only one.

4.2 Centrifugal Chiller

4.2.1 Centrifugal Chiller Specification

The centrifugal Carrier chiller was selected for the first set of tests. It was noted that the centrifugal machine facilitates easier recording of some key parameters. Values for the heat exchanger inlet and outlet temperatures and pressures, and for the voltage, current and power factor of the machine are displayed on a digital readout called the Chiller Visual Control (CVC). The York machines also have CVC units, but theirs do not display as comprehensive a set of data, as pointed out in section 4.3 below. The installation of the Carrier machine also provides a number of possible points where coolant water temperatures can be measured by external instruments if the fitted instruments and CVC readings are deemed unsatisfactory. The specifications of the chiller have been taken from the Carrier Installation Manual [23] and are summarised in Table 4.1 below.

Table 4.1: Carrier Chiller Specifications, (Carrier Installation Manual [23])

Description	Hermetic Centrifugal Liquid Chiller
Type of Compressor	Centrifugal
Number of Compression Stages	One
Refrigerant	R134a
Nominal Refrigeration Capacity	1230-2813kW
Control System	Direct digital product integrated controls (PIC)
Other Features	Digital read-out of control variables

The refrigeration capacity is not specified exactly in the table since the machine was custom built for the Investec installation. Carrier sometimes manufactures machines according to client specification, with different types of chillers made to operate at different ranges of refrigeration capacity. The family of Hermetic Centrifugal Liquid Chillers caters for loads of between 1230 and 2813kW. No specific information could be obtained about the exact capacity of the machine and so its nominal range is given.

The serial number of the chiller used for testing is 19XR-3132363CMS62, from which information about the machine's constituent components can be obtained according to Carrier's coding standards. A brief overview of the main components is given below.

The evaporator, or cooler, is situated directly underneath the compressor and is designed as a two-pass shell-and-tube heat exchanger with the chilled water running through the tubes. It is made to handle 190kg of refrigerant in its shell and 241ℓ of water in its 240 tubes at any one time. The condenser can hold 118kg of refrigerant and 282ℓ of coolant water in its 316 tubes and is also a two-pass shell-and-tube heat exchanger with the condenser water in the tubes and the refrigerant in the shell. Table 4.2 below is adapted from the Carrier Installation Manual [23] and summarises the key heat exchanger data.

Table 4.2: Carrier Heat Exchanger Data, (Carrier Installation Manual [23])

Description	Units	Evaporator	Condenser
Refrigerant	NA	R134a	R134a
Chilled Medium	NA	Water/Brine	Water/Brine
Number of Passes	NA	2	2
Tubes per Pass	NA	120	158
Total Number of Tubes	NA	240	316
Tube Material	NA	CuNi	CuNi
Refrigerant Charge	Kg	190	118
Water Volume	ℓ	242	282
Dry Rigging Weight	Kg	1959	1860

The centrifugal compressor employs one compression stage but includes electronically actuated, variable inlet guide vanes that provide high operating efficiencies through a wide operating range. Table 4.3 below gives the key compressor data adapted from the Carrier Installation Manual [23].

Table 4.3: Carrier Compressor Data, (Carrier Installation Manual [23])

Description	Units	Compressor
Type	NA	Centrifugal
Refrigerant	NA	R134a
Number of Stages	NA	1
Power Supply	V/-/Hz	380/3/50
Design Pressure	kPa	1276
Maximum Pressure	kPa	1600
Total Weight	Kg	1207

4.2.2 Centrifugal Chiller Set-Up

Apart from the main components described above, the Carrier Centrifugal Chiller also comprises many other parts. Figure 4.1 below, taken from the Carrier Installation Manual [23], gives a schematic of the machine and all its components and Table 4.4 identifies the parts labelled on the figure.

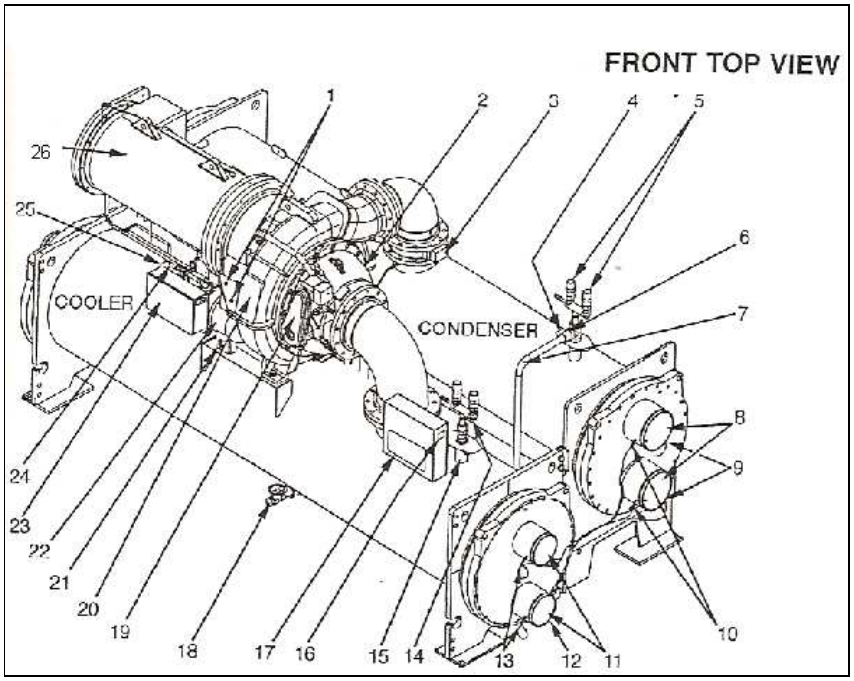

Figure 4.1: Carrier Centrifugal Machine Set-Up, (Carrier Installation Manual [23])

Table 4.4: Centrifugal Chiller Components, (Carrier Installation Manual [23])

Number	Component
1	Oil Level Sight Glass
2	Diffuser Actuator
3	Discharge Isolation Valve
4	Condenser Pumpout Connection
5	Condenser Safety Relief Valves
6	Three-Way Condenser Relief Valve
7	Hot Gas Bypass Line
8	Condenser Waterbox Nozzles
9	Condenser In/Out Temperature Thermistors
10	Condenser Waterflow Device
11	Cooler Waterbox Nozzles
12	Cooler In/Out Temperature Thermistors
13	Cooler Waterflow Device
14	Cooler Safety Relief Valves
15	Cooler Pumpout Connection
16	Chiller Identification Nameplate
17	Chiller Visual Control
18	Refrigerant Charging Valve
19	Guide Vane Actuator
20	Compressor/Transmission
21	Oil Drain/Charging Valve
22	Oil Pump
23	Auxiliary Power Panel
24	Oil Filter Isolation Valve
25	Oil Filter
26	Motor

Key operating data are displayed on the *Chiller Visual Control* (CVC), labelled as component 17 in Figure 4.1. The main data displayed are the inlet and outlet water temperatures at the heat exchangers, an indication of whether the machine is approaching its trip-out point and power information such as voltage, current and power factor for the entire installation. However, the water temperatures at the heat exchanger inlets and outlets are only displayed on the CVC with a resolution of 0.1˚C, which is too imprecise for the purposes of this investigation. Thus, a digital thermometer with a resolution of 0.01˚C was instead used for the water temperature readings.

It is important to note that the voltage, current and power factor values displayed on the CVC take into account the power drawn by the whole chiller and not just by the compressor motor. The power drawn by the oil pump, labelled component 22, and that drawn by the compressor must both be considered when assessing the performance of the machine to obtain an accurate COP reading. If the CVC displayed only the power drawn by the compressor then the oil pump would have to be monitored separately. Instead, only the displayed values need to be recorded since they show all power inputs to the entire chiller.

4.2.3 Centrifugal Chiller Measurement Points

Although the inlet and outlet water temperatures at the heat exchangers can be read off a digital thermometer placed at the respective pipes, as mentioned in 4.2.2 above, and all the necessary power readings can be obtained directly from the Chiller Visual Control, several other measurements also need to be taken from the installation.

The water pressures at the condenser and evaporator inlets and outlets are displayed on pressure gauges that are inserted into pockets at the respective inlet and outlet pipes. Directional arrows on the pipes allow for easy differentiation between inlet and outlet. Isolating valves at the ends of the pockets enable users to insert or remove gauges while the water system is running and under pressure. In figure 4.1, the components labelled as number 8 show where the condenser inlet and outlet pressure gauges are connected and the components labelled number 11 show where the evaporator inlet and outlet gauges are connected.

The mass flow rates of water through the condenser and evaporator can be obtained by using an ultra-sonic flow meter. This device determines flow in a non-intrusive way by mounting two sensors on the outside of the pipe and sending an electronic signal from one to the other. The time taken for the signal to travel between sensors is used in the computation of the flow-rate since the density of the medium through which the signal travels affects the path and time that it takes. Appendix E shows how the mass flow rates through the heat exchangers was obtained through the ultra-sonic meter in more detail.

Additional, confirming measurements are also required to verify the pressure and power supply readings that are read off the CVC. These were taken from independent measurement instruments, whose accuracy must be proven in order for their readings to be used with confidence.

A glycerine-filled differential pressure gauge that reduces the oscillation on the indicator needle was used to verify the displayed pressure values. The overall voltages, currents and power factors for the chiller could be confirmed and corrected using a digital multimeter at the chiller's power box. Current was measured by clamping the multimeter around one of the live wires feeding the chiller, while the voltage was recorded by placing the multimeter probes across any two of the live phase wires. The multimeter had a built-in function that measures and displays the power factor for a three-phase supply when the clamp and probes are in place.

4.2.4 Centrifugal Chiller Measuring Equipment

Table 4.5 below summarises the key information on the measuring equipment that was used for tests on the centrifugal chiller.

Table 4.5: Measuring Equipment for Centrifugal Chiller

Measurement Category	Device	Manufacturer	Resolution	Uncertainty
Water Mass Flow Rate	Ultra-Sonic Flow meter	Fujitsu Electronics	1kg/s	0.5kg/s
Evaporator Inlet/Outlet Water Temperature	Digital Thermometer	Hellerman Tyton	0.01˚C	0.01˚C
Condenser Inlet/Outlet Water Temperature	Digital Thermometer	Hellerman Tyton	0.01˚C	0.01˚C
Overall Voltage	Chiller Visual Control	Carrier	1V	0.5V
Overall Current	Chiller Visual Control	Carrier	1A	0.5A
Overall Power Factor	Chiller Visual Control	Carrier	0.01	0.005
Evaporator Inlet/Outlet Water Pressure	Chiller Visual Control	Carrier	1kPa	0.5kPa
Condenser Inlet/Outlet Water Pressure	Chiller Visual Control	Carrier	1kPa	0.5kPa
Calibrated Overall Voltage	Digital Multimeter	Brymen (Toptronic)	1V	0.5V
Calibrated Overall Current	Digital Multimeter	Brymen (Toptronic)	1A	0.5A
Calibrated Overall Power Factor	Digital Multimeter	Brymen (Toptronic)	0.1	0.05
Calibrated Evaporator Pressure Difference	Analogue Differential Pressure Gauge	Honeywell	1kPa	0.5kPa
Calibrated Condenser Pressure Difference	Analogue Differential Pressure Gauge	Honeywell	1kPa	0.5kPa

Note: The resolution and uncertainty for the water mass flow rate were determined by fluctuations in the displayed values and not on the characteristics of the flow meter

4.3 Reciprocating Chiller

4.3.1 Reciprocating Chiller Specification

It was decided to perform additional tests on one of the York reciprocating chillers. As mentioned above, one of the drawbacks of these machines is the lack of data available from the Chiller Visual Control. The CVC units on the York chillers are mainly used to program the operation of the machine and so almost all the experimental measurements need to be taken using external instrumentation. Nevertheless, tests were still performed to verify the Universal Thermodynamic Model for this different type of refrigeration machine.

The chiller itself is a York semi-hermetic, water-cooled machine that employs two identical reciprocating compressors with identical refrigerant circuits. The York Installation and Operation Manual [24] quotes the key technical data for the chiller and these are presented in Table 4.6 below.

Table 4.6: York Chiller Specifications, (York Installation and Operation Manual [24])

Description	York Semi-Hermetic Reciprocating Liquid Chiller
Type of Compressor	Reciprocating
Number of Compressors	Two
Refrigerant	R 22
Refrigeration Capacity	760kW
Control System	York Micro-Computer Control Centre
Additional Features	Digital Readout of Certain Control Variables

The direct expansion evaporator of the reciprocating chiller has twin refrigerant circuits. It is constructed with a steel shell and copper tubes with inner fins, rolled into steel tube sheets. The condenser also has twin refrigerant circuits with a steel shell and copper tubes rolled into steel tube sheets. Water passes through the tubes and refrigerant through the shell. The technical details and design specification of the heat exchangers are quoted in the York Installation and Operation Manual [24] and are given in Table 4.7.

Table 4.7: York Heat Exchanger Data, (York Installation and Operation Manual [24])

Description	Units	Evaporator	Condenser
Refrigerant	NA	R134a	R134a
Chilled Medium	NA	Water	Water
Number of Tubes	NA	576	340
Tubes Per Pass	NA	2	2
Entering Water Temperature	˚C	12.3	29
Leaving Water Temperature	˚C	5.5	35
Cooling Capacity	kW	760	NA
Heat Rejection Capacity	kW	NA	947.5
Water Pressure Drop	kPa	35	22
Tube Material	NA	Cu	Cu
Water Volume	ℓ	145	234
Water Flow Rate	ℓ/s	26.7	37.7

Both of the compressors in the York chiller are identical reciprocating devices. Table 4.8 contains their key technical data and is adapted from the York Installation and Operation Manual [24].

Table 4.8: York Compressor Data, (York Installation and Operation Manual [24])

Description	Units	Compressor (Each)
Type	NA	Reciprocating
Refrigerant	NA	R 22
Number of Stages	NA	1
Power Supply	V/NA/Hz	380/3/50
Design Motor Power	kW	93.7
Maximum Motor Power	kW	104
Design Amperage	Amps	166
Full Load Amperage	Amps	200

4.3.2 Reciprocating Chiller Set-Up

The way in which the York reciprocating chiller is constructed and assembled is shown in the orthogonal projections of Figure 4.2 below, which have been taken from the York Installation and Operation Manual [24]. Understanding where each component is situated and how they interact with one another is imperative when determining where the appropriate measurement points are. Table 4.9 identifies the parts labelled numerically in the figure.

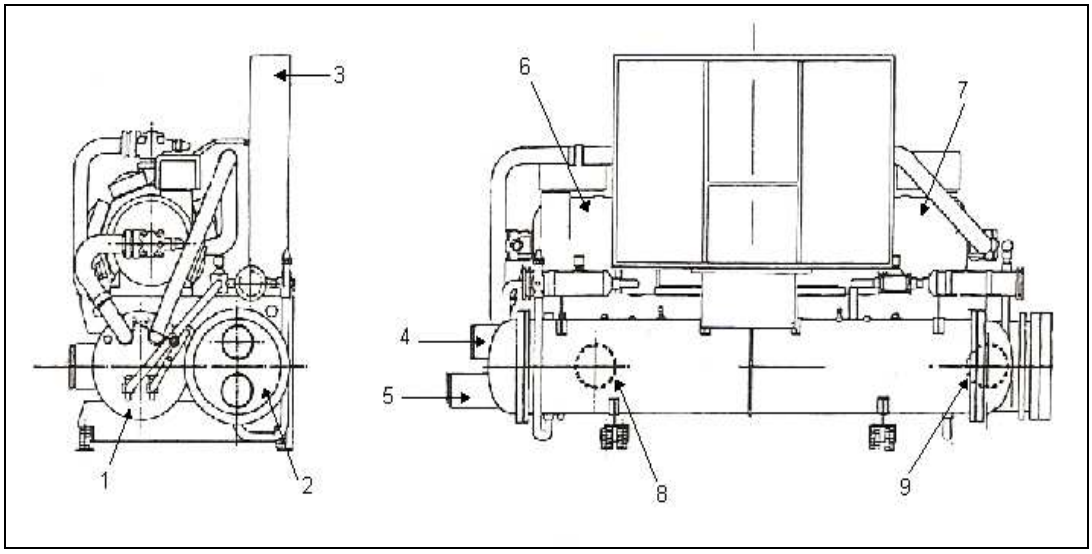

Figure 4.2: York Reciprocating Machine Setup, (York Installation and Operation Manual [24])

Table 4.9: Reciprocating Chiller Components, (York Installation and Operation Manual [24])

Number	Component
1	Evaporator
2	Condenser
3	Chiller Visual Control
4	Condenser Water Outlet
5	Condenser Water Inlet
6	Compressor 1
7	Compressor 2
8	Evaporator Water Inlet
9	Evaporator Water Outlet

As mentioned above, the Chiller Visual Control, labelled number 3 in Figure 4.2, cannot be used to record experimental values since it does not display all of the necessary values. Inspection of its display panel reveals that it is mainly for control purposes so that operators can program the chiller to run under specified conditions for a set period of time. Instead, measurements must be recorded from site-fitted instruments, as discussed below.

4.3.3 Reciprocating Chiller Measurement Points

The condenser water inlet and outlet temperatures can be recorded from digital thermometers placed inside thermal pockets at the condenser inlet and outlet pipes, respectively. The inlet water pipe connects to the chiller at the point labelled number 5 in Figure 4.2, while the outlet pipe connects to the point labelled number 4. Correspondingly, the evaporator water inlet and outlet temperatures can be recorded using thermometers placed inside thermal pockets at its inlet and outlet pipes. The evaporator inlet pipe connects to the point labelled number 8 in the figure and its outlet pipe connects to the point labelled number 9.

The inlet and outlet water pressures at the evaporator and condenser are obtainable from pressure gauges inserted into pockets at the corresponding water pipe. The pockets for the pressure gauges are all situated slightly above the corresponding thermal pocket, where the thermometers are positioned. Valves at the ends of the pressure pockets enable the water flow through them to be shut off or turned back on, depending on whether a gauge needs to be fitted or removed.

The overall voltages, currents and power factors for the reciprocating machine were directly recorded from a multimeter connected to the power supply cables as was done when calibrating the centrifugal chiller's power supply readings, which is described in Section 4.2.3.

The mass flow rates of water through the heat exchangers can be obtained in the same way as for the centrifugal machine using an ultra-sonic flow meter fitted to the outside of the appropriate pipe.

4.3.4 Reciprocating Chiller Measuring Equipment

The technical specifications of the measuring equipment used for the tests on the reciprocating chiller are summarised in Table 4.10 below.

Table 4.10: Measuring Equipment for Reciprocating Chiller

Measurement Category	Device	Manufacturer	Resolution	Uncertainty
Water Mass Flow Rate	Ultra-Sonic Flow Meter	Fujitsu Electronics	1kg/s	0.5 kg/s
Evaporator Inlet/Outlet Water Temperature	Digital Thermometer	Hellerman Tyton	0.01˚C	0.01˚C
Condenser Inlet/Outlet Water Temperature	Digital Thermometer	Hellerman Tyton	0.01˚C	0.01˚C
Overall Voltage	Digital Multimeter	Brymen (Toptronic)	1V	0.5V
Overall Current	Digital Multimeter	Brymen (Toptronic)	1A	0.5A
Overall Power Factor	Digital Multimeter	Brymen (Toptronic)	0.01	0.005
Evaporator Inlet/Outlet Water Pressure	Analogue Pressure Gauge	SpecValve	1kPa	0.5kPa
Condenser Inlet/Outlet Water Pressure	Analogue Pressure Gauge	SpecValve	1kPa	0.5kPa
Evaporator Suction/Discharge Pressure	Analogue Pressure Gauge	SpecValve	1kPa	0.5kPa
Condenser Suction/Discharge Pressure	Analogue Pressure Gauge	SpecValve	1kPa	0.5kPa

Note: The resolution and uncertainty for the water mass flow rate were determined by fluctuations in the displayed values and not on the characteristics of the flow meter

5. EXPERIMENTATION

5.1 Centrifugal Chiller

5.1.1 Experimental Procedure

The approach adopted in verifying the Universal Thermodynamic Model for the Carrier centrifugal chiller at the Investec building was similar to that followed by Gordon and Ng [1] and by Thomas [11]. Measurements were recorded for a range of different condenser water inlet temperatures.

One way of obtaining different condenser water inlet temperatures is to wait for the ambient air wet-bulb temperature to change from low values in the very early hours of the morning to higher values during the afternoon. Since the cooling towers that feed the condenser are situated on the roof of the building, these changes in environmental temperature cause corresponding variations in the condenser water inlet temperature. This non-intrusive approach in obtaining different inlet water temperatures also allows sufficient time for the chiller and the associated measuring devices to adjust to the changes and achieve a steady operating state so that experimental readings will be less prone to highly variable and potentially erroneous fluctuations.

A fluctuating cooling demand dictated by the building occupants does introduce an unpredictable element to the experiment that cannot be controlled. As Air-Handling Units and Fan Coil Units call for more chilled water to maintain specified room temperatures the water flow through the chillers will necessarily increase. However, it can be assumed that the effect of a varying cooling load will have a minimal impact on the experiment for three main reasons.

Firstly, it was pointed out in Section 4.1 that the building is served by eight chillers and any change in cooling load will be shared between them, making the relative impact on each chillers water flow eight times smaller. Secondly, the tests were carried out in the first week of January when the building was not fully occupied and

company operations were not at full capacity. The variation in cooling demand of the fairly empty building can be considered very small especially since most meeting rooms, which are usually cooled by Fan Coil Units that are only turned on when a meeting is in progress, were probably not used at all. Thirdly, the Investec building, like many large office buildings, uses an open-plan layout for the majority of its employees and so a large space, with many people, is under the same environmental conditions, which makes for fewer thermostat adjustments and less variation in cooling demand.

The procedure adopted in calibrating and recording the values for the centrifugal machine was as follows. Tests on the centrifugal machine were conducted between 4 and 5 January 2010, immediately following the year-end holidays, while the building was not fully occupied.

1. The values displayed on the machine's digital readout and on the pressure gauges were first verified. The pressure values were confirmed using a calibrated pressure gauge placed at the heat exchanger's inlet and outlet that measures the system pressure relative to the atmosphere. The power measurements from the display were verified with a digital multimeter connected to the chiller's power supply cables. The details of the subsequent calibration and the instruments used are given in section 4.2 and in Appendix C. A conformance certificate was obtained for the digital multimeter but one could not be found for the pressure gauge.

2. The first set of data was obtained at approximately 8 o' clock on the morning of 4 January 2010. Experimental values were recorded for the first fixed condenser water inlet temperature from the machine's Chiller Visual Control and from the pressure gauges and digital thermometers placed at the inlet and outlet water pipes of the heat exchangers. The condenser and evaporator inlet and outlet water temperatures, pressures and flow-rates, the voltage across the machine's power supply cables, the current drawn by the machine and the overall power factor for the installation were all measured.

3. The procedure outlined in the point above was repeated once the condenser water inlet temperature had increased significantly. A significant increase in this temperature was taken to be at least 0.5˚C and it took between 30 and 90 minutes for such a change to occur, depending on the time of day. For the new condenser water inlet temperature seven sets of data were recorded. Each set took about 1-2 minutes to record.

4. The whole process outlined in the point above was repeated a further three times so that five different condenser water inlet temperatures were tested for in total. Between seven and nine sets of data were recorded at each condenser water inlet temperature depending on how rapidly the temperature changed.

5. The following day, on 5 January 2010, identical tests as described above were conducted on the same machine but with the throttling valve on the condenser water inlet pipe tightened to approximately two-thirds of its maximum capacity to simulate the effects of condenser fouling. Thereafter, the same procedure defined in points 2 to 4 was repeated to collect operating data for performance under fouled conditions. Data for four different condenser water inlet temperatures were recorded under throttled conditions and between six and seven sets of data were recorded for each condenser water inlet temperature.

5.1.2 Precautions

Several experimental precautions also needed to be followed to ensure that the recorded measurements would accurately depict the way in which the machine adjusted to the imposed loads, and to be certain that the loads did not damage the device itself in any way. The precautions observed were as follows:

1. The instruments used to verify the digital read-out were confirmed to be highly accurate before they were used. Only reliably accurate instruments were used and copies of certification (except for the differential pressure gauges) are included in Appendix C.

2. For each data set, values for the different quantities were recorded as quickly as possible to try and ensure that they didn't change significantly before they were taken down. Fortunately, almost all of the data could be obtained from only two different display screens on the Chiller Visual Control and from the digital thermometers, which facilitated quick recording.

3. The machine was operating at a steady state before both the throttled and un-throttled tests were performed on it by allowing it to run non-intrusively for over an hour. The derivation of the Universal Thermodynamic Model is based on a steadily operating machine and transient effects would impact the readings in a way not predicted by the model.

4. The other cooling machines used in the installation also needed to be maintained at a steady state. Any significant deviations in their operating conditions would have impacted the device under analysis and cause the results to deviate in an unexpected way.

5. Careful attention was paid to the machine's specified operating limits when the artificial throttling load was imposed to avoid the machine tripping out. If the condenser water inlet temperature is high enough the machine will trip out due to the increased load on the centrifugal compressor as it tries to adjust to the higher condensing temperature.

5.1.3 Data Processing

The experimental data obtained was then processed so that it could be used with the Universal Thermodynamic Model to obtain the desired outputs. Spreadsheets were set up so that required quantities could be calculated automatically via programmed mathematical formulae and experimental input values.

The first procedure was to adjust the experimental readings according to the calibration exercise discussed above. Values were adjusted according to correction

factors or calibration curves to ensure their accuracy. These corrected quantities were then converted into SI units and used as inputs to corresponding equations so that important parameters could be obtained. Appendix D shows the spreadsheets that were used to process the information recorded for the centrifugal machine.

In order to evaluate the heat transfers at the evaporator and condenser, the corresponding water specific volumes and specific heats were required at relevant temperatures. These two quantities were obtained via linear interpolation between thermodynamic property data tabulated by Moran and Shapiro [3], Table A-2 and Table A-19 pp. 721-722 and p. 754 respectively. The temperature used to fix the state of the water at either the evaporator or condenser was taken as the average between the respective inlet and outlet values.

It was mentioned in section 3.2 that, strictly speaking, water specific volume and specific heat should be obtained at the log mean temperature of either the evaporator or condenser, depending on which component is being analysed, but that the use of an average value might also prove to be feasible. Indeed, this latter hypothesis can be shown to be valid by inspection of how slightly the values of specific volume and specific heat of water change with temperature from the thermodynamic property tables in Moran and Shapiro [3] pp. 721-722 and p. 754. Between 0°C and 27°C the specific heat of water only changes by about 0.9% and the specific volume only changes by about 0.27%. Thus the inaccuracies that accrue from adopting this procedure can be assumed to be negligibly small.

5.1.4 Results

The procedure outlined above was followed and the data obtained was tabulated. Appendix D contains all of the data recorded and also includes the calibrated and SI values of the readings.

As was mentioned previously, the older version of the Universal Thermodynamic Model was used to predict the COP. This method entails constructing a number of graphs to determine the values of the lumped parameters that characterise the

particular machine. In the pages that follow, the respective graphs are shown and the ways in which they are derived are described.

The method adopted in constructing the graphs and thus obtaining the lumped parameters is similar to that adopted by Thomas [11] and Lee [18]. Data recorded and manipulated for when the condenser's throttling valve is left open is referred to as *normal operating data* since the machine operates without any imposed faults, while the data for when the valve is partially closed is termed *throttled*.

5.1.4.1 Results for Normal Operation

The following makes extensive reference to the temperature-dependent version of the Universal Thermodynamic Model and the lumped parameters it employs to characterise a particular machine. For convenience the model is reproduced in Equation [5.1] below.

$$\frac{1}{COP} = -1 + \frac{T_{Ci}}{T_{Eo}} + \frac{-C_0 + C_1 \cdot T_{Ci} - C_2 \cdot \frac{T_{Ci}}{T_{Eo}}}{Q_E} \qquad [5.1]$$

Values were recorded for five different condenser water inlet temperatures while the condenser's throttling valve was left fully open. According to Gordon and Ng [1], a plot of $\alpha = [1/COP + 1 - (T_{Ci}/T_{Eo})].Q_E$ versus T_{Ci}/T_{Eo} from the measured data should yield a set of parallel straight lines, one for each of the fixed condenser water inlet temperatures. The average gradient of these lines is then the negative value of the parameter C_2 in the Universal Thermodynamic Model. Figure 5.1 below shows the graphs of α versus T_{Ci}/T_{Eo} for each of the five temperatures tested for and an explanation of the linear relationship and gradient is given in Appendix A.

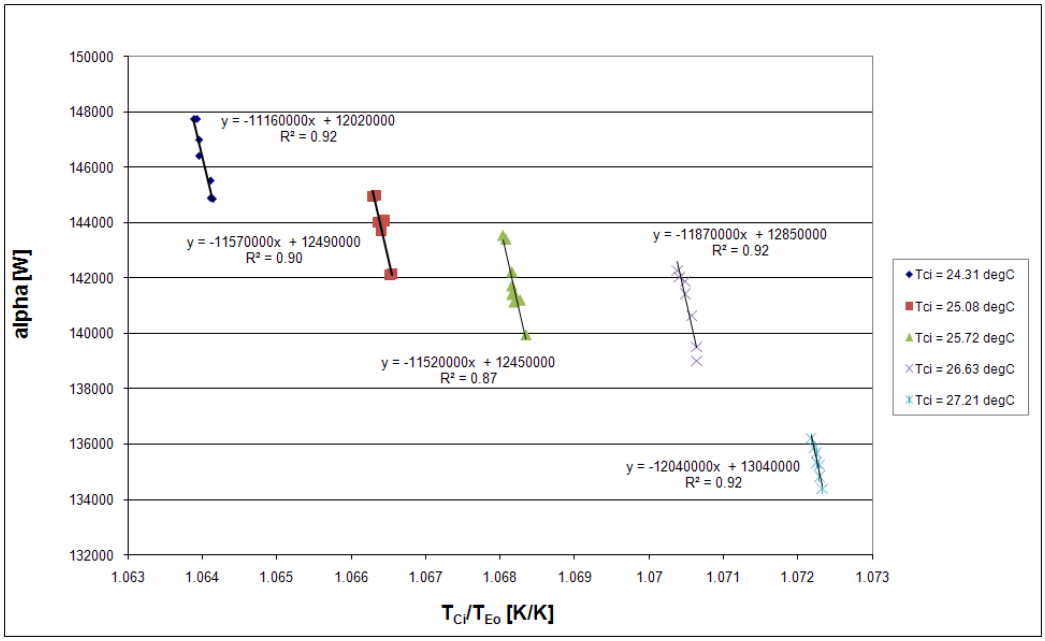

Figure 5.1: α Versus T_{Ci}/T_{Eo} under Normal Conditions for Centrifugal Chiller

Table 5.1 below summarises the relevant data from the figure above that are necessary to obtain an accurate value for the parameter C_2.

Table 5.1: Summary of Normal Centrifugal Data for Parameter C_2

Condenser Inlet Water Temperature	Gradient	C_2	R^2 Value
24.31	-1.116E+07	1.116E+07	0.92
25.08	-1.157E+07	1.157E+07	0.90
25.72	-1.152E+07	1.152E+07	0.87
26.63	-1.187E+07	1.187E+07	0.92
27.21	-1.204E+07	1.204E+07	0.92

From the above, the mean value for C_2 from the six graphs is -11630000 and the average R^2 value is approximately 0.91. The mean value for C_2 was then taken as the final value in the model and was used to find the other parameters and the predicted COP.

Next, the parameters C_0 and C_1 were found via a plot of $\beta = [\alpha + C_2(T_{Ci}/T_{Eo})]$ versus T_{Ci}, which should fall onto a straight line with gradient C_1 and an intercept with the ordinate of $-C_0$. Figure 5.2 below shows this graph and an explanation of this relationship is given in Appendix B.

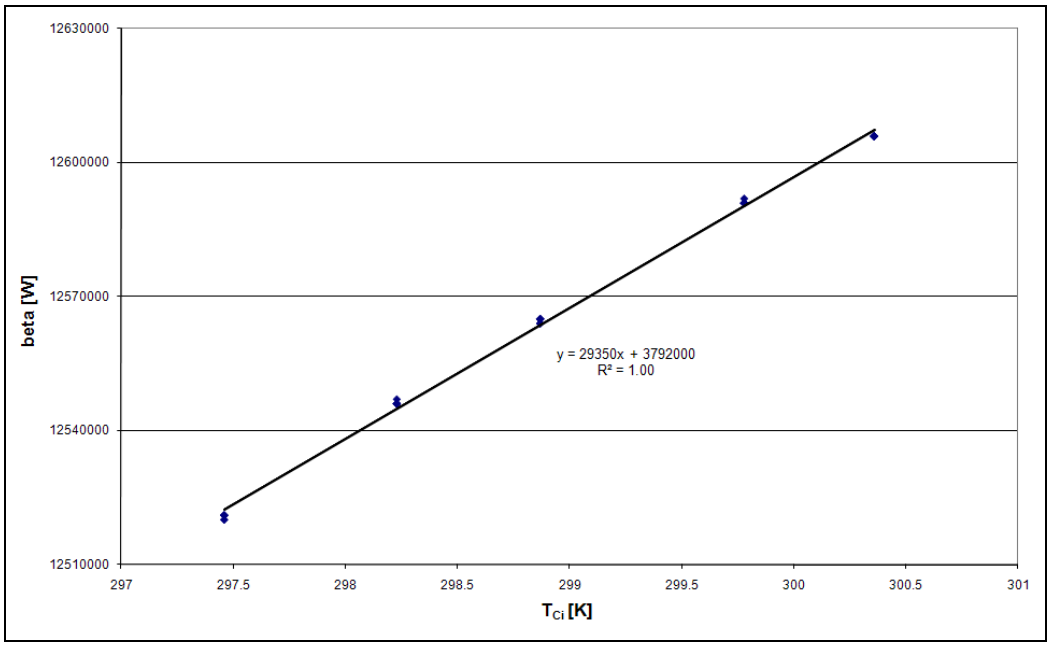

Figure 5.2: β Versus T_{Ci} under Normal Conditions for Centrifugal Chiller

Table 5.2 below summarises the data obtained from the above figure.

Table 5.2: Summary of Normal Centrifugal Data for Parameters C_1 and C_0

	Gradient	Intercept	R^2 Value
Fitted Curve	2.935E+04	3.792E+06	1.00
C_0	-	-3.792E+06	-
C_1	2.935E+04	-	-

The table reveals a value of 29350 for C_1 and a C_0 value of -3792000. The R^2 value for the straight line fitted to the data is 1.00. The values for C_1 and C_0, along with the value for C_2 obtained above were then substituted into the Universal Thermodynamic Model of Equation [5.1] to find predicted COP values for different operating conditions.

Figure 5.3 below shows the characteristic curve of 1/COP versus 1/ (Cooling Rate) predicted by the Universal Thermodynamic Model given in Equation [5.1] for the centrifugal machine operating under normal conditions.

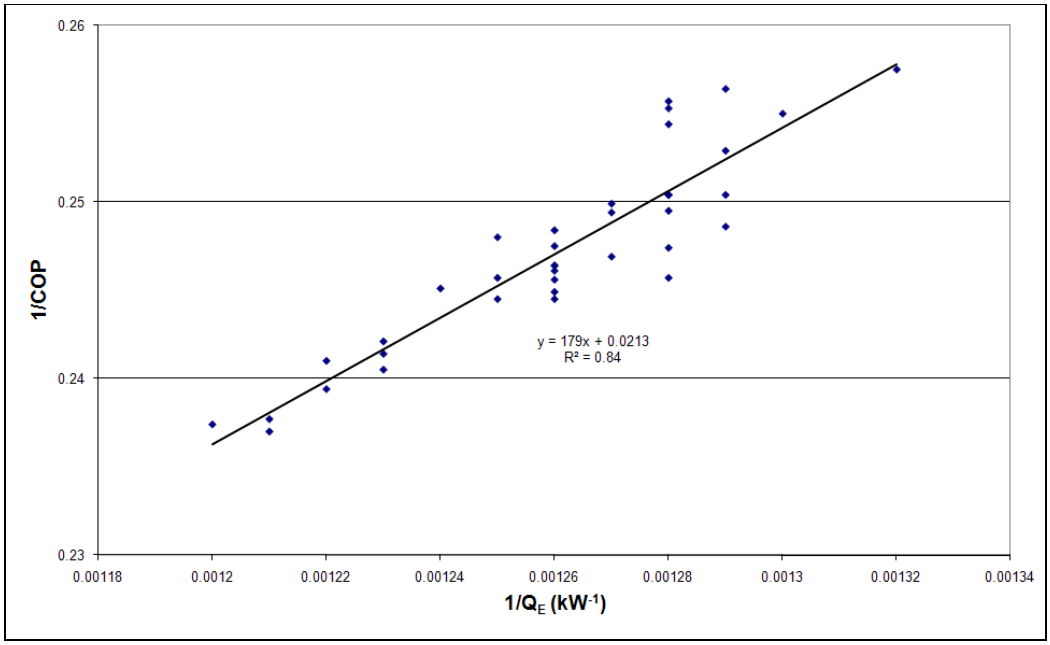

Figure 5.3: Characteristic Curve [1/COP vs. 1/ (Cooling Rate)] under Normal Conditions for Centrifugal Chiller

As was mentioned in section 3.2, the COP can also be obtained by measurement since it is defined as the ratio between the cooling effect achieved and the input power required by the machine. Employing this relation allows a comparison to be drawn between the measured COP and the values predicted by the Universal Thermodynamic Model. Figure 5.4 below shows this relationship graphically by plotting the two sets of data for the same quantity against each other. The ideal curve of y = x, or Measured COP = Predicted COP, is also overlaid on the graph to indicate where the experimental data points deviate.

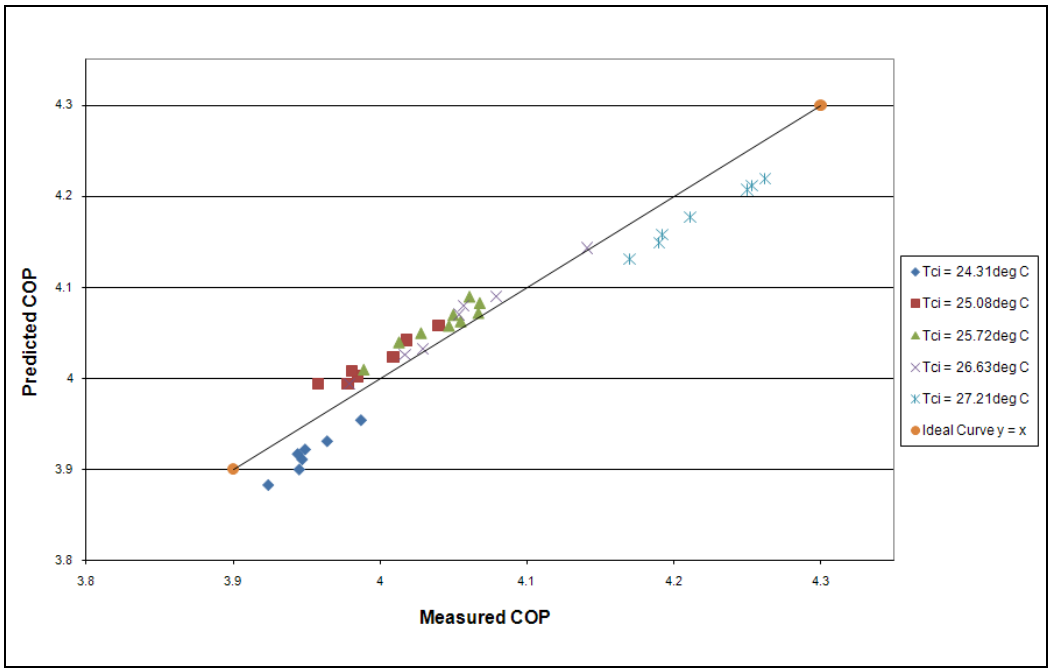

Figure 5.4: Predicted Versus Measured COP under Normal Conditions for Centrifugal Chiller

5.1.4.2 Results for Throttled Conditions

As for the tests conducted under normal operating conditions, the results that follow are in line with the Universal Thermodynamic Model given in Equation [5.1] above.

Readings at four different condenser inlet temperatures were taken for when the condenser's throttling valve was closed to approximately two-thirds of its maximum throttling capacity. Again, plots of $\alpha = [1/COP + 1 - (T_{Ci}/T_{Eo})].Q_E$ versus T_{Ci}/T_{Eo} were used to determine the value of C_2 in the same way as for normal operating conditions. The graph is shown in Figure 5.5 below.

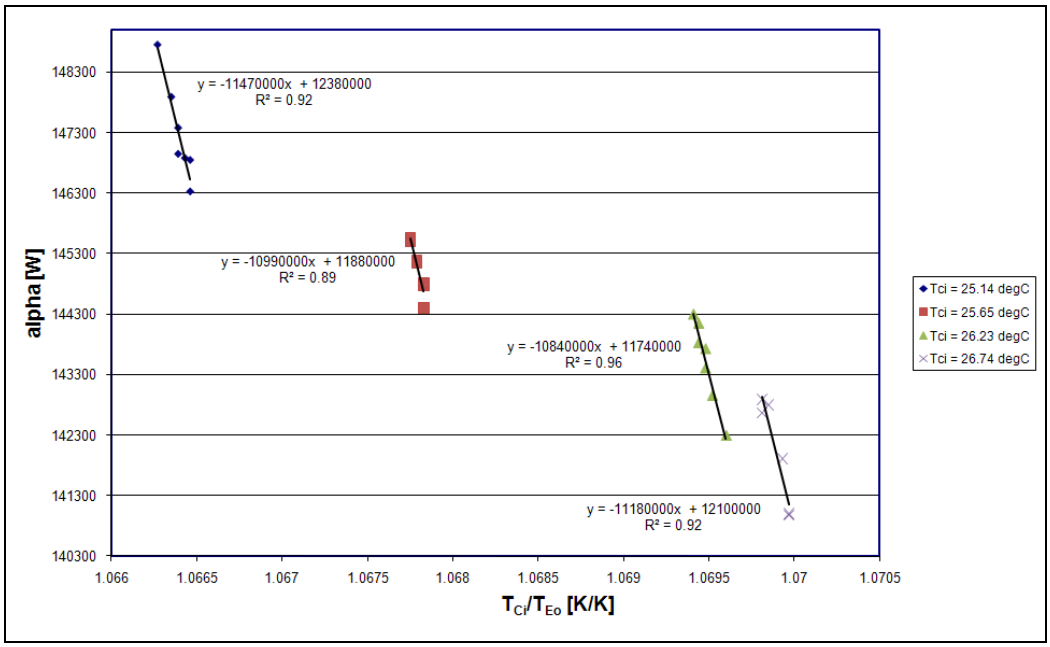

Figure 5.5: α Versus T_{Ci}/T_{Eo} under Throttled Conditions for Centrifugal Chiller

Table 5.3 below summarises the major information for the above four graphs to reveal the mean value of the parameter C_2 under throttled conditions. From the table it can be calculated that the mean value for C_2 is 11120000 and the mean R^2 value is approximately 0.92.

Table 5.3: Summary of Throttled Centrifugal Data for Parameter C_2

Temperature	Gradient	C_2	R^2 Value
25.14	-1.147E+07	1.147E+07	0.92
25.65	-1.099E+07	1.099E+07	0.89
26.23	-1.084E+07	1.084E+07	0.96
26.74	-1.118E+07	1.118E+07	0.92

Again, using this mean value for C_2 a graph of $\beta = [\alpha + C_2 (T_{Ci}/T_{Eo})]$ versus T_{Ci} reveals the values of the other two lumped parameters in the Universal Thermodynamic Model. Figure 5.6 below shows this plot.

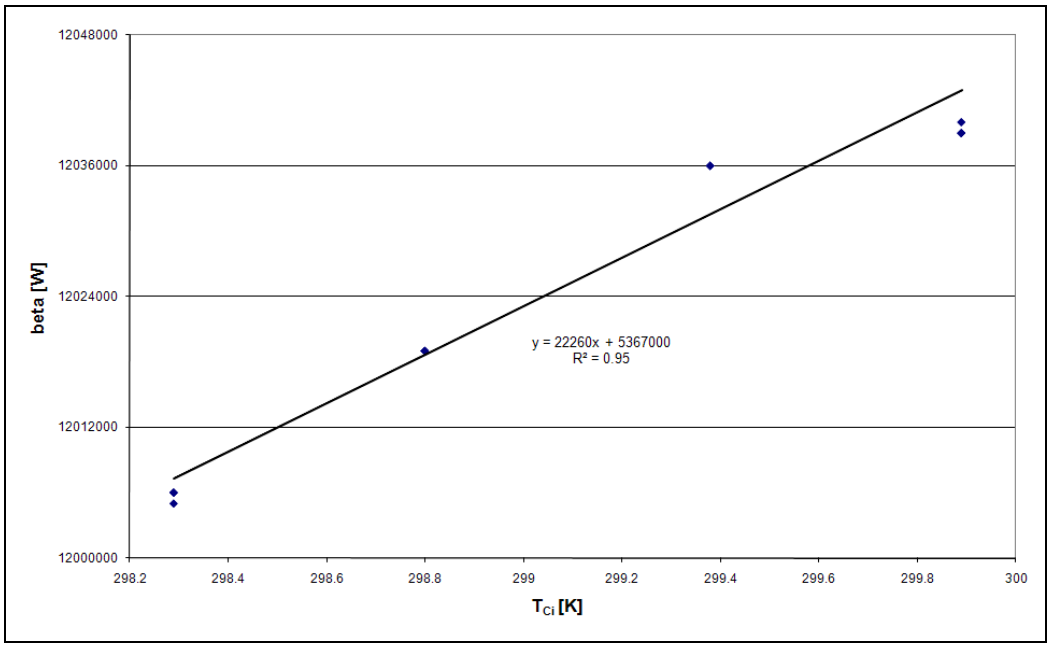

Figure 5.6: β Versus T_{Ci} under Throttled Conditions for Centrifugal Chiller

Table 5.4 summarises the relevant data from the above figure to give the values of the parameters C_0 and C_1 for when the condenser's throttling valve was tightened. The R^2 value of the fitted curve is also given as 0.95.

Table 5.4: Summary of Throttled Centrifugal Data for Parameters C_1 and C_0

	Gradient	Intercept	R^2 Value
Fitted Curve	2.26E+04	5.367E+06	0.95
C_0	-	-5.367E+06	-
C_1	2.26E+04	-	-

The above values for C_0 and C_1 were substituted into the model and COP values were then predicted from it. The characteristic curve for throttled conditions is given in Figure 5.7 below.

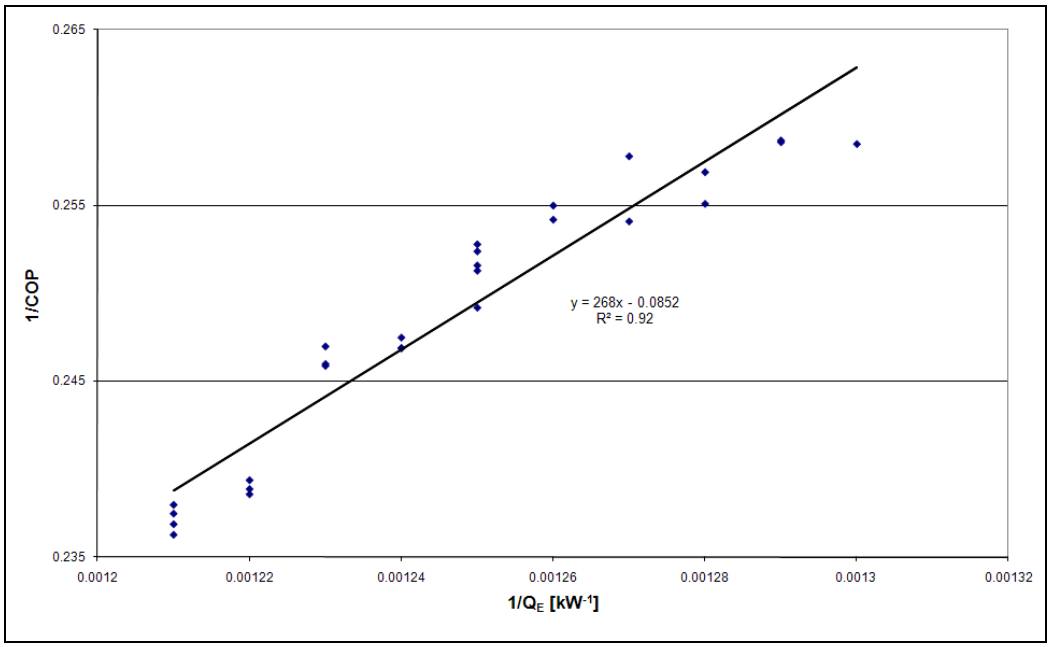

Figure 5.7: Characteristic Curve [1/COP vs. 1/ (Cooling Rate)] under Throttled Conditions for Centrifugal Chiller

Figure 5.8 below shows the comparative plot of measured versus predicted COP for when the condenser's throttling valve was tightened. The ideal curve of y = x is also shown on the graph.

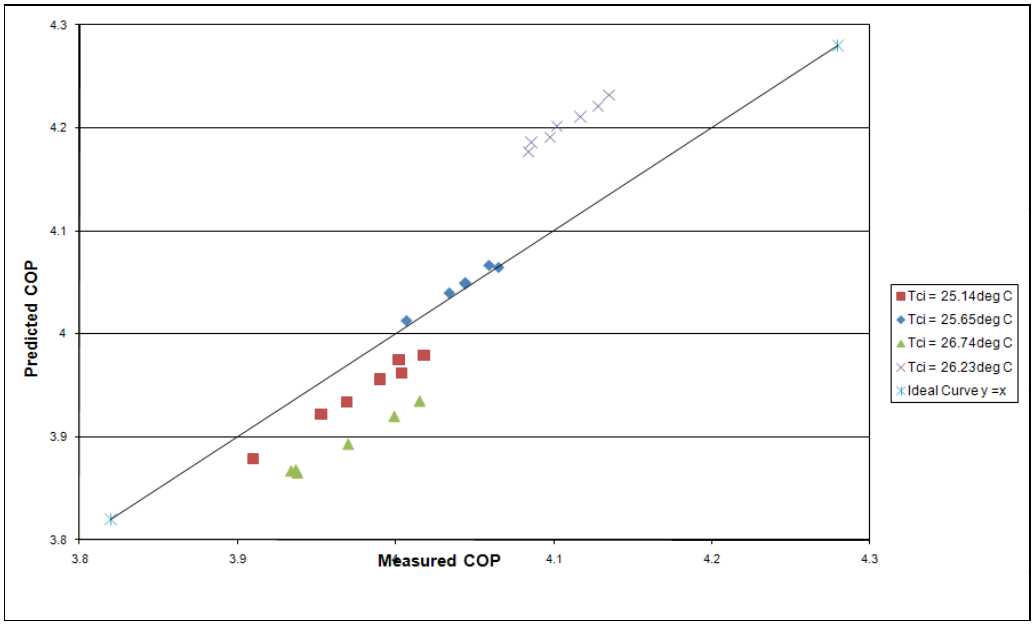

Figure 5.8: Measured Versus Predicted COP under Throttled Conditions for Centrifugal Chiller

5.1.4.3 Comparison between Normal and Throttled Conditions

The characteristic curves for both the normal and throttled tests on the centrifugal chiller are shown in Figures 5.3 and 5.7 above. Figure 5.9 below overlays these two graphs on the same set of axes to allow for easy comparison between the two data sets.

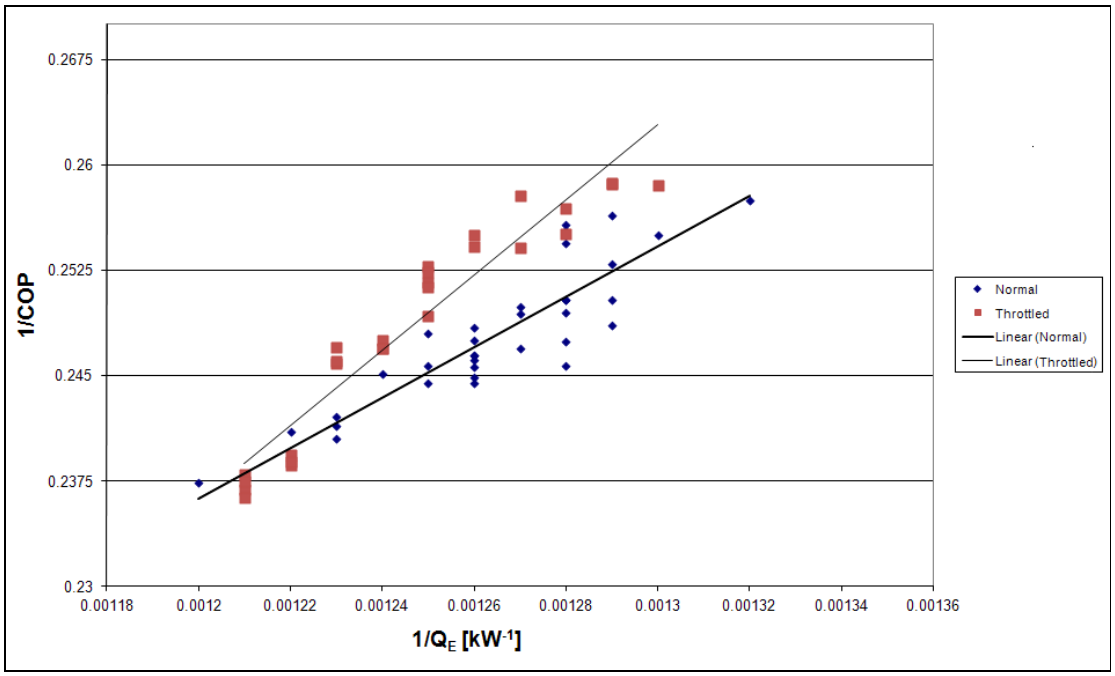

Figure 5.9: Characteristic Curve for Normal and Throttled Conditions for Centrifugal Chiller

5.2 Reciprocating Chiller

5.2.1 Experimental Procedure

Further tests were performed on one of the York reciprocating chillers at the Investec building. The tests were conducted from the morning until the afternoon on 7 January 2010 and values were recorded as the condenser water temperature changed naturally, as the ambient wet-bulb temperature rose throughout the day.

Unlike the centrifugal chiller, the Chiller Visual Control on the reciprocating machine did not display all of the required quantities and therefore all measurements were obtained manually from the calibrated equipment used to verify and correct the CVC readings from the centrifugal machine. As mentioned in Section 5.1.2 above, a copy of the calibration certificate for the multimeter is in Appendix C.

The experimental procedure adopted for the reciprocating machine was the same as for the centrifugal chiller, which is described in Section 5.1.1 above. Between six and seven sets of data were obtained for each of seven fixed condenser water inlet temperature.

5.2.2 Precautions

1. The tests performed on the reciprocating machine observed the same precautions as the tests on the centrifugal machine. These are detailed in section 5.1.2 above.

5.2.3 Results

For the reciprocating machine seven different condenser water inlet temperatures were tested for and the tabulated readings that were obtained are given fully in Appendix F. The same approach was adopted as for the centrifugal machine when processing the reciprocating machine's data. In the following pages the respective graphs are shown and their derivations are described.

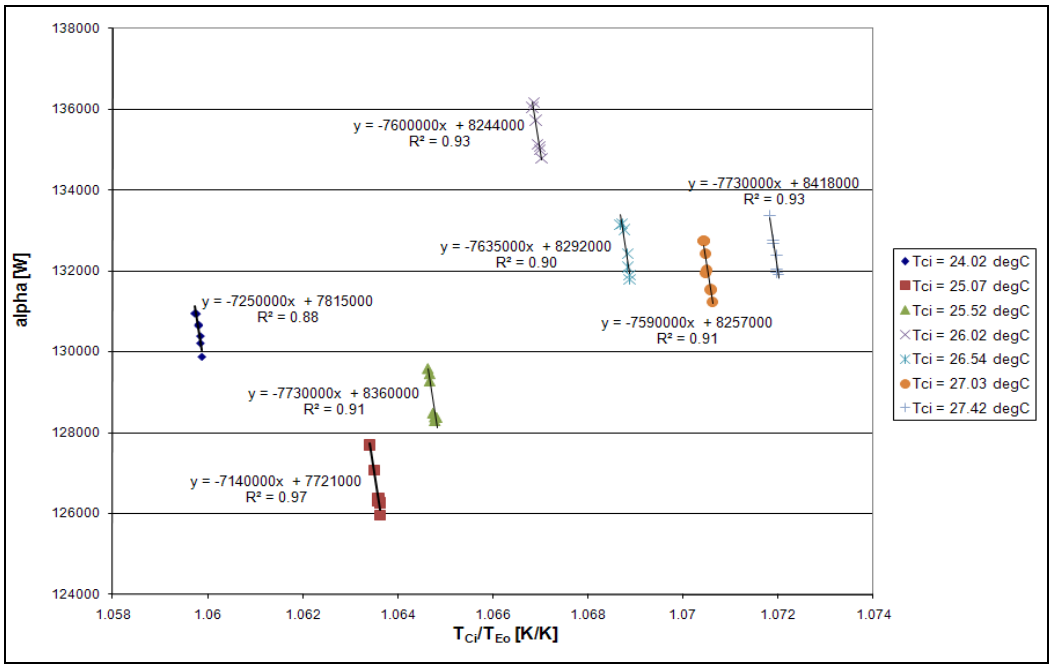

Figure 5.10: α Versus T_{Ci}/T_{Eo} for Reciprocating Chiller

Table 5.5 below summarises the relevant data from the figure above that are necessary to obtain an accurate value for the parameter C_2.

Table 5.5: Summary of Reciprocating Data for Parameter C_2

Temperature	Gradient	C_2	R^2 Value
24.02	-7.25E+06	7.25E+06	0.88
25.07	-7.14E+06	7.14E+06	0.97
25.52	-7.73E+06	7.73E+06	0.91
26.02	-7.60E+06	7.60E+06	0.93
26.54	-7.635E+06	7.635E+06	0.90
27.03	-7.59E+06	7.59E+06	0.91
27.42	-7.73E+06	7.73E+06	0.93

The average value for C_2 can be calculated from the above to be 7525000, which can then be used to determine the other equation parameters. The average R^2 value for the straight line fitted to the data points is approximately 0.92.

Figure 5.11 below shows a plot of $\beta = [\alpha + C_2 (T_{Ci}/T_{Eo})]$ versus T_{Ci} for the reciprocating chiller. The gradient of this graph reveals the value for C_1, while its intercept gives the value for C_0. The equation for the fitted straight line and the R^2 value of the fit are both given in the graph.

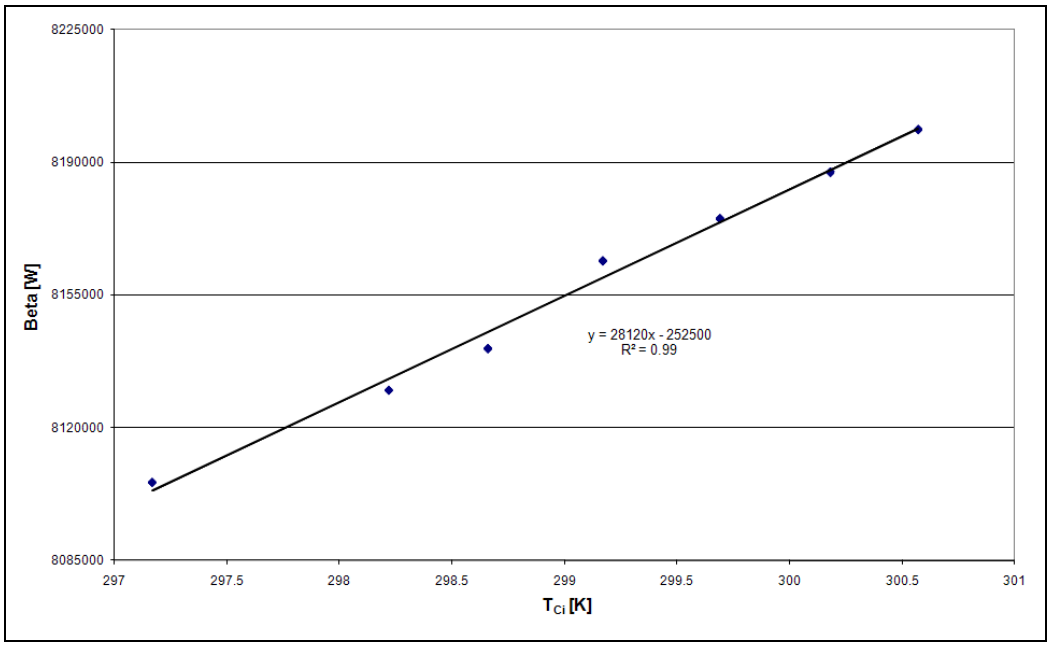

Figure 5.11: β Versus T_{Ci} for Reciprocating Chiller

Table 5.6 shows the relevant data from the curve above, with respect to the parameters in the Universal Thermodynamic Model. The R^2 value of the fitted curve in the figure is 0.99.

Table 5.6: Summary of Reciprocating Data for Parameters C_0 and C_1

	Gradient	Intercept	R^2 Value
Fitted Curve	2.812E+04	-2.525E+05	0.99
C_0	-	2.525E+05	-
C_1	2.812E+04	-	-

Once all parameters were obtained, their respective values were substituted into the Universal Thermodynamic Model so that predicted COP values could be calculated. Figure 5.12 below shows the characteristic curve of 1/COP versus 1/ (Cooling Rate) for the reciprocating machine.

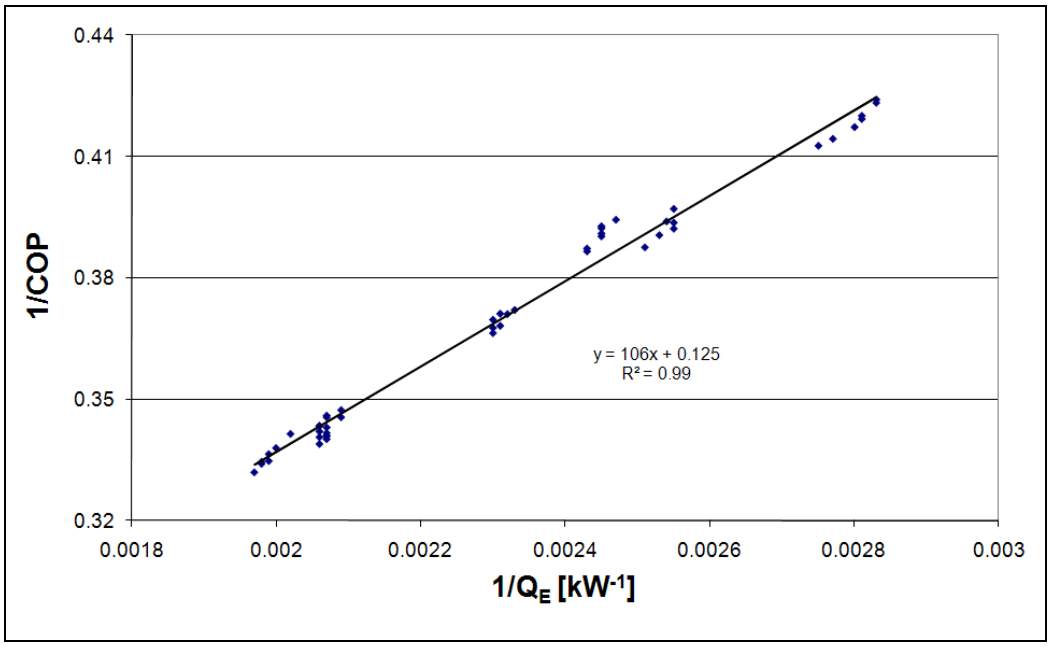

Figure 5.12: Characteristic Curve [1/COP vs. 1/ (Cooling Rate)] for Reciprocating Chiller

As was done for the centrifugal chiller, a graph of measured versus predicted COP was constructed to illustrate the degree of correlation between the Universal Thermodynamic Model and direct experimental measurement. The ideal y = x curve is also shown on the graph. This graph is given in Figure 5.13 below.

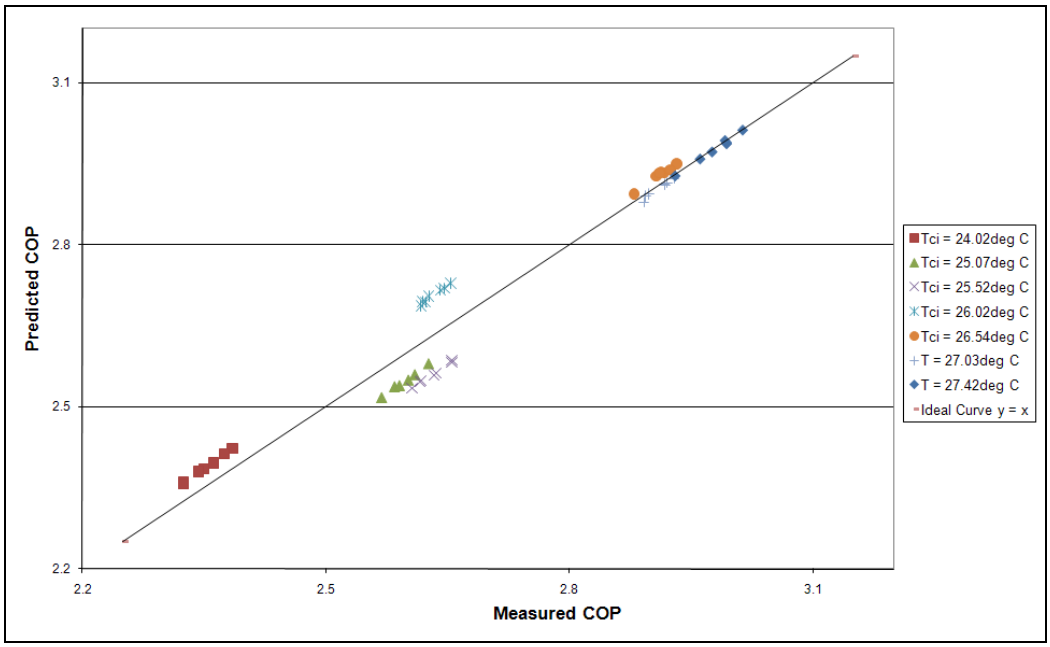

Figure 5.13: Measured Versus Predicted COP for Reciprocating Chiller

5.3 Experimental Uncertainty Analysis

The importance of knowing the uncertainty inherent in an experiment is stressed by Wheeler and Ganji [25] p. 113, who state that "measurement processes usually introduce a certain amount of variability or randomness into the results and this randomness can affect the conclusions drawn from experiments." In order to draw reliable conclusions from any sort of test the degree of confidence with which the data can be trusted must be ascertained. Although two methods of confirming the measured quantities were introduced above, namely the overall energy balance and the comparison between measured and predicted COP values, an experimental uncertainty analysis was also conducted.

Bowker and Lieberman [26] observe that the uncertainty of an experiment gives an indication of the error inherent to it in much the same way as confidence intervals are used for statistical analyses; they basically set parameters on the experimental outcomes that determine whether they can be treated as reliable or not. When broken down to its most fundamental level, the experimental uncertainty is a function of the fluctuations and resolutions of recorded values and gives an indication of the accuracy of the measured values relative to true values.

The deviations recorded between measured and predicted COP values can be compared to the experimental uncertainty in measuring COP to determine whether they are sufficiently accurate. This is achieved by assessing whether the measured deviations lie within the bounds set by the analysis.

An uncertainty analysis was performed on all data sets recorded. The method adopted was taken from Wheeler and Ganji [25] where applicable, but in certain scenarios where a direct application was not feasible an applied version of the method was devised. Appendix G shows all the formulae used to arrive at the final experimental uncertainty and the corresponding tabulated results are given in Appendix H.

6. DISCUSSION

6.1 Centrifugal Chiller under Normal Operation

As mentioned above, five different condenser inlet water temperatures were tested for with the condenser throttling valve left fully open for a total of 37 sets of data. The outcomes have been presented graphically and the details of the different curve fits have been summarised in the preceding chapter. A discussion of the results obtained and their accuracy is given below.

6.1.1 Determination of Equation Parameters

The graphs of $\alpha = [1/COP + 1 - (T_{Ci}/T_{Eo})].Q_E$ versus T_{Ci}/T_{Eo} for the machine operating under normal conditions are shown in Figure 5.1 in the preceding chapter. As was mentioned, each of the graphs corresponds to a fixed condenser water inlet temperature and they should all be approximately parallel to one another. The negative of the average value of the gradients reveals the lumped parameter C_2 in the Universal Thermodynamic Model.

The mean R^2 value for the graphs was calculated from Table 5.1 to be 0.91. This high value suggests that the processed experimental data in Figure 5.1 for each condenser water inlet temperature closely approximates a straight line, as predicted by Gordon and Ng [(1)]. In addition, the fitted straight lines for each of the fixed condenser water inlet temperatures all had similar gradients, which the Universal Thermodynamic Model predicts. In fact, the difference between the maximum and minimum values for the gradients can be calculated to be approximately 7.3%. The gradients were also all negative in value, which is consistent with the predictions of Gordon and Ng [(1)].

Determination of the parameters C_0 and C_1 was also performed graphically, but by constructing a plot of $\beta = [\alpha + C_2 (T_{Ci}/T_{Eo})]$ versus T_{Ci} as shown in Figure 5.2. As predicted by the Universal Thermodynamic Model, the data falls on a straight line and the spread of the data points reflects the different condenser water inlet temperatures tested for. The gradient of the straight line reveals the value for C_1, while the intercept with the y-axis is the negative of the value for C_0.

The R^2 value for the β versus T_{Ci} plot is 1.00, which is representative of how accurately the data fits the straight line and suggests that the measured data agree closely with predictions and assumptions made in formulating the Universal Thermodynamic Model.

In sum, determination of the lumped parameters in the Universal Thermodynamic Model reveals that the experimental data obtained for the centrifugal machine operating normally can be viewed as reliable because of the nature and shape of graphs required in finding the values for C_0, C_1 and C_2. These all behaved in predictable and expected ways that are similar to those of previous studies.

The values obtained for the three constants can then be inserted into the Universal Thermodynamic Model of Equation [3.5] to predict COP at a range of operating conditions outside of those already tested for so that a characteristic curve of the machine under normal operating conditions can be devised and used for performance assessment.

6.1.2 Characteristic Curve

Using the Universal Thermodynamic Model and other recorded data, the graph of Figure 5.3, which shows a plot of 1/COP versus 1/ (Cooling Rate), was obtained. The expected features of this characteristic curve were discussed in section 3.1 and it was observed that, for a large majority of cooling capacities, a linear relationship should occur.

The experimentally obtained characteristic curve reflects the straight-line relationship between the reciprocals of COP and cooling rate to confirm the hypothesis stated above. The data points relate strongly with the straight line fitted to them and the R^2 value for this fit is 0.84, which reflects the close correlation. This further verifies the accuracy of the Universal Thermodynamic Model with respect to the experimental data obtained since the curve behaves almost exactly as predicted by the model.

It is interesting to note that the data points that correspond to the highest COP are for when the condenser inlet water temperature was at its highest towards midday. This phenomenon agrees with what was discussed in Section 3.1 that the COP of a refrigeration machine increases with cooling capacity until it reaches the upper limit of its range. Furthermore, it also indicates that the chiller did not operate at its highest capacity during the experiment because non-linearity of the characteristic curve would have occurred if the maximum were reached. This is consistent with Section 5.1 above, which points out that the building was not fully occupied when the tests were conducted and so cooling demand would not have been at its highest.

6.1.3 Data Confirmation

The experimental data was directly confirmed in three ways. The first and most illustrative check was to compare the measured and predicted values for COP against one another to observe how closely they correspond. The second method was to perform a simple energy balance on the machine as a whole, which would indicate whether the recorded data is sufficiently accurate or not. Finally, the calculated deviations between measured and predicted COP values were compared against the expected experimental uncertainty to deduce whether the deviations are within the allowable limits. Complete, tabulated data for the centrifugal machine is given in Appendix D and that for the reciprocating chiller is given in Appendix F. The percentage errors between measured and predicted COP values and the energy imbalance percentage are listed in the Processed Data tables.

Previous work performed in verifying the Universal Thermodynamic Model by Gordon and Ng [5], Ng, Chua et al. [13], Thomas [11] and Lee [18] all utilise a comparative plot of predicted versus measured COP as a powerful tool for determining its accuracy. The COP of a machine has been introduced and defined as the cooling effect achieved divided by the power required and can thus be determined from direct measurement for each set of data recorded under all of the condenser water inlet temperatures. Theoretically, the predicted and measured COP values should yield a straight line with a gradient of 1 and an intercept at the origin if they correspond exactly.

Figure 5.4 shows the graph of predicted versus measured COP under normal operating conditions. No curve was fitted to the data since the error induced when trying to fit a straight line to the points might suggest that the correlation between the predicted and measured readings is weaker than it actually is. This might come about because the fitted curve may actually be further from the ideal ($y = x$) curve than the data points are. Instead, for each data point the percentage deviation between measured and predicted COP is calculated. From Table D6 in Appendix D it can be seen that the maximum deviation between the COP values is slightly more than 1.14%.

It can be seen from Figure 5.4 that the experimental data points for predicted versus measured COP are evenly distributed around the ideal y = x curve and Table D6 shows that the percentage errors between predicted and measured COPs are all very small. The maximum positive deviation is 1.141% and the maximum negative deviation is -0.714%. Data sets for three out of the five different condenser water inlet temperatures have the predicted COP marginally higher than measured COP, while the data for the other two condenser water inlet temperatures have the predicted COP slightly smaller than measured COP. This combination of small percentage errors and even distribution of positive and negative deviations explains the close correlation between the data points and ideal curve in Figure 5.4.

An energy balance was also performed on the water circuit of the machine to try and gain a further insight into the accuracy of the experiment. As mentioned in section 3.2 the balance takes into account the heat rejection at the condenser, the addition of heat energy at the evaporator and the input power to the chiller as a whole. If all other heat transfer mechanisms to and from the surroundings are considered negligible, a summation of the relevant quantities should ideally equal zero. A large amount of energy left unaccounted for would suggest inaccurate measuring equipment.

The details of the energy balance are contained in Table D6, which provides a column for the energy left unaccounted for due to inaccuracies in the measuring instruments and uncertainties in their resolution. It can be seen that the maximum amount unaccounted for is about 28.5kW, which is less than 3% of the heat transferred at the condenser for that data point.

As was noted above, the maximum deviation between measured and predicted COP values for the centrifugal machine operating normally was calculated to be approximately 1.14%. Inspection of the experimental uncertainty for the same machine under the same operating conditions reveals that this maximum deviation falls safely within the allowable limits. The uncertainty can be seen in Table H2 and is approximately 7.86% so the deviations in COP can be considered acceptable. Therefore, tests performed on the centrifugal machine under normal operating

conditions suggest that the Universal Thermodynamic Model reliably and accurately predicts the performance of the centrifugal chiller under normal operation.

6.2 Centrifugal Chiller under Throttled Conditions

Only four different condenser water inlet temperatures were tested for when the centrifugal chiller's throttling valve was tightened, which resulted in 27 data sets being recorded. The outcomes have been shown graphically and the main details of the relevant curve fits have been outlined. A more detailed analysis of the results obtained and the accuracy thereof is presented below.

6.2.1 Determination of Equation Parameters

Figure 5.5 shows the curves of $\alpha = [1/COP + 1 - (T_{Ci}/T_{Eo})].Q_E$ versus T_{Ci}/T_{Eo} for the four fixed condenser water inlet temperatures. As can be seen, all four graphs have similar gradients, as predicted by the Universal Thermodynamic Model, and the curves all have negative gradients as encountered above for the machine operating normally. The maximum deviation between gradients for the centrifugal machine under throttled conditions can be calculated to be approximately 3%.

The R^2 values for the curves of α versus T_{Ci}/T_{Eo} are also high, as was encountered above for the machine operating normally. The mean R^2 value has been calculated to be 0.92, which suggests a very close correspondence between the data points and the straight line fitted to them. This strong straight line correlation, combined with the fact that the lines are all approximately parallel, are all in agreement with predictions dictated by the model.

As was done for the machine operating normally, a plot of $\beta = [\alpha + C_2(T_{Ci}/T_{Eo})]$ versus T_{Ci}, as shown in Figure 5.6, revealed the values for the parameters C_0 and C_1 once the value for C_2 was obtained. Table 5.4 shows that this graph has an R^2 value of 0.95 when compared to the straight line fitted to its data points, which is in agreement with the Universal Thermodynamic Model.

Thus, determination of the constants C_0, C_1 and C_2 for the centrifugal machine under throttled conditions further verifies the Universal Thermodynamic Model. As for the machine operating normally, the respective graphs used in determining the values for the parameters behaved as expected. The parameters can then be inserted into the model to yield COP values for a broad range of cooling rates.

6.2.2 Characteristic Curve

Figure 5.7 gives the characteristic plot of 1/COP versus 1/ (Cooling Rate) for the centrifugal chiller under throttled conditions. As was the case for the machine under normal operation, the plots closely approximate a straight line.

The straight line that was fitted to the data points was shown to have an R^2 value of 0.92. This value indicates the strong correlation between the points and the line, further justifying the hypothesis put forward by Gordon and Ng [(1)] in the derivation of their Universal Thermodynamic Model that the reciprocals of COP and cooling rate share a linear relationship.

The curve reveals that the COP values for the four different temperatures are all very similar, with less than a 9% difference between maximum and minimum and that the maximum COP values occur at the second highest condenser inlet water temperature. This is in contrast to what occurred with the centrifugal chiller under normal operation and is discussed further in the following sub-section and in Section 6.3.

6.2.3 Data Confirmation

As for the experimental results obtained for the centrifugal machine under normal operating conditions, the data for throttled conditions was confirmed via a comparative check between predicted and measured COP values, by a water-circuit energy balance, and by comparing the calculated deviations with the experimental uncertainty.

A plot of measured versus predicted COP values for the throttling tests is given in Figure 5.8. Ideally, a straight-line relationship of gradient 1 and intercept at the origin should exist for the two sets of values. However, as for the data obtained under normal operation, no line was fitted to the data points since the errors incurred through fitting an approximate curve might make the data points appear less accurate than what they actually are. Instead, the percentage deviation between predicted and measured COP for each data point was evaluated. From Table D11, it can be seen that the maximum error encountered for the COP is approximately 2.45%.

The experimental data points in Figure 5.8 can be seen to be spread around the ideal curve of y = x. The points for condenser inlet water temperatures of 25.65°C and 26.23°C are above the ideal curve, while those for 25.14 °C and 26.74°C are below.

It is also evident from Figure 5.8 that the highest COP values do not correspond to the maximum condenser water inlet temperature. In fact the maximum condenser water inlet temperature yielded some of the lowest COPs for the throttled test. This is in contrast to what was found for un-throttled operation where the COP values continued to increase with condenser water inlet temperature in a linear fashion. Since the only explicit difference between the two experiments was closing off of the condenser valve it may be that this throttling resulted in the chiller operating in the undesirable non-linear region of Figure 3.1 near its maximum cooling capacity where COP rapidly drops off with increasing cooling capacity. This explanation is consistent with the fact that throttling artificially simulates an operational fault that hinders performance.

A waterside energy balance was also performed for the throttled data. Only the condenser, evaporator and overall power drawn by the chiller were considered in the balance. As for this chiller's normal operation, the 'unaccounted energy transfers' can be attributed to inaccuracies in the recording instruments and uncertainties in their resolution.

The results of the energy balance for each data point are given in Table D11. It can be seen that the maximum amount of energy left unaccounted for is 27.7kW, which constitutes approximately 2.85% of the energy transferred at the condenser.

The experimental uncertainty analysis, given in Tables H3 and H4, for the centrifugal machine operating under throttled conditions reveals that errors of up to 8.1% can be expected in the measured COP values. The 2.5% maximum deviation between measured and predicted COP can then be considered acceptable and so the accuracy of the throttled experiment and any conclusions made thereof are reliable.

6.3 Comparison between Centrifugal Normal and Throttled Tests

Further insight into the accuracy and diagnostic capability of the Universal Thermodynamic Model can be obtained by comparing the results obtained for the normal and throttled tests. The most direct and informative comparison between the two operating conditions is to analyse their respective characteristic curves of 1/COP versus 1/ (Cooling Rate).

Figure 5.9 gives the characteristic curves for both operating regimes on the same set of axes and straight lines are fitted to the relevant data for easy comparison. As discussed above, fewer condenser inlet water temperatures were tested for when the throttling valve was tightened than for when it was left fully open and so the throttled data covers a smaller range than the normal data.

The most striking characteristic of Figure 5.9 is that the fitted curve for normal operation generally lies noticeably below that for throttled operation except for at high cooling rates where the two tend to approach one another. It is expected for the un-throttled curve to be the lower of the two since throttling impairs performance but the tendency for the curves to approach one another at high cooling rates seems surprising because it suggests that throttling does not have an adverse effect on performance at the point of approach.

However, the nature of the characteristic curve was described in Section 3.1 and it was shown that there is a point where a further increase in cooling rate causes the relationship between the reciprocals of cooling rate and COP to become non-linear. The point at which the throttled and un-throttled curves approach one another in Figure 5.9 may be, as mentioned in Section 6.2.3, near the point where the machine reaches its maximum cooling capacity under throttled operation. Here, the Universal Thermodynamic Model becomes invalid.

In sum, a simple comparative analysis of the normal and throttled characteristic curves exhibits how the Universal Thermodynamic Model can be used to detect faults in a machine's operation. When heat transfer in the condenser or evaporator is present the characteristic curve will shift vertically upward from its normal position for the majority of cooling rates, indicating that the COP value is below its normal reading for the corresponding cooling rate. At, or near, the point of maximum cooling capacity the curves may begin to behave in unpredictable ways as the relationship between reciprocals of cooling rate and COP becomes non-linear.

In addition to an analysis of the respective characteristic curves, a comparison of the constants, C_0, C_1 and C_2, for normal and throttled operation provides some further insight into the diagnostic capability of the Universal Thermodynamic Model. The values for C_2, given in Sections 5.1.4.1 and 5.1.4.2 above, stay almost the same for both operating conditions and a 4.38% difference can be calculated between the normal and throttled conditions. There is a greater discrepancy of 24.15% between normal and throttled C_1 values and the difference in C_0 values is the highest at approximately 29.35%.

It can be recalled from Section 3.1 that for a fixed condenser water inlet temperature the constants C_0 and C_1 loosely represent irreversibilities in the condenser and C_2 represents the evaporator irreversibilities. The significant deviations of C_0 and C_1 can then be explained because the condenser throttling valve was tightened to simulate fouling. The evaporator was left untouched and so the C_2 values remained almost constant.

6.4 Reciprocating Chiller

Further tests were performed on one of the York reciprocating machines at the Investec installation. The results have been presented graphically to try and illustrate the correlation between the Universal Thermodynamic Model and measured values. A discussion into the accuracy and reliability of the results is presented below.

6.4.1 Determination of Equation Parameters

For the York reciprocating machine operating under normal conditions the parameter C_2 was again obtained via a series of graphs, one for each defined condenser water inlet temperature. The plots of $\alpha = [1/COP + 1 - (T_{Ci}/T_{Eo})].Q_E$ versus T_{Ci}/T_{Eo} used to obtain an experimental value have been shown in Figure 5.10 and the summarised data is presented in Table 5.5.

Consistent with predictions made by Gordon and Ng [(1)] and with the findings from the centrifugal tests, the curves all have similar gradients and the data points for each closely correlate to a straight line. The average R^2 value for the graphs has been calculated to be approximately 0.92, which reflects this close correlation and suggests that the data is indicative of the Universal Thermodynamic Model's predictions.

Thereafter, a graph of $\beta = [\alpha + C_2 (T_{Ci}/T_{Eo})]$ versus T_{Ci} was constructed for the reciprocating chiller and is shown in Figure 5.11. This plot is meant to closely

approximate a straight line, with its gradient as the value for C_1 and its vertical intercept as the negative value of C_0.

The R^2 value for the graph of β versus T_{Ci} is shown on the figure as approximately 0.99 and the spread of the data points can be observed to be indicative of the different condenser water inlet temperatures specified. The high R^2 value can be taken as an indication that the experimental data and the Universal Thermodynamic Model are in close agreement.

Thus, manipulation of the experimental data collected from the reciprocating machine shows a close agreement with the predictions made by Gordon and Ng [1]. The trends and spread of the data points are very similar to what is expected from the Universal Thermodynamic Model. The resultant values obtained for C_0, C_1 and C_2 can then be inserted into the model with a high level of confidence.

6.4.2 Characteristic Curve

The characteristic plot of 1/COP versus 1/ (Cooling Rate) for the reciprocating chiller is shown in Figure 5.12. This curve was discussed in section 3.1 and it was shown that the graph displays linearity across its entire range except where the point of maximum cooling capacity is reached. Employing the assumption that the building is not calling for maximum cooling, a straight line was fitted to the data points as a means of validating the universal model with the experiment.

The R^2 value for the characteristic curve is shown on the graph to be approximately 0.99, which reflects its strong correlation to the fitted straight line. This then helps to further confirm the accuracy of the Universal Thermodynamic Model since the curve behaves as expected.

Consistent with the observations made for the centrifugal machine under normal conditions the data points that correspond to the maximum COP are also those for which the condenser inlet water temperature was at its highest and so the reciprocating machine probably didn't operate at its maximum capacity.

6.4.3 Data Confirmation

The same means of confirming the experimental data as for the centrifugal chiller were employed for the reciprocating machine. A graphical and numerical comparison of the COP values obtained via measurement and prediction is used as the primary confirming method and a waterside energy balance of the main components is used as a quantitative, supplementary check. A third check is also employed that compares the deviations in COP values with the experimental uncertainty.

A graph of predicted versus measured COP is given in Figure 5.13. Ideally, the data points should collapse to a straight line through the origin with a gradient of 1 to show that each measured COP matches each predicted COP exactly. However, in order to avoid incurring any additional errors associated with fitting a straight line to the points the graph does not fit any curve and only the points themselves are given. Instead, the deviation between the measured and predicted values is calculated for each individual data point and is tabulated, as shown in Table F5.

Inspection of Figure 5.13 shows that the data points approximate the ideal straight line but the degree to which it does so cannot be quantitatively assessed from the curve. Analysis of the tabulated data of Table F5 reveals that there is a very small deviation between the measured and actual COP readings for each data point and that the maximum difference recorded is 2.97%.

The energy balance performed is also tabulated in Table F5. This balance only takes into account the entering and leaving states of the evaporator and condenser water circuits and the power drawn by the chiller. The amount of energy left unaccounted for after the balance is performed can be attributed to inaccuracies in the recording instruments and uncertainties in their resolution.

The maximum amount of energy left unaccounted for after the energy balance was performed was calculated to be about 14kW, which is just above 2.22% of the energy transferred at the condenser.

The uncertainty analysis performed on the reciprocating chiller shows that errors of up to 6.64% could be expected in the measured COP values. Therefore the 2.97% maximum deviation between measured and predicted COPs discussed above is acceptable when compared to the uncertainty and the accuracy of the experiment, and any related conclusions can be viewed as reliably accurate.

7. CONCLUSION AND RECOMMENDATIONS

7.1 Conclusion

The project objectives were listed in section 1.4 and the subsequent research undertaken and experiments performed have been aimed at achieving these intended outcomes. The degrees to which the different aims of the study have been satisfied are discussed below.

Through following its derivation and critically discussing several papers that verified its accuracy, familiarity and insight were gained into the Universal Thermodynamic Model. An understanding was acquired of the model's main assumption that a linear relationship exists between the reciprocals of COP and cooling rate of a refrigeration machine except for at the upper extremity of its operating range. The model was then applied to three different scenarios, two on a centrifugal chiller and one on a reciprocating machine.

The accuracy of the model was verified for two large installations, with operating capacities both in excess of 700kW. The correlation between the measured COP and that predicted by the model was shown to be very strong for both machines and within the experimental uncertainty boundaries. In fact, the maximum deviation obtained for all experiments was below 3%, which is testament to the accuracy of the results.

Artificially imposing a machine fault and comparing the results with those from the same machine under fault-free conditions also confirmed that the Universal Thermodynamic Model has some fault diagnosis capability. A comparison of the key equation constants of the temperature-independent version of the model revealed that significant condenser fouling should be easily detectable by noticeable deviations in the constants C_0 and C_1 from their regular values. Constant C_2 will vary to a lesser extent than C_0 and C_1.

The comparative test also revealed the effect that heat exchanger fouling has on the overall performance of a machine and it has been shown graphically that the COP is lower for the majority of cooling rates when significant condenser fouling exists. However, as the machine approaches its maximum cooling capacity, its characteristic curve of reciprocals of cooling rate and COP approaches the non-linear region, where the Universal Thermodynamic Model becomes invalid.

The Universal Thermodynamic Model can therefore be viewed as a valuable tool with distinct benefits over other fault assessment techniques because it provides a means to compare corresponding actual and normal performance for a wide range of cooling capacities below the machine's upper limit. Once a normal benchmark has thereby been set for a machine's permissible operating range, it then becomes a simple task to assess that machine's actual performance for any actual operating regime it encounters.

7.2 Recommendations for Further Work

It was described in Section 5.1.1 and 5.2.1 that experimental measurements were taken manually from the machine's digital display and from instruments located on the machine. This introduced an unreliable element into the experiment because of the time lag between readings. Further studies that verify the Universal Thermodynamic Model will benefit from using an automatic data logger like the one employed by Thomas [11]. This will facilitate the ease of measurement since it can be programmed to record and store critical values at set time intervals, and also provide greater accuracy and reliability by recording values simultaneously.

Further studies will also benefit through more thorough testing of refrigeration machines at their maximum capacities, under both normal and fault-simulated operating regimes. These may reveal key, generally applicable details of the limitations of the Universal Thermodynamic Model at maximum capacities, and

hence yield useful caveats when using the model to diagnose faults when machines operate at or near maximum capacities.

8. REFERENCES

1. Gordon, J.M and Ng, K.C. (2000). *Cool Thermodynamics – The Engineering and Physics of Predictive, Diagnostic and Optimization Methods for Cooling Systems,* Cambridge International Science Publishing, Cambridge, United Kingdom, pp1-2.

2. Chamber of Mines South Africa. (2010). INTERNET. The South African Mining Industry Fact Sheet. http://www.bullion.org.za/Publications/Facts&Figures2008/Text2008.pdf, cited January 2010.

3. Moran, MJ and Shapiro, HN. (2000*). Fundamentals of Engineering Thermodynamics*, SI Version, 3rd edition, John Wiley and Sons, West Sussex, UK.

4. Grimmelius, HT, Klein Woud, J and Been, G. (1995). On-Line Failure Diagnosis for Compression Refrigeration Plants, *International Journal of Refrigeration,* vol.18, no.1, January 1995, pp31-41.

5. Gordon, JM and Ng, KC. (1995). Predictive and Diagnostic Aspects of a Universal Thermodynamic Model for Chillers, *International Journal of Heat and Mass Transfer*, vol. 38, no. 5, pp. 807-818.

6. Gordon, JM and NG, KC. (1994). Thermodynamic Modelling of Reciprocating Chillers, Journal of Applied Physics, Vol. 75, No. 6, 15 March 1994, pp. 2769-2774

7. ESKOM. (2010). INTERNET. ESKOM Demand-Side Management. www.eskomdsm.co.za, cited October 2010.

8. Bailey-McEwan, M. (1998). Assessing Site Performance of Large Mine Water Chilling Machines Using Refrigerant-Circuit Measurements and Machine Modelling. PhD Thesis, 1998, University of the Witwatersrand, Johannesburg, South Africa.

9. Stewart, JM. (1982). Practical Aspects of Human Heat Stress, Environmental Engineering on South African Mines, 1982, the Mine Ventilation Society of South Africa, pp. 535-539.

10. Isermann, R. (1982). Process Fault Detection Based on Modelling and Estimation Methods, Proceeding, IFAC Conference on Identification and System Parameter Estimation, Washington DC, USA, 1982, pp. 7-30.

11. Thomas, G. (2004). Detecting Under-Performance and Faults in a Refrigeration Machine by Second-Law Analysis. Project Report, 2004, University of the Witwatersrand, Johannesburg, South Africa.

12. Phelan, J, Brandemuehl, MJ, Krarti, M. (1997). In-Situ Performance Testing of Chillers for Energy Analysis, ASHRAE Transactions, 1997, vol. 103, no. 1, pp290-302.

13. Ng, KC, Chua, HT, Ong, W, Lee, SS and Gordon, JM. (1997). Diagnostics and Optimization of Reciprocating Chillers: Theory and Experiment, *Applied Thermal Engineering*, vol.17, no. 3, pp. 263-276.

14. Gluckman, R. (1986). Inefficient Operation of Refrigeration Plant, *Proceedings, Joint Seminar on Cutting Refrigeration Energy Costs*, Institute of Refrigeration and Institution of Mechanical Engineers (UK), 19 November 1986 (Institute of Refrigeration (UK), 1986).

15. Hall, AE and Unsted, AD. (1976). Computer Modelling of Underground Refrigeration Equipment, in: Proceedings of the Second IFAC Symposium on Automation in Mining, Mineral and Metal Processing, Johannesburg, South Africa, 1976; South African Council for Automation and Computation, Pretoria, South Africa, 1997, pp 75-80.

16. Hemp, R, Cilliers, PF, Starfield, AM and Fallon, P. (1986). Computer Analysis of Underground Refrigeration Plant Performance, *Journal of the Mine Ventilation Society of South Africa,* vol. 39, no. 6, June 1986, pp. 77-85.

17. Ng, KC, Gordon, JM and Chua, HT. (2003). New Thermodynamic Tools for Chiller Diagnostics and Optimisation, Proceedings, International Congress of Refrigeration, 2003, Washington D.C.

18. Lee, TS. (2004). Thermodynamic Modelling and Experimental Validation of Screw Liquid Chillers, ASHRAE 4689 Transactions, 2004.

19. Gordon, Ng and Chua. (1995). Centrifugal Chillers: Thermodynamic Modelling and the Diagnostic Case Study, International Journal of Refrigeration, vol. 18, no. 4, pp 253-257.

20. Gordon, JM and Ng, KC. (1995). Thermodynamic Modelling of Reciprocating Chillers, *Heat Recovery System & CHP*, vol. 15, pp 73-83.

21. Cengel, YA and Turner, RH. (2001). *Fundamentals of Thermal-Fluid Sciences*, McGraw-Hill Higher Education, New York, 2001, pp881-928.

22. McPartland, JF and Novak, WJ. (1964). *Practical Electricity*, McGraw-Hill Inc., USA.

23. Carrier Installation Manual. Obtained via private correspondence with Enviroware Construction.

24. York Installation and Operation Manual. Obtained via private correspondence with Enviroware Construction.

25. Wheeler, AJ and Ganji, AR. (1996). *Introduction to Engineering Experimentation*, Prentice-Hall Inc., New Jersey.

26. Bowker, AH and Lieberman, GJ. (1960). *Engineering Statistics*, Prentice-Hall Inc., New Jersey.

APPENDIX A: Obtaining Constant C_2

Gordon and Ng [1] state that a plot of $\alpha = [1/COP + 1 - (T_{Ci}/T_{Eo})].Q_E$ versus T_{Ci}/T_{Eo} should yield a set of parallel straight lines, one for each fixed condenser water inlet temperature (T_{Ci}), and that the gradient of these lines gives the negative value of parameter C_2 in the Universal Thermodynamic Model. The following will explain how this conclusion was reached.

The Universal Thermodynamic Model has been introduced in the following format:

$$\frac{1}{COP} = -1 + \frac{T_{Ci}}{T_{Eo}} + \frac{-C_0 + C_1 \cdot T_{Ci} - C_2 \cdot \frac{T_{Ci}}{T_{Eo}}}{Q_E} \qquad [A.1]$$

Rearranging terms from the above equation leads to Equation [A.2].

$$\left[\frac{1}{COP} + 1 - \frac{T_{Ci}}{T_{Eo}}\right].Q_E = -C_0 + C_1 \cdot T_{Ci} - C_2 \cdot \frac{T_{Ci}}{T_{Eo}} \qquad [A.2]$$

Since $\alpha = [1/COP + 1 - (T_{Ci}/T_{Eo})].Q_E$, the relationship in Equation [A.3] must be valid by equality.

$$\alpha = -C_0 + C_1 \cdot T_{Ci} - C_2 \cdot \frac{T_{Ci}}{T_{Eo}} \qquad [A.3]$$

For a fixed condenser water inlet temperature the value T_{Ci} is constant, say θ, and so Equation [A.3] can be rearranged to Equation [A.4].

$$\alpha = -C_0 + C_1 \cdot \theta - C_2 \cdot \frac{\theta}{T_{Eo}} \qquad [A.4]$$

Now, a plot of α versus T_{Ci}/T_{Eo} effectively becomes a plot of $-C_0 + C_1.\theta - C_2.(\theta/T_{E0})$ versus θ/T_{Eo}, which fits the general straight line equation y = (m.x + c) with y = α and $x = \theta/T_{Eo.}$ The gradient of the line (m) can be seen to be $-C_2$ and so the value of C_2 is the negative of the gradient.

APPENDIX B: Obtaining Constants C_0 and C_1

Gordon and Ng [1] state that a plot of $\beta = [\alpha + C_2.(T_{Ci}/T_{Eo})]$ versus TCi should yield a straight line with gradient C_1 and intercept with the vertical axis $-C_0$. The following will illustrate this relationship.

Invoking Equation [A.3] above into the relationship $\beta = [\alpha + C_2.(T_{Ci}/T_{Eo})]$ results in Equation [B.1]:

$$\beta = -C_0 + C_1 \cdot T_{Ci} \qquad [B.1]$$

Equation [B.1] above fits the general straight line equation $y = (m.x + c)$ with $y = \beta$ and $x = T_{Ci.}$ The gradient of the line (m) can be seen to be C_1 and the intercept with the vertical (y) axis is the negative of C_0.

APPENDIX C: Instrument Calibration

The evaporator and condenser water pressures on the centrifugal chiller's visual display were calibrated using an analogue differential pressure gauge placed at the inlet and outlet of the particular heat exchanger. Since the pressures at the heat exchanger's inlets and outlets remains approximately constant for a particular operating regime, only one calibration measurement was recorded. The pressures recorded from the digital display were corrected by multiplying them by a correction factor, which was obtained by dividing the calibrated pressure difference by the displayed pressure difference. Table C1 summarises the calibration exercise for the evaporator pressure, while Table C2 summarises that for the condenser.

The calibration certificate for the differential pressure gauge had been lost but the maintenance staff at Investec verbally assured its accuracy and calibration history.

Table C1: Evaporator Water Pressure Calibration

EVAPORATOR	
Recorded inlet water pressure	411kPa
Recorded outlet water pressure	471kPa
Recorded pressure difference	60kPa
Correct pressure difference	68kPa
Pressure correction factor	1.1333

Table C2: Condenser Water Pressure Calibration

CONDENSER	
Recorded inlet water pressure	479kPa
Recorded outlet water pressure	410kPa
Recorded pressure difference	69kPa
Correct pressure difference	67kPa
Pressure correction factor	0.971

The voltage, current and power factor values were all obtained from the Carrier machine's digital display, or Chiller Visual Control unit. These values were all calibrated using a digital multimeter connected to the corresponding power supply cables. The values obtained from the display are adjusted according to a correction factor, which is the calibrated value divided by the recorded value. The details of this exercise have been discussed in section 4 and Table C3 below summarises the results of the calibration.

The conformance certificate for the meter, which was issued when the instrument was bought, is given overleaf.

Table C3: Voltage, Current and Power Factor Calibration

POWER	
Recorded voltage	405.9V
Correct voltage	406.3V
Voltage correction factor	1.001
Recorded current	359A
Correct current	355A
Current correction factor	0.989
Recorded power factor	0.61
Correct power factor	0.596
Power factor correction factor	0.977

TYCOM (PTY) LTD.
The best in test & measurement

Tel: (011) 787 8508/9
Fax: (011) 787 8518
Email: sales@tycom-sa.com
Website: www.tycom-sa.com
Reg No: 56/00195/07

Certificate of Conformance

Make : TOPTRONIC MULTI-METER
Model TBM126
Serial No : 074481008
Certificate No. : TC28894

The following equipment was used to calibrate the above instrument.

Description	Model	Serial No.	Certificate No.	Expiry Date
FLUKE	5100B	780015	200805065	2009.05.30
FLUKE	8840A	4427035	200707038	2008.07.10
EDC	3200	7499	200707035	2008.07.11

The above instrument conforms to the manufacturers specifications, within the confines of calibration environment.

Calibrated for : **ENVIROWARE CONSTRUCTION**

Date of issue : **2009/04/08**

Date of Expiry : **2010/04/07**

Calibrated by :

APPENDIX D: Tabulated Centrifugal Data

Table D1 summarises the abbreviated terms used throughout Appendix D.

Table D1: Appendix D Nomenclature

TERM	DESCRIPTION	UNITS
T_{ci} R	Recorded condenser inlet water temperature	˚C
T_{Ci} C	Calibrated condenser inlet water temperature	˚C
T_{Ci}SI	SI condenser inlet water temperature	K
T_{Co} R	Recorded condenser outlet water temperature	˚C
T_{Co} C	Calibrated condenser outlet water temperature	˚C
T_{Co}SI	SI condenser outlet water temperature	K
T_{Ei} R	Recorded evaporator inlet water temperature	˚C
T_{Ei} C	Calibrated evaporator inlet water temperature	˚C
T_{Ei}SI	SI evaporator inlet water temperature	K
T_{Eo} R	Recorded evaporator outlet water temperature	˚C
T_{Eo} C	Recorded evaporator outlet water temperature	˚C
T_{Eo}SI	SI evaporator outlet water temperature	K
V R	Recorded voltage	V
V C	Calibrated voltage	V
I R	Recorded current	Amps
I C	Calibrated current	Amps
cosφ R	Recorded power factor	None
cosφ C	Calibrated power factor	None
Power	Power drawn by chiller	W
P_{Ci}	Condenser inlet water pressure	kPa
P_{Co}	Condenser outlet water pressure	kPa
ΔP_c R	Recorded condenser differential pressure	kPa
ΔP_c C	Calibrated condenser differential pressure	kPa
P_{Ei}	Evaporator inlet water pressure	kPa
P_{Eo}	Evaporator outlet water pressure	kPa
ΔP_E R	Recorded evaporator differential pressure	kPa
ΔP_E C	Calibrated evaporator differential pressure	kPa
TE_{ave}	Average evaporator water temperature	˚C
TC_{ave}	Average condenser water temperature	˚C
v_E	Evaporator specific volume	m^3/kg

TERM	DESCRIPTION	UNITS
C_E	Evaporator specific heat	J/(kg.K)
v_C	Condenser specific volume	m^3/kg
C_C	Condenser specific heat	J/(kg.K)
vol_{flow} C	Condenser water volumetric flow	m^3/s
vol_{flow} E	Evaporator water volumetric flow	m^3/s
m_{fl}E	Evaporator water mass flow	kg/s
m_{fl}C	Condenser water mass flow	kg/s
Q_E	Evaporator heat transfer	W
Q_C	Condenser heat transfer	W
COP	Measured coefficient of performance	None
COP P	Predicted coefficient of performance	None
balance	Amount of energy left unaccounted for after an energy balance	W
diffCOP%	Percentage differential between measured and predicted COP values	None

Table D2 below shows the various evaporator and condenser inlet and outlet water temperatures obtained under normal operating conditions. The recorded, calibrated and SI values are given for all data sets.

Table D2: Temperature Data for Normal Operation for Centrifugal Chiller

T_{Ci} R [°C]	T_{Ci}SI [K]	T_{Co} R [°C]	T_{Co}SI [K]	T_{Ei} R [°C]	T_{Ei}SI [K]	T_{Eo} R [°C]	T_{Eo}SI [K]
24.31	297.46	27.65	300.8	9.76	282.91	6.39	279.54
24.31	297.46	27.69	300.84	9.81	282.96	6.38	279.53
24.31	297.46	27.74	300.89	9.81	282.96	6.39	279.54
24.31	297.46	27.76	300.91	9.87	283.02	6.43	279.58
24.31	297.46	27.77	300.92	9.89	283.04	6.45	279.6
24.31	297.46	27.78	300.93	9.89	283.04	6.44	279.59
24.31	297.46	27.76	300.91	9.88	283.03	6.43	279.58
25.08	298.23	28.38	301.53	9.91	283.06	6.47	279.62
25.08	298.23	28.39	301.54	9.94	283.09	6.48	279.63
25.08	298.23	28.4	301.55	9.92	283.07	6.5	279.65
25.08	298.23	28.44	301.59	9.98	283.13	6.52	279.67
25.08	298.23	28.41	301.56	10.01	283.16	6.54	279.69
25.08	298.23	28.46	301.61	10.03	283.18	6.51	279.66
25.08	298.23	28.43	301.58	9.99	283.14	6.53	279.68
25.72	298.87	29.09	302.24	10.09	283.24	6.6	279.75
25.72	298.87	29.11	302.26	10.14	283.29	6.62	279.77
25.72	298.87	29.09	302.24	10.13	283.28	6.64	279.79
25.72	298.87	29.12	302.27	10.16	283.31	6.65	279.8
25.72	298.87	29.21	302.36	10.16	283.31	6.64	279.79
25.72	298.87	29.19	302.34	10.18	283.33	6.65	279.8
25.72	298.87	29.21	302.36	10.19	283.34	6.65	279.8
25.72	298.87	29.2	302.35	10.18	283.33	6.68	279.83
25.72	298.87	29.22	302.37	10.17	283.32	6.67	279.82
26.63	299.78	30.04	303.19	10.36	283.51	6.89	280.04
26.63	299.78	30.08	303.23	10.39	283.54	6.85	280
26.63	299.78	30.05	303.2	10.42	283.57	6.87	280.02
26.63	299.78	30.12	303.27	10.44	283.59	6.85	280
26.63	299.78	30.11	303.26	10.44	283.59	6.89	280.04
26.63	299.78	30.15	303.3	10.44	283.59	6.91	280.06
26.63	299.78	30.13	303.28	10.45	283.6	6.92	280.07
27.21	300.36	30.67	303.82	10.57	283.72	6.97	280.12
27.21	300.36	30.72	303.87	10.61	283.76	6.95	280.1
27.21	300.36	30.76	303.91	10.57	283.72	6.98	280.13
27.21	300.36	30.75	303.9	10.63	283.78	6.96	280.11
27.21	300.36	30.72	303.87	10.62	283.77	6.96	280.11
27.21	300.36	30.74	303.89	10.65	283.8	6.97	280.12
27.21	300.36	30.79	303.94	10.62	283.77	6.99	280.14

Table D3 below contains the power supply data for the machine under normal operating conditions. The recorded and calibrated values for the voltage, current and power factor are all displayed and these are used to calculate the power values.

Table D3: Power Supply Data for Normal Operation for Centrifugal Chiller

V R	V C	I R	I C	cosϕ R	cosϕ C	Power
[V]	[V]	[A]	[A]			[W]
402.9	403.3	432.4	427.6	0.663	0.648	193550
403.1	403.5	433.9	429.1	0.664	0.649	194630
403.6	404	433.1	428.3	0.665	0.65	194810
402.9	403.3	434.1	429.3	0.668	0.653	195820
403.6	404	435.1	430.3	0.671	0.656	197520
403.7	404.1	434.4	429.6	0.672	0.657	197550
405.2	405.6	434.7	429.9	0.667	0.652	196910
403.3	403.7	433.1	428.3	0.663	0.648	194060
403.6	404	433.5	428.7	0.661	0.646	193790
403.9	404.3	432.9	428.1	0.667	0.652	195460
404.8	405.2	434.4	429.6	0.664	0.649	195680
405.4	405.8	434.7	429.9	0.667	0.652	197010
404.1	404.5	433.4	428.6	0.669	0.654	196390
405.3	405.7	434.1	429.3	0.668	0.653	196990
403.4	403.8	432.4	427.6	0.662	0.647	193490
404.4	404.8	433.5	428.7	0.665	0.65	195370
403.8	404.2	434.1	429.3	0.664	0.649	195060
404.5	404.9	434.9	430.1	0.665	0.65	196060
405.1	405.5	428.3	423.6	0.674	0.658	195760
403.9	404.3	428.6	423.9	0.675	0.659	195620
404.6	405	431.2	426.5	0.669	0.654	195660
404.7	405.1	434.2	429.4	0.669	0.654	197040
404.5	404.9	435.6	430.8	0.668	0.653	197290
402.1	402.5	436.6	431.8	0.668	0.653	196570
399.2	399.6	438.4	433.6	0.668	0.653	195970
398.7	399.1	437.3	432.5	0.675	0.659	197020
398.4	398.8	437.1	432.3	0.674	0.658	196480
403.8	404.2	438.7	433.9	0.669	0.654	198670
402.5	402.9	438.8	434	0.669	0.654	198070
404.5	404.9	438.4	433.6	0.668	0.653	198570
397.7	398.1	434.5	429.7	0.672	0.657	194660
398.3	398.7	435.6	430.8	0.668	0.653	194270
404.1	404.5	436.3	431.5	0.658	0.643	194390
405.2	405.6	436.3	431.5	0.657	0.642	194610
404.6	405	435.2	430.4	0.659	0.644	194430

V R [V]	V C [V]	I R [A]	I C [A]	cosϕ R	cosϕ C	Power [W]
403.2	403.6	435.5	430.7	0.664	0.649	195400
403.1	403.5	433.3	428.5	0.667	0.652	195260

Table D4 below contains the evaporator and condenser inlet and outlet pressure data. The recorded changes in pressure across the heat exchangers are calculated and calibrated.

Table D4: Pressure Data for Normal Operation for Centrifugal Chiller

P_{Ci} [kPa]	P_{Co} [kPa]	ΔP_C R [kPa]	ΔP_C C [kPa]	P_{Ei} [kPa]	P_{Eo} [kPa]	ΔP_E R [kPa]	ΔP_E C [kPa]
478	408	70	67.97	469	411	58	65.73
478	408	70	67.97	469	411	58	65.73
478	408	70	67.97	469	411	58	65.73
478	408	70	67.97	469	411	58	65.73
478	408	70	67.97	469	411	58	65.73
478	408	70	67.97	469	411	58	65.73
478	408	70	67.97	469	411	58	65.73
478	408	70	67.97	469	411	58	65.73
478	408	70	67.97	469	411	58	65.73
478	408	70	67.97	469	411	58	65.73
478	408	70	67.97	469	411	58	65.73
478	408	70	67.97	469	411	58	65.73
478	408	70	67.97	469	411	58	65.73
478	408	70	67.97	469	411	58	65.73
478	408	70	67.97	469	411	58	65.73
478	408	70	67.97	469	411	58	65.73
478	408	70	67.97	469	411	58	65.73
477	408	69	67	469	411	58	65.73
478	408	70	67.97	470	412	58	65.73
477	408	69	67	470	412	58	65.73
478	409	69	67	472	411	61	69.13
478	409	69	67	472	412	60	67.998
478	410	68	67	473	412	61	69.13
478	408	70	67.97	470	411	59	66.86
478	408	70	67.97	470	412	58	65.73
478	408	70	67.97	470	411	59	66.86
477	407	70	67.97	469	411	58	65.73
477	408	69	67	469	412	57	64.6

P_{Ci}	P_{Co}	ΔP_C R	ΔP_C C	P_{Ei}	P_{Eo}	ΔP_E R	ΔP_E C
[kPa]	[kPa]	[kPa]	[kPa]	[kPa]	[kPa]	[kPa]	[kPa]
478	408	70	67.97	470	412	58	65.73
478	407	71	68.94	470	412	58	65.73
478	408	70	67.97	470	411	59	66.86
477	408	69	67	470	411	59	66.86
477	408	69	67	470	411	59	66.86
478	407	71	68.94	469	412	57	64.6
477	408	69	67	469	412	57	64.6
478	408	70	67.97	470	412	58	65.73
478	409	69	67	470	412	58	65.73

The first set of processed data for the centrifugal chiller under normal operation is given in Table D5 below. These quantities are mainly used to simplify the calculations of the final values shown in the subsequent table.

Table D5: Processed Data 1 for Normal Operation for Centrifugal Chiller

TE_{ave}	TC_{ave}	v_E	C_E	v_C	C_C	$m_{fl}E$	$m_{fl}C$
[°C]	[°C]	[m^3/kg]	[J/(kg.K)]	[m^3/kg]	[J/(kg.K)]	[kg/s]	[kg/s]
8.075	25.98	0.001	4205	0.001005	4181	53.6	69.1
8.095	26	0.001	4205	0.001005	4181	53.8	69.1
8.1	26.025	0.001	4205	0.001005	4181	53.5	69.1
8.15	26.035	0.001	4205	0.001005	4181	53.4	69.1
8.17	26.04	0.001	4205	0.001005	4181	53.9	69.1
8.165	26.045	0.001	4205	0.001005	4181	53.7	69.1
8.155	26.035	0.001	4205	0.001005	4181	53.8	69.1
8.19	26.73	0.001	4205	0.001005	4181	53.9	69.1
8.21	26.735	0.001	4205	0.001005	4181	53.4	69.1
8.21	26.74	0.001	4205	0.001005	4181	53.8	69.1
8.25	26.76	0.001	4205	0.001005	4181	53.5	69.1
8.275	26.745	0.001	4205	0.001005	4181	53.8	69.1
8.27	26.77	0.001	4205	0.001005	4181	53.6	69.1
8.26	26.755	0.001	4205	0.001005	4181	53.9	69.1
8.345	27.405	0.001	4205	0.001005	4181	53.4	69.1
8.38	27.415	0.001	4205	0.001005	4181	53.6	69.1
8.385	27.405	0.001	4205	0.001005	4181	53.9	69.1
8.405	27.42	0.001	4205	0.001005	4181	53.5	69.1
8.4	27.465	0.001	4205	0.001005	4181	53.8	69.1
8.415	27.455	0.001	4205	0.001005	4181	53.6	69.1

TE_{ave}	TC_{ave}	v_E	C_E	v_C	C_C	$m_{fl}E$	$m_{fl}C$
[°C]	[°C]	[m^3/kg]	[J/(kg.K)]	[m^3/kg]	[J/(kg.K)]	[kg/s]	[kg/s]
8.42	27.465	0.001	4205	0.001005	4181	53.2	69.1
8.43	27.46	0.001	4205	0.001005	4181	53.4	69.1
8.42	27.47	0.001	4205	0.001005	4181	53.8	69.1
8.625	28.335	0.001	4205	0.001005	4181	53.6	69.1
8.62	28.355	0.001	4205	0.001005	4181	53.7	69.1
8.645	28.34	0.001	4205	0.001005	4181	53.5	69.1
8.645	28.375	0.001	4205	0.001005	4181	53.9	69.1
8.665	28.37	0.001	4205	0.001005	4181	54	69.1
8.675	28.39	0.001	4205	0.001005	4181	53.6	69.1
8.685	28.38	0.001	4205	0.001005	4181	53.9	69.1
8.77	28.94	0.001	4205	0.001005	4181	53.9	69.1
8.78	28.965	0.001	4205	0.001005	4181	53.8	69.1
8.775	28.985	0.001	4205	0.001005	4181	53.7	69.1
8.795	28.98	0.001	4205	0.001005	4181	53.6	69.1
8.79	28.965	0.001	4205	0.001005	4181	53.2	69.1
8.81	28.975	0.001	4205	0.001005	4181	53.7	69.1
8.805	29	0.001	4205	0.001005	4181	53.6	69.1

Table D6 shows the second and final set of processed data for the centrifugal machine operating normally. These values constitute the main outcomes of the experiment.

Table D6: Processed Data 2 for Normal Operation for Centrifugal Chiller

T_{Ci} R	QE	QC	1/QE	COP	alpha	beta	1/COP P	COP P	balance	bal%	diffCOP%
[°C]	[W]	[W]	[kW^{-1}]		[W]	[W]			[W]		
24.31	759560	964950	0.00132	3.924	144880	12520000	0.2575	3.883	11840	1.227	1.045
24.31	775970	976510	0.00129	3.987	144850	12521000	0.2529	3.954	5910	0.605	0.828
24.31	769390	990950	0.0013	3.949	145510	12521000	0.255	3.922	26750	2.699	0.684
24.31	772440	996730	0.00129	3.945	146400	12520000	0.2564	3.9	28470	2.856	1.141
24.31	779670	999620	0.00128	3.947	147730	12521000	0.2557	3.911	22430	2.244	0.912
24.31	779040	1002500	0.00128	3.944	147730	12521000	0.2553	3.917	25910	2.585	0.685
24.31	780490	996730	0.00128	3.964	146980	12521000	0.2544	3.931	19330	1.939	0.832
25.08	779670	953390	0.00128	4.018	142150	12546000	0.2474	4.042	-20340	-2.133	-0.597
25.08	776930	956280	0.00129	4.009	142120	12546000	0.2486	4.023	-14440	-1.51	-0.349
25.08	773700	959170	0.00129	3.958	144070	12547000	0.2504	3.994	-9990	-1.042	-0.91
25.08	778390	970730	0.00128	3.978	144020	12546000	0.2504	3.994	-3340	-0.344	-0.402
25.08	785010	962060	0.00127	3.985	144950	12546000	0.2499	4.002	-19960	-2.075	-0.427
25.08	793370	976510	0.00126	4.04	143700	12546000	0.2464	4.058	-13250	-1.357	-0.446
25.08	784210	967840	0.00128	3.981	144970	12546000	0.2495	4.008	-13360	-1.38	-0.678

T_{Ci} R	QE	QC	1/QE	COP	alpha	beta	1/COP P	COP P	balance	bal%	diffCOP%
[°C]	[W]	[W]	[kW^{-1}]		[W]	[W]			[W]		
25.72	783670	973620	0.00128	4.05	139940	12565000	0.2457	4.07	-3540	-0.364	-0.494
25.72	793370	979400	0.00126	4.061	141200	12565000	0.2445	4.09	-9340	-0.954	-0.714
25.72	791010	973620	0.00126	4.055	141130	12564000	0.2461	4.063	-12450	-1.279	-0.197
25.72	789640	982280	0.00127	4.028	142220	12565000	0.2469	4.05	-3420	-0.348	-0.546
25.72	796330	1008300	0.00126	4.068	141450	12565000	0.2449	4.083	16210	1.608	-0.369
25.72	795620	1002500	0.00126	4.067	141400	12564000	0.2456	4.072	11260	1.123	-0.123
25.72	791920	1008300	0.00126	4.047	141710	12564000	0.2464	4.058	20720	2.055	-0.272
25.72	785910	1005400	0.00127	3.989	143540	12565000	0.2494	4.01	22450	2.233	-0.526
25.72	791800	1011200	0.00126	4.013	143400	12565000	0.2475	4.04	22110	2.187	-0.673
26.63	782100	985170	0.00128	3.979	141430	12591000	0.2504	3.994	6500	0.66	-0.377
26.63	799360	996730	0.00125	4.079	139500	12591000	0.2445	4.09	1400	0.14	-0.27
26.63	798630	988060	0.00125	4.054	140640	12591000	0.2457	4.07	-7590	-0.768	-0.395
26.63	813670	1008300	0.00123	4.141	139010	12591000	0.2414	4.143	-1850	-0.183	-0.048
26.63	806100	1005400	0.00124	4.057	141870	12592000	0.2451	4.08	630	0.063	-0.567
26.63	795620	1017000	0.00126	4.017	142040	12591000	0.2484	4.026	23310	2.292	-0.224
26.63	800070	1011200	0.00125	4.029	142270	12591000	0.248	4.032	12560	1.242	-0.074
27.21	815940	999620	0.00123	4.192	135690	12606000	0.2405	4.158	-10980	-1.098	0.811
27.21	828000	1014100	0.00121	4.262	134380	12606000	0.237	4.219	-8170	-0.806	1.009
27.21	810650	1025600	0.00123	4.17	135860	12606000	0.2421	4.131	20560	2.005	0.935
27.21	827170	1022700	0.00121	4.25	134830	12606000	0.2377	4.207	920	0.09	1.012
27.21	818760	1014100	0.00122	4.211	135240	12606000	0.2394	4.177	910	0.09	0.807
27.21	830980	1019800	0.0012	4.253	135340	12606000	0.2374	4.212	-6580	-0.645	0.964
27.21	818160	1034300	0.00122	4.19	136210	12606000	0.241	4.149	20880	2.019	0.979

Table D7 below contains the evaporator and condenser inlet and outlet water temperatures for the centrifugal chiller operating under throttled conditions. As for the data corresponding to normal operation, the recorded, calibrated and SI values are given.

Table D7: Temperature Data for Throttled Operation for Centrifugal Chiller

T_{ci} R [°C]	T_{Ci}SI [K]	T_{Co} R [°C]	T_{Co}SI [K]	T_{Ei} R [°C]	T_{Ei}SI [K]	T_{Eo} R [°C]	T_{Eo}SI [K]
25.14	298.29	29.17	302.32	10.14	283.29	6.57	279.72
25.14	298.29	29.19	302.34	10.13	283.28	6.58	279.73
25.14	298.29	29.18	302.33	10.11	283.26	6.6	279.75
25.14	298.29	29.18	302.33	10.13	283.28	6.55	279.7
25.14	298.29	29.17	302.32	10.14	283.29	6.57	279.72
25.14	298.29	29.17	302.32	10.12	283.27	6.56	279.71
25.14	298.29	29.18	302.33	10.13	283.28	6.55	279.7
25.65	298.8	29.7	302.85	10.27	283.42	6.68	279.83
25.65	298.8	29.71	302.86	10.27	283.42	6.67	279.82
25.65	298.8	29.72	302.87	10.29	283.44	6.67	279.82
25.65	298.8	29.69	302.84	10.27	283.42	6.69	279.84
25.65	298.8	29.72	302.87	10.29	283.44	6.68	279.83
25.65	298.8	29.72	302.87	10.28	283.43	6.67	279.82
25.65	298.8	29.73	302.88	10.3	283.45	6.69	279.84
26.23	299.38	30.39	303.54	10.45	283.6	6.77	279.92
26.23	299.38	30.37	303.52	10.44	283.59	6.78	279.93
26.23	299.38	30.39	303.54	10.45	283.6	6.8	279.95
26.23	299.38	30.38	303.53	10.43	283.58	6.75	279.9
26.23	299.38	30.39	303.54	10.46	283.61	6.78	279.93
26.23	299.38	30.39	303.54	10.47	283.62	6.79	279.94
26.23	299.38	30.38	303.53	10.46	283.61	6.79	279.94
26.74	299.89	30.75	303.9	10.6	283.75	7.14	280.29
26.74	299.89	30.74	303.89	10.63	283.78	7.13	280.28
26.74	299.89	30.74	303.89	10.68	283.83	7.17	280.32
26.74	299.89	30.75	303.9	10.65	283.8	7.13	280.28
26.74	299.89	30.72	303.87	10.63	283.78	7.16	280.31
26.74	299.89	30.73	303.88	10.64	283.79	7.17	280.32

The power supply data for the centrifugal machine under throttled conditions is given in Table D8. The recorded and calibrated voltage, current and power factor values are shown.

Table D8: Power Supply Data for Throttled Conditions for Centrifugal Chiller

V R	V C	I R	I C	cosϕ R	cosϕ C	Power
[V]	[V]	[A]	[A]			[W]
412.3	412.3	442.1	442.1	0.635	0.635	200480
412.4	412.4	443.4	443.4	0.633	0.633	200480
411.1	411.1	441.9	441.9	0.638	0.638	200750
409.2	409.2	442.5	442.5	0.638	0.638	200090
413.8	413.8	441.9	441.9	0.632	0.632	200170
410.6	410.6	442.4	442.4	0.634	0.634	199470
411.2	411.2	442.9	442.9	0.633	0.633	199670
411.8	411.8	443.9	443.9	0.631	0.631	199780
411.3	411.3	442.3	442.3	0.633	0.633	199450
413.3	413.3	442.4	442.4	0.631	0.631	199830
411.9	411.9	443.9	443.9	0.631	0.631	199830
413.8	413.8	444.4	444.4	0.628	0.628	200030
411.8	411.8	441.6	441.6	0.633	0.633	199380
412.8	412.8	444.2	444.2	0.631	0.631	200400
412.2	412.2	444.4	444.4	0.632	0.632	200520
413.2	413.2	444	444	0.631	0.631	200510
413.9	413.9	445.9	445.9	0.63	0.63	201390
413.1	413.1	443.9	443.9	0.629	0.629	199780
413.5	413.5	444.1	444.1	0.632	0.632	201020
413.9	413.9	443.9	443.9	0.633	0.633	201440
413.3	413.3	444.9	444.9	0.632	0.632	201280
411.7	411.7	438.7	438.7	0.626	0.626	195830
412.1	412.1	439.5	439.5	0.624	0.624	195750
412.8	412.8	443.1	443.1	0.623	0.623	197370
412.5	412.5	441.2	441.2	0.622	0.622	196070
413.5	413.5	441.3	441.3	0.623	0.623	196910
412.9	412.9	440.2	440.2	0.626	0.626	197070

The condenser and evaporator inlet and outlet water temperatures are given in Table D9 when the centrifugal machine operates with the throttling valve tightened. The recorded differential pressures and the calibrated differential pressures for both heat exchangers are also given.

Table D9: Pressure Data for Throttled Operation for Centrifugal Chiller

P_{Ci} [kPa]	P_{Co} [kPa]	ΔP_C R [kPa]	ΔP_C C [kPa]	P_{Ei} [kPa]	P_{Eo} [kPa]	ΔP_E R [kPa]	ΔP_E C [kPa]
570	519	51	49.52	470	412	58	65.73
570	519	51	49.52	470	412	58	65.73
570	519	51	49.52	470	412	58	65.73
570	519	51	49.52	470	412	58	65.73
570	519	51	49.52	470	412	58	65.73
570	519	51	49.52	470	412	58	65.73
570	519	51	49.52	470	412	58	65.73
570	519	51	49.52	470	412	58	65.73
570	519	51	49.52	470	412	58	65.73
570	519	51	49.52	470	412	58	65.73
570	519	51	49.52	470	412	58	65.73
570	519	51	49.52	470	412	58	65.73
570	519	51	49.52	470	412	58	65.73
570	519	51	49.52	470	412	58	65.73
570	519	51	49.52	470	412	58	65.73
570	519	51	49.52	470	412	58	65.73
570	519	51	49.52	470	412	58	65.73
570	519	51	49.52	470	412	58	65.73
570	519	51	49.52	470	412	58	65.73
570	519	51	49.52	470	412	58	65.73
570	519	51	49.52	470	412	58	65.73
570	519	51	49.52	470	412	58	65.73
570	519	51	49.52	470	412	58	65.73
570	519	51	49.52	470	412	58	65.73
570	519	51	49.52	470	412	58	65.73
570	519	51	49.52	470	412	58	65.73
570	519	51	49.52	470	412	58	65.73
570	519	51	49.52	470	412	58	65.73
570	519	51	49.52	470	412	58	65.73
570	519	51	49.52	470	412	58	65.73
570	519	51	49.52	470	412	58	65.73

The first set of processed data for throttled conditions is given in Table D10 below. The data shown is predominantly used to arrive at the final processed data given in Table D11.

Table D10: Processed Data 1 for Throttled Operation for Centrifugal Chiller

TE_{ave}	TC_{ave}	v_E	C_E	v_C	C_C	$m_{fl}E$	$m_{fl}C$
[°C]	[°C]	[m^3/kg]	[J/(kg.K)]	[m^3/kg]	[J/(kg.K)]	[kg/s]	[kg/s]
8.355	27.155	0.001	4204	0.001004	4181	53.3	57.8
8.355	27.165	0.001	4204	0.001004	4181	53.1	57.8
8.355	27.16	0.001	4204	0.001004	4181	53.2	57.8
8.34	27.16	0.001	4204	0.001004	4181	53.2	57.8
8.355	27.155	0.001	4204	0.001004	4181	53.4	57.8
8.34	27.155	0.001	4204	0.001004	4181	52.9	57.8
8.34	27.16	0.001	4204	0.001004	4181	53.3	57.8
8.475	27.675	0.001	4204	0.001004	4181	53.4	57.8
8.47	27.68	0.001	4204	0.001004	4181	53.3	57.8
8.48	27.685	0.001	4204	0.001004	4181	53.3	57.8
8.48	27.67	0.001	4204	0.001004	4181	53.2	57.8
8.485	27.685	0.001	4204	0.001004	4181	53.3	57.8
8.475	27.685	0.001	4204	0.001004	4181	53.4	57.8
8.495	27.69	0.001	4204	0.001004	4181	53.4	57.8
8.61	28.31	0.001	4204	0.001004	4181	53.5	57.8
8.61	28.3	0.001	4204	0.001004	4181	53.4	57.8
8.625	28.31	0.001	4204	0.001004	4181	53.6	57.8
8.59	28.305	0.001	4204	0.001004	4181	53.4	57.8
8.62	28.31	0.001	4204	0.001004	4181	53.3	57.8
8.63	28.31	0.001	4204	0.001004	4181	53.6	57.8
8.625	28.305	0.001	4204	0.001004	4181	53.3	57.8
8.87	28.745	0.001	4204	0.001004	4181	53	57.8
8.88	28.74	0.001	4204	0.001004	4181	53.2	57.8
8.925	28.74	0.001	4204	0.001004	4181	53.1	57.8
8.89	28.745	0.001	4204	0.001004	4181	53.2	57.8
8.895	28.73	0.001	4204	0.001004	4181	53.1	57.8
8.905	28.735	0.001	4204	0.001004	4181	53.2	57.8

The final set of processed data for the centrifugal machine under throttled conditions is given in Table D11 below. The values are used as the main experimental outcomes for measurement and discussion.

Table D11: Processed Data 2 for Throttled Operation for Centrifugal Chiller

T_{Ci} R	QE	QC	1/QE	COP	alpha	beta	1/COP P	COP P	balance	bal%	diffCOP%
[°C]	[W]	[W]	[kW^{-1}]		[W]	[W]			[W]		
25.14	799940	973900	0.00125	3.99	147380	12006000	0.2528	3.956	-26520	2.723	0.852
25.14	792480	978730	0.00126	3.953	147890	12006000	0.255	3.922	-14230	1.454	0.784
25.14	785020	976310	0.00127	3.91	148750	12006000	0.2578	3.879	-9460	0.969	0.793
25.14	800680	976310	0.00125	4.002	146850	12006000	0.2516	3.975	-24460	2.505	0.675
25.14	801440	973900	0.00125	4.004	146950	12005000	0.2524	3.962	-27710	2.845	1.049
25.14	791710	973900	0.00126	3.969	146880	12006000	0.2542	3.934	-17280	1.774	0.882
25.14	802180	976310	0.00125	4.018	146330	12005000	0.2513	3.979	-25540	2.616	0.971
25.65	805930	978730	0.00124	4.034	145150	12019000	0.2475	4.04	-26980	2.757	-0.149
25.65	806660	981150	0.00124	4.044	144760	12019000	0.2469	4.05	-24960	2.544	-0.148
25.65	811140	983560	0.00123	4.059	144820	12019000	0.2459	4.067	-27410	2.787	-0.197
25.65	800680	976310	0.00125	4.007	145570	12019000	0.2492	4.013	-24200	2.479	-0.15
25.65	808900	983560	0.00124	4.044	145190	12019000	0.2469	4.05	-25370	2.579	-0.148
25.65	810420	983560	0.00123	4.065	144400	12019000	0.246	4.065	-26240	2.668	0
25.65	810420	985980	0.00123	4.044	145490	12019000	0.247	4.049	-24840	2.519	-0.124
26.23	827680	1005300	0.00121	4.128	142960	12036000	0.2369	4.221	-22900	2.278	-2.253
26.23	821650	1000500	0.00122	4.098	143410	12036000	0.2386	4.191	-21660	2.165	-2.269
26.23	822470	1005300	0.00122	4.084	144300	12036000	0.2394	4.177	-18560	1.846	-2.277
26.23	826140	1002900	0.00121	4.135	142300	12036000	0.2363	4.232	-23020	2.295	-2.346
26.23	824590	1005300	0.00121	4.102	143730	12036000	0.238	4.202	-20310	2.02	-2.438
26.23	829230	1005300	0.00121	4.117	143830	12036000	0.2375	4.211	-25370	2.524	-2.283
26.23	822350	1002900	0.00122	4.086	144150	12036000	0.2389	4.186	-20730	2.067	-2.447
26.74	770930	969060	0.0013	3.937	141910	12040000	0.2585	3.868	2300	0.237	1.753
26.74	782780	966650	0.00128	3.999	140980	12039000	0.2551	3.92	-11880	1.229	1.975
26.74	783550	966650	0.00128	3.97	142670	12039000	0.2569	3.893	-14270	1.476	1.94
26.74	787260	969060	0.00127	4.015	141000	12039000	0.2541	3.935	-14270	1.473	1.993
26.74	774620	961810	0.00129	3.934	142800	12040000	0.2586	3.867	-9720	1.011	1.703
26.74	776080	964230	0.00129	3.938	142890	12039000	0.2587	3.865	-8920	0.925	1.854

APPENDIX E: Recording Water Flow Rates

The volumetric flow rates of water through the condenser and evaporator for all of the experiments were obtained from an ultrasonic flow-meter. The complete device is comprised of a linear sensor, with adjustable sensing pads, and a programming device. The sensor is strapped to the outside of the pipe being tested along its longitudinal axis and sends triangulated pulses between two sensing pads, as indicated in Figure E1.

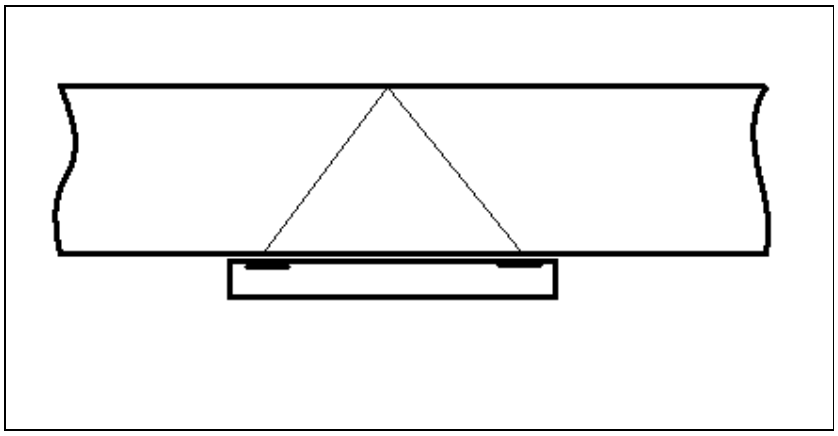

Figure E1: Ultrasonic Flow-Meter Triangulated Pulses

Users only need to specify the outer diameter, wall thickness and material of the pipe being tested and specify the type of fluid flowing through the pipe. With this information, the display device calculates and indicates the distance at which the adjustable pads must be set. Once this is set up correctly the sensor is connected to the display device via two cables, one at each sensing pad.

The time taken used for pulses to be sent from one pad to the other is used to calculate the flow through the pipe and the flow rate is displayed in either m/s, m^3/s or kg/s.

The pages that follow are taken from the ultrasonic meter manual and they contain the key steps that are followed to obtain flow measurements.

Instruction Manual

PORTABLE TYPE ULTRASONIC FLOWMETER (PORTAFLOW X)

TYPE: CONVERTER FLC-2
DETECTOR FLD-1

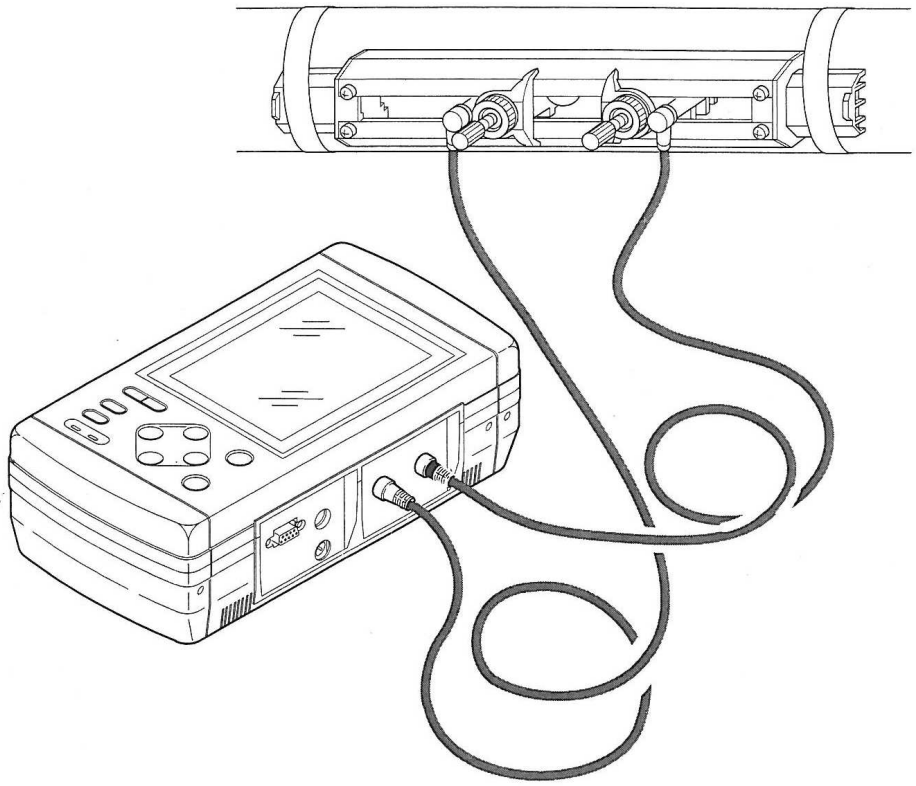

Fuji Electric Systems Co., Ltd.

INF-TN2FLCc-E

6. INPUT OF PIPING SPECIFICATIONS

Before installing the detector, set the specifications of a pipe in the main unit to allow measurements.

Caution) Measurements cannot be accomplished without these settings.

6.1 Display of pipe setup screen

① Press the ◀ key on the "MEASURE" screen to invert the "Tab".

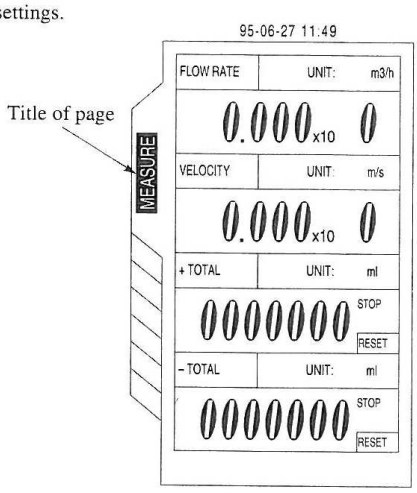

② Press the ▼ key, and the "SITE SETUP" menu screen is displayed.

To move the cursor on the screen, press the ▶ key or ENT key.

To invert "PIPE PARAMETER" on the menu screen , press the ▼ key on the "SITE SETUP" screen.

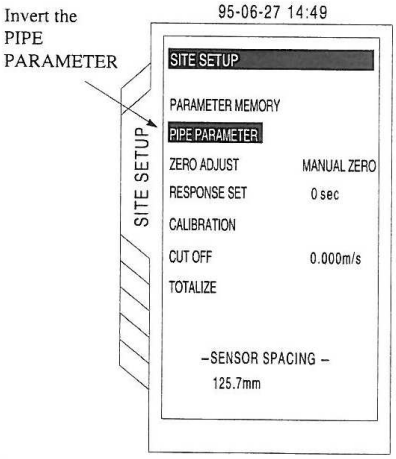

③ Press the ENT key, and "PIPE PARAMETER" screen is displayed.

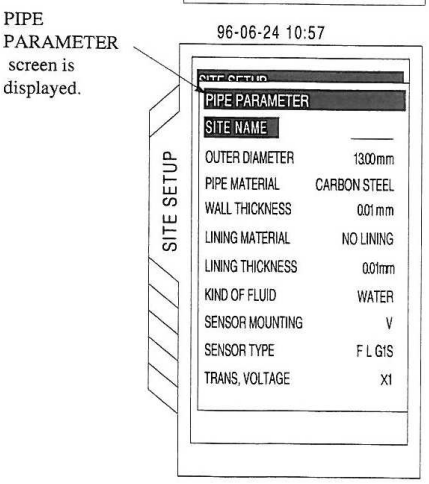

④ Outline of PIPE PARAMETER

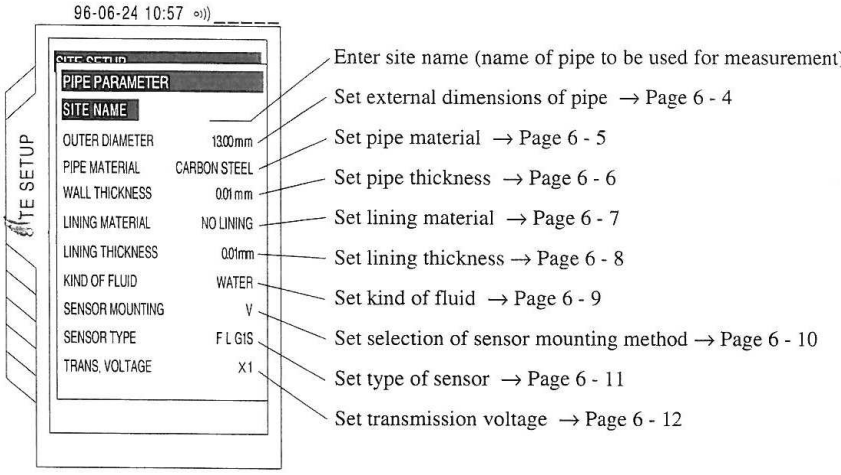

⑤ Display of mounting dimensions

When the settings are completed on the "PIPE PARAMETER" screen, press the (ESC) key to display the "SITE SETUP" menu screen.
At the last line the "SENSOR SPACING" value is displayed.

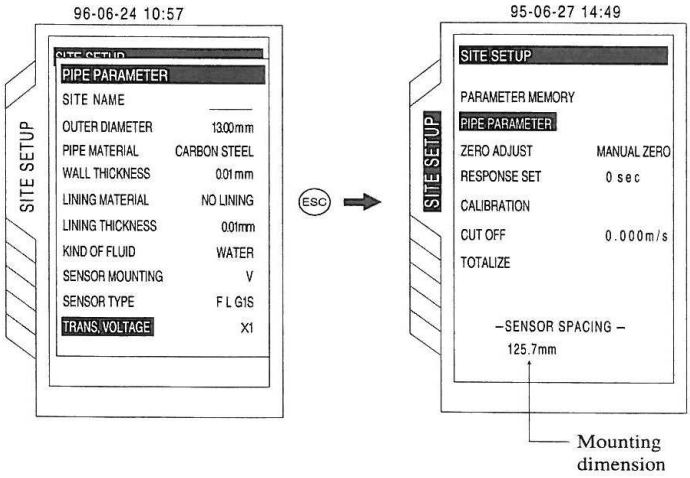

Install the sensor according to chapter 7. MOUNTING OF DETECTOR and the mounting dimension is as displayed on the last line.

6.3 Outer diameter of piping (unit: mm) (range: 13 to 6100 mm)

Press the ▼ key on the "PIPE PARAMETER" screen to invert the "OUTER DIAMETER".
Press the ENT key, and you can enter the outer dimension.

Use the ◀ or ▶ key to cause the digit to move in the right and left direction
Use the ▲ or ▼ key to enter the numeric.
After entry, press the ENT key.

Note) Enter outer dimensions, but not nominal diameter (example: 20A → 20).

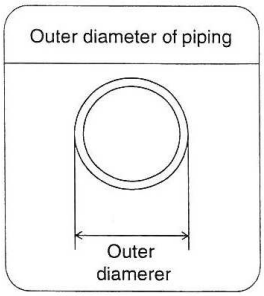

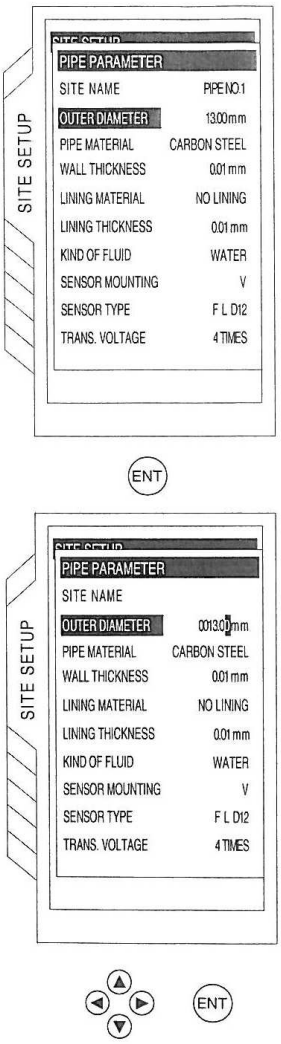

Example) When the outer diameter of piping is 318.5 mm:

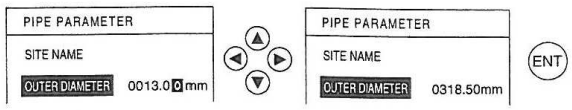

6.4 Piping material

Press the ▼ key to invert the "PIPE MATERIAL".
Press the ENT key, and the "PIPE MATERIAL" screen will appear.

Select the material by using the ▲ or ▼ key. After entry, press the ENT key.

Note) If you select "OTHER", enter the sound velocity (range: 1000 to 3700m/s). See page 15 - 6, Table ㉑.

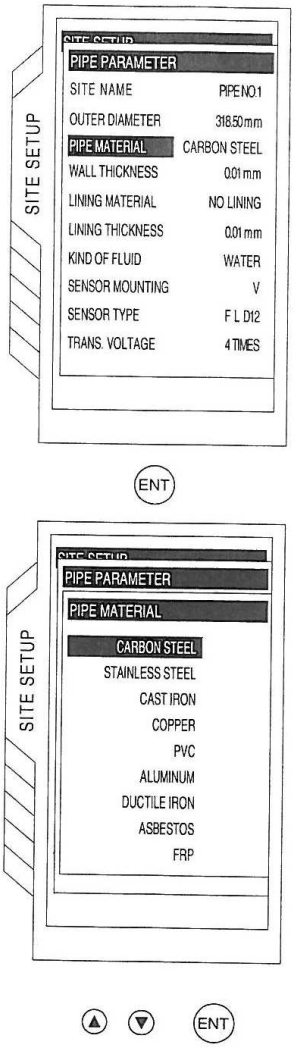

Example) When the piping material is cast iron:

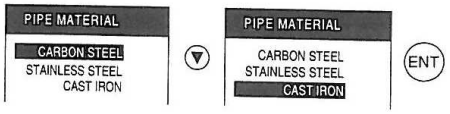

6.5 Wall thickness (unit: mm) (range: 0.01 to 100.00mm)

Press the ▼ key to invert the "WALL THICKNESS".
Press the ENT key, and wall thickness can be entered (See pages 15 -1 to 15 - 6, Piping Data).
Use the ◀ or ▶ key to move the digit to the right and left.
Using the ▲ or ▼ key, enter the numeral. After entry, press the ENT key.

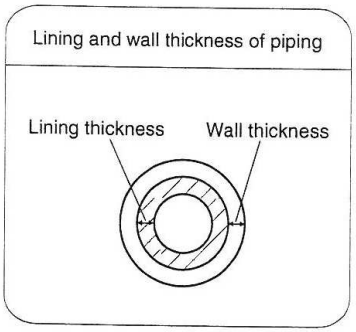

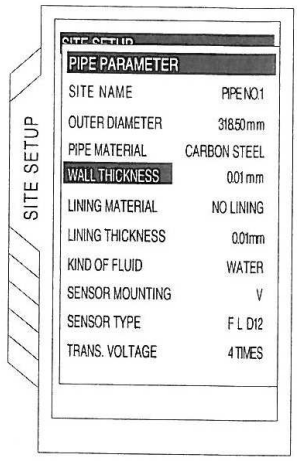

ENT

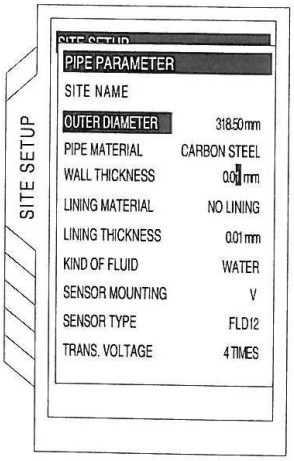

▲ ◀ ▶ ▼ ENT

Example) When the wall thickness is 1.25mm

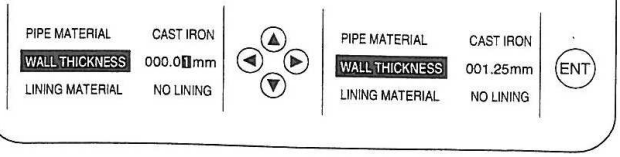

6.6 Lining material

Press the ▼ key to invert "LINING MATERIAL".
Press the ENT key, and "LINING MATERIAL" screen will appear.

Using the ▲ or ▼ key, select the material. After selection, press the ENT key.

Note) If you select "OTHER", enter the sound velocity (range 1000 to 3700m/s). See page 15-6, Table ㉑.

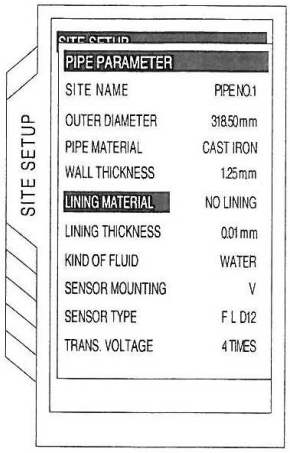

ENT

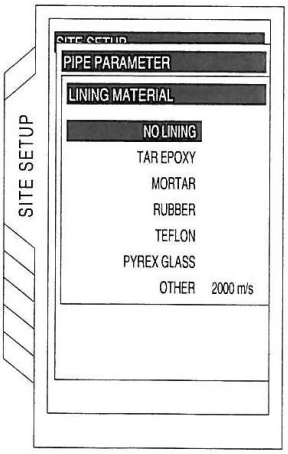

▲ ▼ ENT

Example) When the lining material is mortar

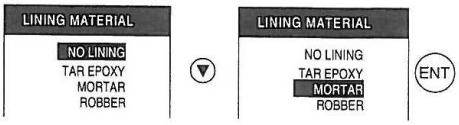

6.7 Lining thickness (unit: mm) (range: 0.01 to 100.00 mm)

When the lining material is set to items other than "None" in 6.6 Lining material.

Press the ▼ key to invert the "LINING THICKNESS".

Press the ENT key, the lining thickness numeric entry can be performed.

The cursor can shift the numeric digit by using the ◀ or ▶ key. The numeric can be entered by using the ▲ or ▼ key.

After entry, press the ENT key.

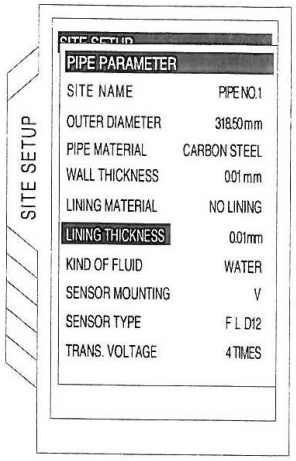

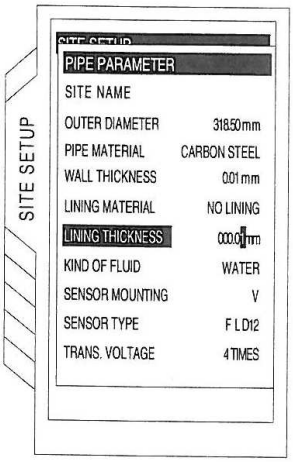

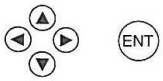

Example) When the lining thickness is 1.25 mm

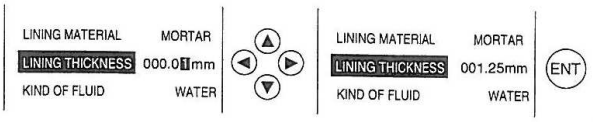

6.8 Kind of fluid

Select kind of fluid and enter the dynamic viscosity coefficient.
For fluid having no item, enter sound velocity. (Range: 500 to 2500 m/s)
Press the ▼ key to invert the "KIND OF FLUID".
Press the ENT key. The "KIND OF FLUID" screen will appear.

Note 1) To return the screen to the "PIPE PARAMETER", press the ESC key.

Select kind of fluid by using the ▲ or ▼ key.
After selection, press the ENT key, the screen will appear, to enter the dynamic viscosity coefficient. The initial value is set to water coefficient.

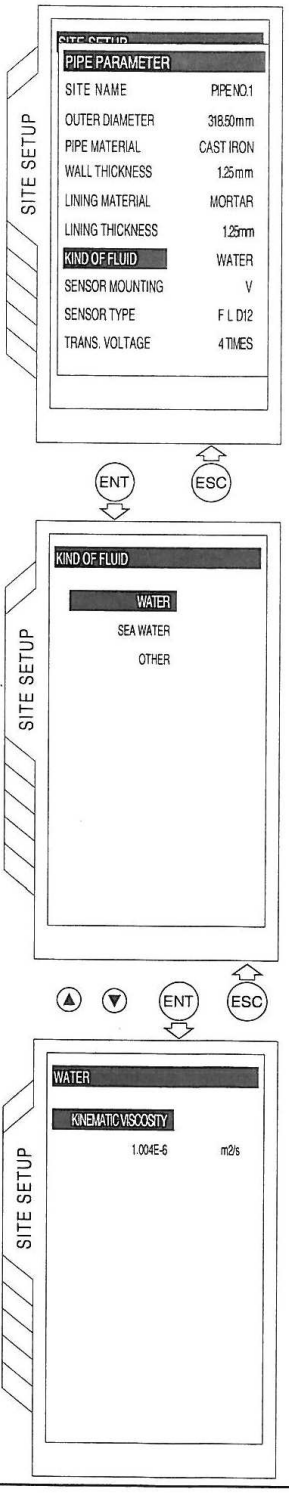

⚠ CAUTION

There is no need to change "1.004 E-6m²/s" when measuring water. Return the screen by pressing the ESC key.

Note 2) When "OTHER" is selected, enter sound velocity. See page 15-6, Tables 20 and 22.

Remarks

Dynamic viscosity coefficient is set to water (20°C).
When measuring accurately or measuring fluid other than water, enter as needed.
(See page 15-6.)
(Range: 0.001×10^{-6} to 999.999×10^{-6}m²/s)

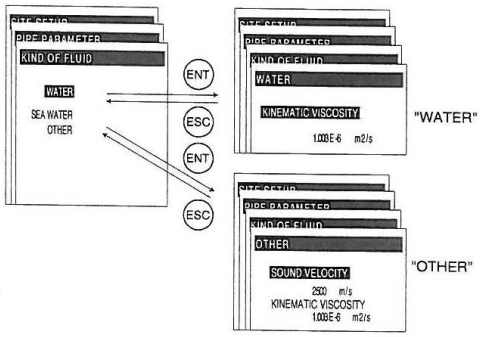

6.9 Selection of sensor mounting method

Mounting methods available for the sensor are V method and Z method as illustrated.

To select the mounting method;

Press the ▼ key to invert the "SENSOR MOUNTING".

Press the ENT key. The "SENSOR MOUNTING" screen will appear.

Select either V or Z method using the ▲ or ▼ key.

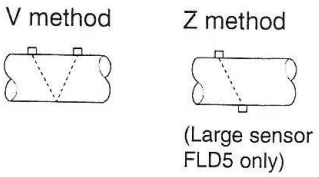

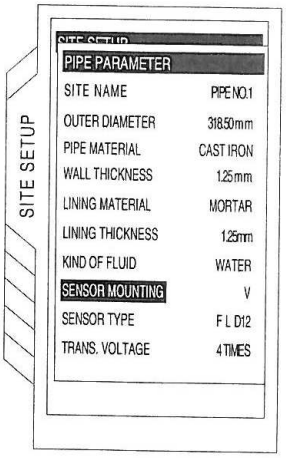

ENT

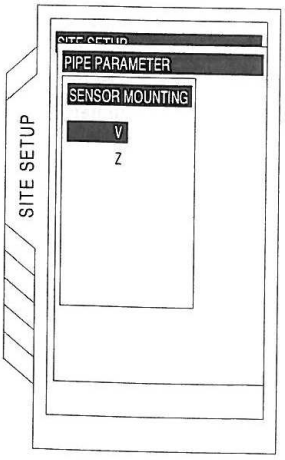

▲ ▼ ENT

Remarks

Select the V method generally. Use the Z method in the following cases:

- Ample space is not provided.
- High turbidity
- Weak receiving waveform
- Thick scale is deposited on the pipe internal surface.

7. MOUNTING OF DETECTOR

7.1 Selection of mounting location

Detector mounting location, i.e., the conditions of the pipe subjected to flow rate measurement exert a great influence on measurement accuracy. So select a location meeting the conditions listed below.

(1) There is a straight pipe portion of 10D or more on the upstream side and that of 5D or more on the downstream side.
(2) No factors to disturb the flow (such as pump and valve) within about 30D on the upstream side.

Classification	For upstream side	For downstream side
90° bend	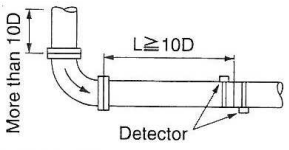	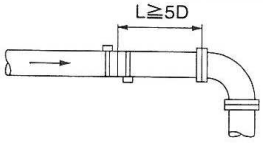
Tee	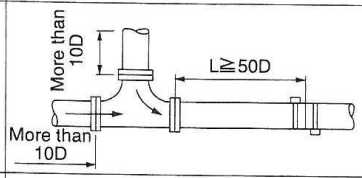	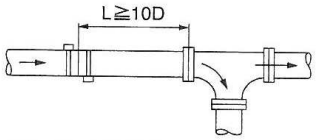
Diffuser	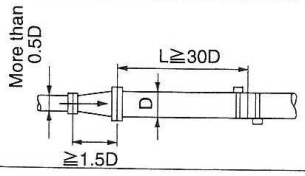	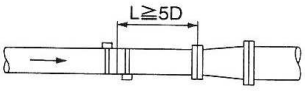
Reducer	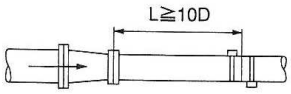	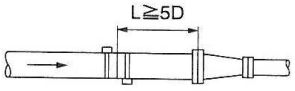
Valves	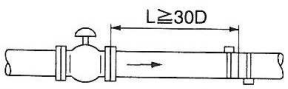 Flow control valve exists on upstream side.	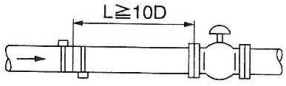 Flow control valve exists on downstream side.
Pump	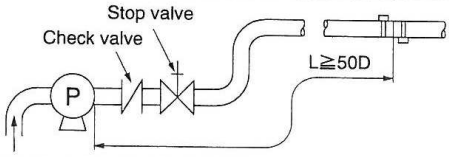	

Extracted from Japan Electric and Machinery Industry Society (JEMIS-032)

(3) Pipe is always filled with fluid. Neither air bubbles nor foreign materials are contained in the fluid.
(4) There is an ample maintenance space around the pipe to which the detector is to be mounted (see figure below).
Note 1) Secure an adequate space for allowing a person to stand and work on both sides of a pipe.
Note 2) D indicates the inside diameter of a pipe.

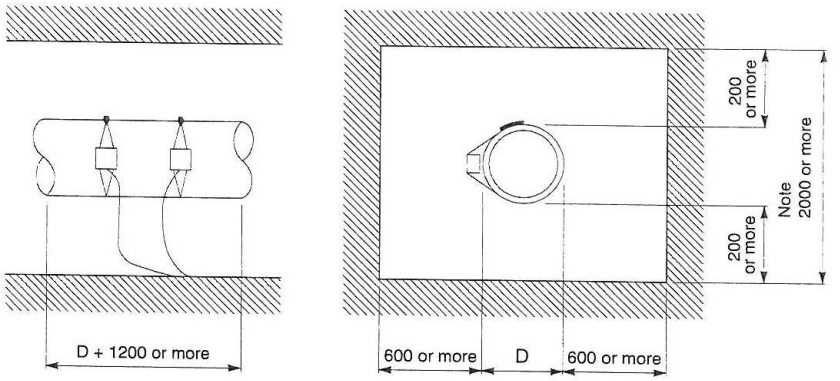

Space required for mounting detector

(5) For a horizontal pipe, mount the detector within ±45° of the horizontal plane.
For a vertical pipe, the detector can be mounted at any position on the outer circumference.

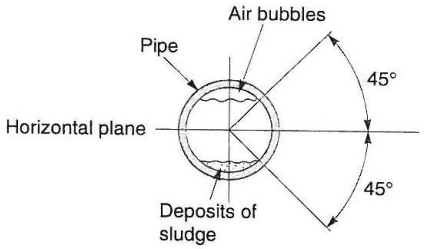

(6) Avoid mounting the detector near a deformation, flange or welded part on the pipe.

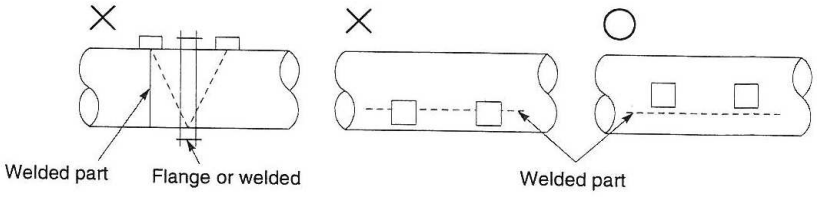

7.2 Selection of detector

(1) Selection of mounting methods

There are 2 methods for mounting the detector; V method and Z method. For the mounting space, see the following sketch.

<Large sensor>

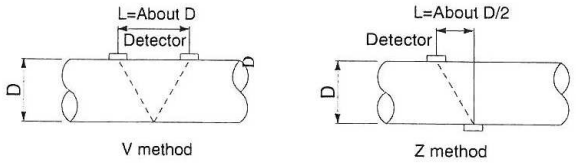

<Small diameter sensor, small sensor or high-temperature sensor>

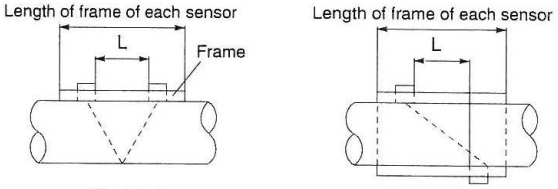

Mounting method

L: Mounting dimension
(mounting dimension for sensor displayed on the SITE SETUP screen)

Employ the Z method in the following cases.

- Mounting space need be saved (mounting space of the Z method is about one half of the V method's).
- Turbid fluid such as sewage is to be measured.
- Pipe has mortar lining.
- A thick film of scale may have been formed on the inner surface of pipe because it is old.

(2) Detector selection standards

The Z method for large size sensor is recommended for outer diameter 300mm or more.
FLD51 should be used as much as possible for pipes such as old pipes, cast iron pipes, and mortar lining pipes, through which it is difficult for ultrasonic signals to pass.

Detector

Type	Diameter	Temperature
FLD22	13 100mm (V method)	-40 +100°C
FLD12	50 350mm (V method) 300 400mm (Z method)	-40 +100°C
FLD32	50 350mm (V method) 300 400mm (Z method)	-40 +200°C
FLD51	200 3000mm (V method) 200 6000mm (Z method)	-40 +80°C

7.4 How to mount small size (standard) sensor and small outer diameter sensor to pipe

① Loosen the lock nut and slide the sensor so as to meet the mounting dimension and then tighten the nut.

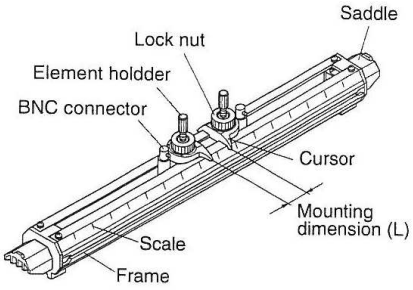

② Apply a coat of silicone grease to the transmitting surface of the sensor. Spread the compound over the entire area.

Keep the sensor retracted by turning the element holder counterclockwise.

After cleaning the surface of the pipe, the sensor should be mounted.

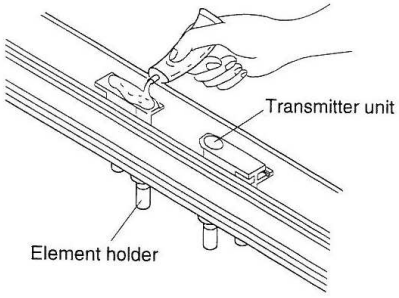

⚠ CAUTION

Apply a small quantity (like toothpaste) of silicon grease to the transmitter unit.

③ Fix the both ends (saddles) of the sensor to the pipe by cloth belts.
Mounting will be facilitated by winding the cloth belts on the pipe in advance.
Cloth belts are usable at 80°C or lower. If beyond 80°C, stainless steel belts should be used.
(High-temperature stainless belt: Drawing No. TK7G7981C1)

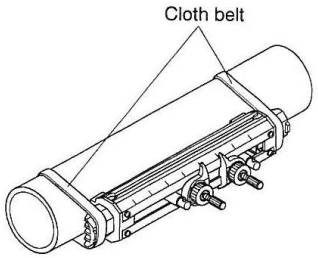

④ Make sure the sensor is mounted in parallel with the pipe axis and the mounting dimension is right. Then, turn the element holder clockwise until the sensor comes in close contact with the pipe.

Stop turning the element holder when it stiffens because the transmitting surface comes in contact with the pipe surface. Be careful not to turn the holder excessively.

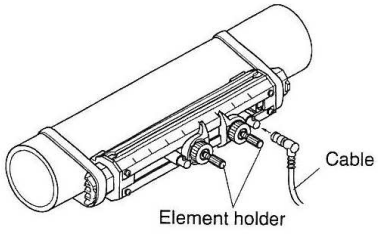

7.5 How to mount large size sensor

7.5.1 How to determine mounting position (large sensor)

Determine the mounting position by carrying out the following work.
For this work, gauge paper is necessary (For the gauge paper, refer to page 7-10).

① Match the edge of gauge paper with the line at about 100mm from one end of the pipe portion treated for detector mounting, and wind the gauge paper so that the line marked on the paper is parallel with the pipe axis (fix with tape not to allow deviation). At this time, the edge of gauge paper should be aligned.

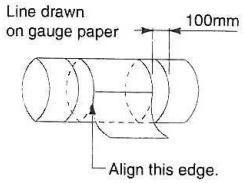

② Extending the line marked on the gauge paper, mark straight line A on the pipe.

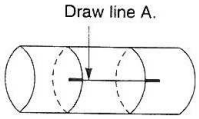

③ Mark a line along on edge of the gauge paper. The intersection of this line and straight line A is replaced with A_0.

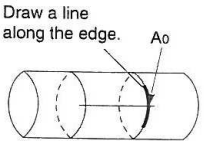

④ In mounting by the V method, peel the gauge paper and measure the mounting dimension from A_0 to determine A_2 position. At this position, mark a line orthogonal to the straight line A.

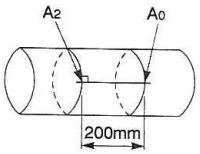

A_0 and A_2 become the mounting positions.

Example) L = 200mm

⑤ In mounting by the Z method, measure the circumference from A_0 with a measuring tape. At 1/2 of the circumference, determine points B_0 and B_1, and mark a line (straight line B) connecting those points.

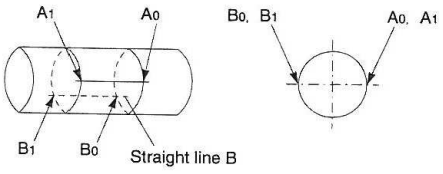

⑥ Mark the points B_0 and peel off the gauge paper.

Measure the mounting dimension from B_0 to determine B_2 position. At this position, make a line orthogonal to the straight line B.

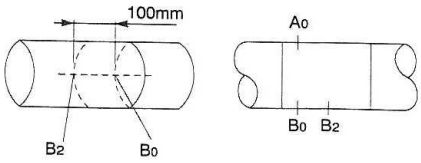

A_0 and B_2 become the mounting positions.

Example) L = 100mm

7.5.3 How to mount large size sensor to pipe

① **Height adjustment of guide plate**

- Place the sensor on the pipe surface in parallel with the pipe axis.
- Loosen the guide plate fixing screw and slide the guide plate until its edge and transmitting surface touch the surface of pipe.
- Then tighten the fixing screw.

② **How to determine the length of wire rope**

- Place the sensor on the marked lines and fit the wire rope and fastening spring.
- Loosen the wire clip and pull the wire rope until the overall length of fastening spring approximates 180mm. Then tighten the wire clip.
  (The fastening spring has a free length of 110mm.)
- While fixing the wire rope, remove the sensor.

③ **Mounting of sensor**

- Wipe off contaminates from the transmitting surface of sensor and the sensor mounting surface of pipe.
- Apply the silicone grease on the transmitting surface of sensor wile spreading it evenly.
- Film thickness of the silicone grease should be about 3mm.
- Spread the wire rope near the marked lines in the left-right direction, bring the sensor in close contact and fit the wire rope.
- Align the matching mark of sensor with the marked line. In addition, make the transmitting direction marks of sensors face each other.
- Make sure the matching mark of sensor is aligned with the marked line and connect the coaxial cable to the converter.

Note) Do not pull the coaxial cable. Otherwise, the sensor will be activated to disturb measurement.

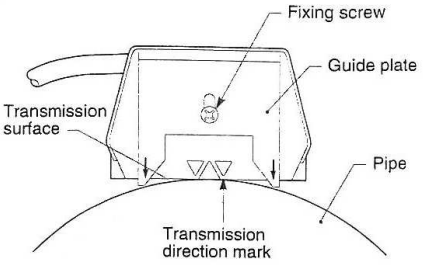

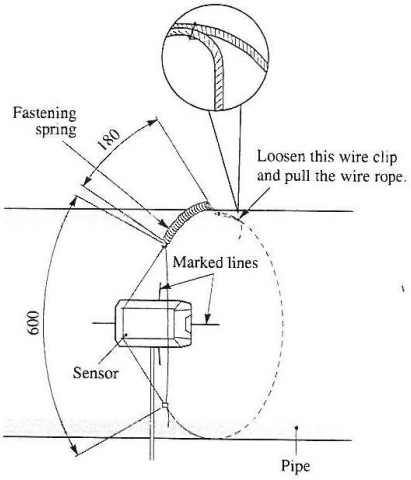

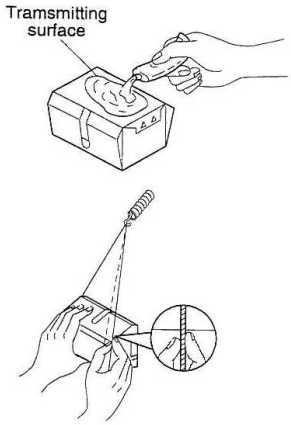

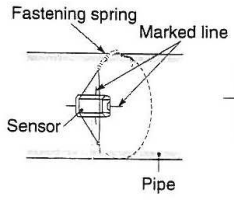

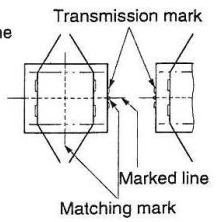

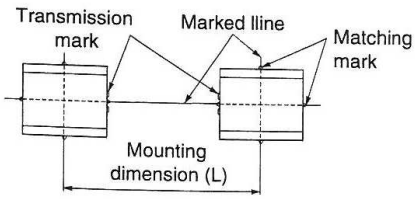

8. MEASUREMENT

When wiring, piping settings and mounting of the sensor are completed, start the measurement.
The contents displayed on the MEASURE screen are as follows.

Instantaneous flow meter

- On the MEASURE screen, instantaneous flow, instantaneous flow velocity, analog output, and analog input are displayed.

  Of the 4 stages displayed on the MEASURE screen, 2 contents can be arbitrarily allocated to the 1st and 2nd stage. Allocation is accomplished by selection of "UNIT".

  If the flow rate is displayed when water flow stops, refer to page 9-3, "ZERO ADJUST" and page 9-5, "CUT OFF".

  If the flow display fluctuates, refer to page 9-3 "RESPONSE SET".

Integrated flow rate

- When the integrated flow rate is displayed, "+TOTAL" and "-TOTAL" are fixed on the third stage and 4th stage, respectively.
- Integrated flow rate value is available in the range from 0000000 to 999999. If the value exceeds 9999999, it reset to 0000000.

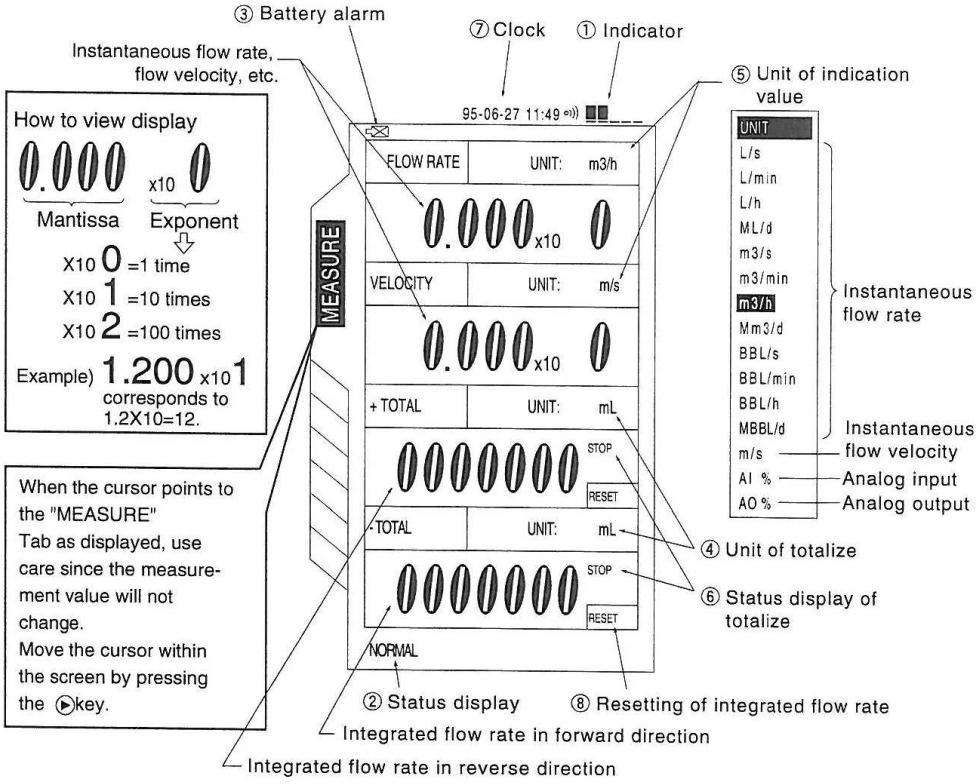

① **"Indicator"**

Shows the intensity of ultrasonic receiving signal.
Check if 2 or more indicators are displayed.
If one or less indicator is displayed, raise the transmission voltage level as shown on page 6-12.
When the sensor is not connected, the indicator may be lighted by sensing noises. But, this is not error.

② **"Status display"**

Check if "NORMAL" is displayed. If the sensor is not connected, other messages may be displayed. This is not an error.
In case other message is displayed after installing and connecting the sensor, take corrective actions according to page 9-33, "System check function".
If "NORMAL" is not displayed when 1 or less indicator is display, refer to page 11-2, "Error in measured value".

③ **"Battery alarm"**

When activating this instrument on the built-in battery, check if the BATTERY ALARM ( ) is not displayed. If "BATTERY ALARM" is displayed, the power is turned OFF in about 20 minutes.
When charging the battery, refer to page 4-1 "To charge the battery".

④ **Unit of integration**

When changing the unit of integration, refer to page 9-6, "TOTALIZE: when performing the integration process of measured data (totalize)".

⑤ **Unit of indication value**

To change the units of flow rate and flow velocity on the MEASURE screen;

① Move the cursor to "UNIT" by pressing the ▲ or ▼ key.

② Press the ENT key, and the screen appears, enabling the unit of flow rate to be selected. Select any unit by pressing the ▲ or ▼ key and press the ENT key.

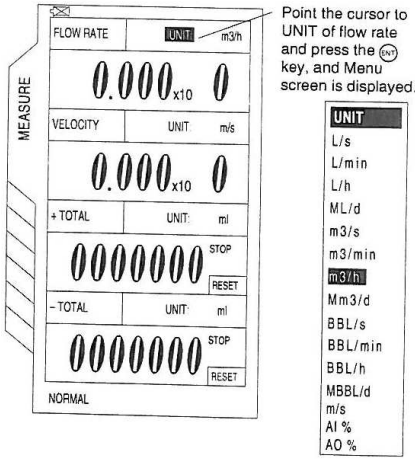

⑥ **Status display of integration**

Meaning of display

STOP:	Not totalized
RUN:	Totalizing in progress

To start the action of integration, refer to page 9-6, "TOTALIZE".

⑦ **"Clock set"**

This instrument has a timer function. For the timer to set the time, refer to page 9-15, "CLOCK SET".
The timer function should be used based on this watch.

⑧ **Reset**

The integration value can be set to 0 or "any other numeric value". To reset the integration value, point the cursor to "RESET" by pressing the ▲ or ▼ key, and then press the ENT key.
When you want to reset to any value or 1000 for example, refer to page 9-7, "To set reset data".

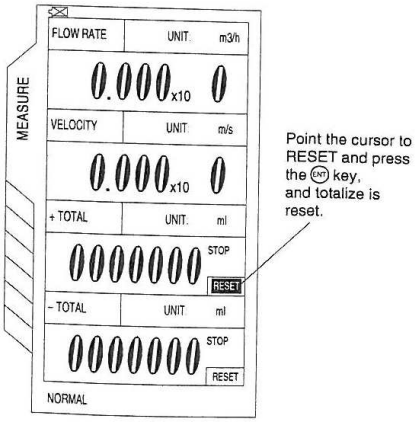

APPENDIX F: Tabulated Reciprocating Machine Data

All of the recorded and processed data for the tests performed on the reciprocating chiller are given in the tables below. The same abbreviations for the tables of Appendix D are used below and a description of all the terms is given in Table D1.

Table F1 contains all of the temperature data for the evaporator and condenser inlet and outlet water flows. The recorded temperatures and their SI conversions are given.

Table F1: Reciprocating Temperature Data

T_{Ci} R [°C]	T_{Ci}SI [K]	T_{Co} R [°C]	T_{Co}SI [K]	T_{Ei} R [°C]	T_{Ei}SI [K]	T_{Eo} R [°C]	T_{Eo}SI [K]
24.02	297.17	27.54	300.69	10.14	283.29	7.24	280.39
24.02	297.17	27.55	300.7	10.13	283.28	7.26	280.41
24.02	297.17	27.53	300.68	10.15	283.3	7.25	280.4
24.02	297.17	27.54	300.69	10.14	283.29	7.27	280.42
24.02	297.17	27.55	300.7	10.13	283.28	7.23	280.38
24.02	297.17	27.57	300.72	10.17	283.32	7.25	280.4
24.02	297.17	27.56	300.71	10.16	283.31	7.24	280.39
25.07	298.22	28.76	301.91	10.43	283.58	7.23	280.38
25.07	298.22	28.77	301.92	10.45	283.6	7.26	280.41
25.07	298.22	28.77	301.92	10.42	283.57	7.24	280.39
25.07	298.22	28.78	301.93	10.44	283.59	7.23	280.38
25.07	298.22	28.78	301.93	10.45	283.6	7.24	280.39
25.07	298.22	28.79	301.94	10.46	283.61	7.29	280.44
25.51	298.66	29.44	302.59	10.67	283.82	7.34	280.49
25.51	298.66	29.45	302.6	10.66	283.81	7.33	280.48
25.51	298.66	29.43	302.58	10.68	283.83	7.37	280.52
25.51	298.66	29.45	302.6	10.65	283.8	7.34	280.49
25.51	298.66	29.45	302.6	10.68	283.83	7.38	280.53
25.51	298.66	29.45	302.6	10.67	283.82	7.37	280.52
25.51	298.66	29.45	302.6	10.66	283.81	7.35	280.5
26.02	299.17	30.19	303.34	10.75	283.9	7.23	280.38
26.02	299.17	30.18	303.33	10.77	283.92	7.26	280.41
26.02	299.17	30.2	303.35	10.78	283.93	7.27	280.42
26.02	299.17	30.14	303.29	10.74	283.89	7.24	280.39
26.02	299.17	30.16	303.31	10.73	283.88	7.25	280.4
26.02	299.17	30.21	303.36	10.77	283.92	7.24	280.39
26.02	299.17	30.18	303.33	10.78	283.93	7.28	280.43
26.54	299.69	31.03	304.18	11.16	284.31	7.28	280.43

T_{Ci} R	T_{Ci}SI	T_{Co} R	T_{Co}SI	T_{Ei} R	T_{Ei}SI	T_{Eo} R	T_{Eo}SI
[°C]	[K]	[°C]	[K]	[°C]	[K]	[°C]	[K]
26.54	299.69	31.01	304.16	11.14	284.29	7.24	280.39
26.54	299.69	31.05	304.2	11.17	284.32	7.27	280.42
26.54	299.69	31.05	304.2	11.15	284.3	7.23	280.38
26.54	299.69	31.02	304.17	11.14	284.29	7.26	280.41
26.54	299.69	31.02	304.17	11.12	284.27	7.23	280.38
26.54	299.69	31.03	304.18	11.14	284.29	7.24	280.39
27.03	300.18	31.47	304.62	11.17	284.32	7.28	280.43
27.03	300.18	31.45	304.6	11.14	284.29	7.24	280.39
27.03	300.18	31.47	304.62	11.15	284.3	7.23	280.38
27.03	300.18	31.47	304.62	11.16	284.31	7.27	280.42
27.03	300.18	31.49	304.64	11.19	284.34	7.28	280.43
27.03	300.18	31.49	304.64	11.19	284.34	7.27	280.42
27.03	300.18	31.47	304.62	11.17	284.32	7.26	280.41
27.42	300.57	32.04	305.19	11.27	284.42	7.28	280.43
27.42	300.57	32.05	305.2	11.3	284.45	7.26	280.41
27.42	300.57	32.04	305.19	11.31	284.46	7.26	280.41
27.42	300.57	32.07	305.22	11.3	284.45	7.24	280.39
27.42	300.57	32.06	305.21	11.31	284.46	7.23	280.38
27.42	300.57	32.08	305.23	11.33	284.48	7.24	280.39
27.42	300.57	32.07	305.22	11.31	284.46	7.24	280.39

Table F2 below contains the power supply data for the reciprocating machine. The voltage, current and power factor values are all given and these are used to arrive at the value for power drawn.

Table F2: Reciprocating Power Supply Data

V R	I R	cosϕ R	Power
[V]	[A]		[W]
396.2	283.1	0.78	151530
394.4	281.8	0.79	152080
397.1	283.3	0.78	151990
393.9	282.2	0.79	152100
395.1	283.4	0.78	151270
395.1	281.9	0.79	152400
394.9	281.3	0.79	152000
395.6	280.1	0.79	151620
394.3	278.3	0.8	152050
394.8	279.9	0.79	151210

V R	I R	cosϕ R	Power
[V]	[A]		[W]
394.5	279.7	0.79	150980
395.6	279.9	0.79	151510
394.8	278.9	0.8	152570
394.9	283.4	0.8	155070
394.2	280.4	0.81	155070
394.1	281.8	0.81	155810
395.6	282.2	0.8	154690
395.4	281.1	0.81	155930
396.2	283.2	0.8	155470
395.8	282.4	0.8	154880
394.1	296.5	0.81	163940
395.6	300.2	0.8	164560
396.1	300.9	0.8	165150
395.7	299.3	0.8	164110
392.1	297.8	0.81	163820
392.7	297.9	0.81	164130
393.4	298.9	0.81	164970
392.6	301.4	0.81	166010
393.6	303.1	0.8	165310
392.7	302.1	0.81	166440
393.1	303.4	0.8	165260
391.9	302.5	0.81	166320
392.8	303.2	0.8	165030
391.2	301.8	0.81	165640
391.4	303.6	0.81	166710
392.6	304.6	0.8	165700
392.2	304.5	0.8	165480
391.7	301.6	0.81	165740
391.6	303.6	0.81	166800
390.4	300.7	0.82	166730
392.6	301.8	0.81	166230
393.8	305.7	0.81	168900
393.9	305.2	0.81	168660
394.2	305.2	0.81	168790
395.3	307.1	0.8	168210
398.1	305.4	0.8	168470
396.4	306.4	0.8	168300
394.1	305.2	0.81	168750

The evaporator and condenser inlet and outlet water pressure data is given in Table F3 below.

Table F3: Reciprocating Pressure Data

P_{Ci} [kPa]	P_{Co} [kPa]	$\Delta P_C R$ [kPa]	P_{Ei} [kPa]	P_{Eo} [kPa]	$\Delta P_E R$ [kPa]
400	378	22	460	369	91
400	378	22	460	369	91
400	378	22	460	369	91
400	378	22	460	369	91
400	378	22	460	369	91
400	378	22	460	369	91
400	378	22	460	369	91
400	378	22	460	369	91
400	378	22	460	369	91
400	378	22	460	369	91
400	378	22	460	369	91
400	378	22	460	369	91
400	378	22	460	369	91
400	378	22	460	369	91
400	378	22	460	369	91
400	378	22	460	369	91
400	378	22	460	369	91
400	378	22	460	369	91
400	378	22	460	369	91
400	378	22	460	369	91
400	378	22	460	369	91
400	378	22	460	369	91
400	378	22	460	369	91
400	378	22	460	369	91
400	378	22	460	369	91
400	378	22	460	369	91
400	378	22	460	369	91
400	378	22	460	369	91
400	378	22	460	369	91
400	378	22	460	369	91
400	378	22	460	369	91
400	378	22	460	369	91
400	378	22	460	369	91
400	378	22	460	369	91
400	378	22	460	369	91
400	378	22	460	369	91
400	378	22	460	369	91
400	378	22	460	369	91
400	378	22	460	369	91
400	378	22	460	369	91

P_{Ci}	P_{Co}	$\Delta P_C R$	P_{Ei}	P_{Eo}	$\Delta P_E R$
[kPa]	[kPa]	[kPa]	[kPa]	[kPa]	[kPa]
400	378	22	460	369	91
400	378	22	460	369	91
400	378	22	460	369	91
400	378	22	460	369	91
400	378	22	460	369	91
400	378	22	460	369	91
400	378	22	460	369	91
400	378	22	460	369	91
400	378	22	460	369	91
400	378	22	460	369	91
400	378	22	460	369	91
400	378	22	460	369	91

The first set of processed data for the reciprocating machine is given in Table F4. The data listed are mainly used to calculate the final set of processed data listed in Table F5.

Table F4: Reciprocating Processed Data 1

TE_{ave}	TC_{ave}	v_E	C_E	v_C	C_C	$m_{fl}E$	$m_{fl}C$
[°C]	[°C]	[m^3/kg]	[J/(kg.K)]	[m^3/kg]	[J/(kg.K)]	[kg/s]	[kg/s]
281.84	298.93	0.0294	4205	0.0346	4179	29.2	34.7
281.845	298.935	0.0294	4205	0.0346	4179	29.3	34.5
281.85	298.925	0.0294	4205	0.0346	4179	29.2	34.8
281.855	298.93	0.0294	4205	0.0346	4179	29.3	34.4
281.83	298.935	0.0294	4205	0.0346	4179	29.3	34.8
281.86	298.945	0.0294	4205	0.0346	4179	29.6	34.3
281.85	298.94	0.0294	4205	0.0346	4179	29.4	34.5
281.98	300.065	0.0294	4205	0.0346	4179	29.6	34.9
282.005	300.07	0.0294	4205	0.0346	4179	29.3	34.7
281.98	300.07	0.0294	4205	0.0346	4179	29.3	34.5
281.985	300.075	0.0294	4205	0.0346	4179	29.1	34.8
281.995	300.075	0.0294	4205	0.0346	4179	29.3	34.6
282.025	300.08	0.0294	4205	0.0346	4179	29.4	34.5
282.155	300.625	0.0294	4205	0.0346	4179	29.4	34.5
282.145	300.63	0.0294	4205	0.0346	4179	29.4	34.7
282.175	300.62	0.0294	4205	0.0346	4179	29.3	34.8
282.145	300.63	0.0294	4205	0.0346	4179	29.3	34.6
282.18	300.63	0.0294	4205	0.0346	4179	29.4	34.4

TE_{ave}	TC_{ave}	v_E	C_E	v_C	C_C	$m_{fl}E$	$m_{fl}C$
[°C]	[°C]	[m^3/kg]	[J/(kg.K)]	[m^3/kg]	[J/(kg.K)]	[kg/s]	[kg/s]
282.17	300.63	0.0294	4205	0.0346	4179	29.2	34.5
282.155	300.63	0.0294	4205	0.0346	4179	29.3	34.3
282.14	301.255	0.0294	4205	0.0346	4179	29.4	34.5
282.165	301.25	0.0294	4205	0.0346	4179	29.2	34.3
282.175	301.26	0.0294	4205	0.0346	4179	29.4	34.6
282.14	301.23	0.0294	4205	0.0346	4179	29.5	34.4
282.14	301.24	0.0294	4205	0.0346	4179	29.3	34.5
282.155	301.265	0.0294	4205	0.0346	4179	29.2	34.2
282.18	301.25	0.0294	4205	0.0346	4179	29.4	34.6
282.37	301.935	0.0294	4205	0.0346	4179	29.3	34.5
282.34	301.925	0.0294	4205	0.0346	4179	29.4	34.4
282.37	301.945	0.0294	4205	0.0346	4179	29.5	34.6
282.34	301.945	0.0294	4205	0.0346	4179	29.4	34.3
282.35	301.93	0.0294	4205	0.0346	4179	29.7	34.5
282.325	301.93	0.0294	4205	0.0346	4179	29.5	34.4
282.34	301.935	0.0294	4205	0.0346	4179	29.4	34.2
282.375	302.4	0.0294	4205	0.0346	4179	29.5	34.5
282.34	302.39	0.0294	4205	0.0346	4179	29.5	34.4
282.34	302.4	0.0294	4205	0.0346	4179	29.4	34.3
282.365	302.4	0.0294	4205	0.0346	4179	29.3	34.5
282.385	302.41	0.0294	4205	0.0346	4179	29.4	34.5
282.38	302.41	0.0294	4205	0.0346	4179	29.5	34.6
282.365	302.4	0.0294	4205	0.0346	4179	29.5	34.4
282.425	302.88	0.0294	4205	0.0346	4179	29.5	34.3
282.43	302.885	0.0294	4205	0.0346	4179	29.4	34.5
282.435	302.88	0.0294	4205	0.0346	4179	29.5	34.5
282.42	302.895	0.0294	4205	0.0346	4179	29.5	34.4
282.42	302.89	0.0294	4205	0.0346	4179	29.6	34.6
282.435	302.9	0.0294	4205	0.0346	4179	29.3	34.3
282.425	302.895	0.0294	4205	0.0346	4179	29.5	34.5

Table F5 contains the final set of processed data for the reciprocating machine. These data sets constitute the main outcomes of the experiment.

Table F5: Reciprocating Processed Data 2

T_{Ci} R	QE	QC	1/QE	COP	alpha	beta	1/COP P	COP P	balance	bal%	diffCOP%
[°C]	[W]	[W]	[kW^{-1}]		[W]	[W]			[W]		
24.02	356080	510440	0.0028	2.35	130210	8105500	0.4193	2.385	2830	0.554	-1.489
24.02	353600	508940	0.0028	2.325	130950	8105700	0.4233	2.362	3260	0.641	-1.591
24.02	356080	510460	0.0028	2.343	130680	8105700	0.4201	2.38	2390	0.468	-1.579
24.02	353600	506030	0.0028	2.325	130960	8105400	0.4241	2.358	330	0.065	-1.419
24.02	357300	513370	0.0028	2.362	129870	8105500	0.4173	2.396	4800	0.935	-1.439
24.02	363450	508860	0.0028	2.385	130650	8105700	0.4127	2.423	-6990	1.374	-1.593
24.02	360990	510380	0.0028	2.375	130390	8105700	0.4144	2.413	-2610	0.511	-1.6
25.07	398300	538180	0.0025	2.627	126270	8130100	0.3876	2.58	-11740	2.181	1.789
25.07	393030	536540	0.0025	2.585	127080	8130000	0.394	2.538	-8540	1.592	1.818
25.07	391800	533450	0.0026	2.591	126300	8129800	0.3937	2.54	-9560	1.792	1.968
25.07	392790	539540	0.0026	2.602	125960	8129800	0.3922	2.55	-4230	0.784	1.998
25.07	395490	536440	0.0025	2.61	126380	8129900	0.3906	2.56	-10560	1.969	1.916
25.07	391900	536330	0.0026	2.569	127700	8129800	0.3971	2.518	-8140	1.518	1.985
25.51	411680	566610	0.0024	2.655	128390	8140900	0.3873	2.582	-140	0.025	2.75
25.51	411680	571340	0.0024	2.655	128370	8141100	0.3866	2.587	4590	0.803	2.561
25.51	407810	570080	0.0025	2.617	129460	8141100	0.3923	2.549	6460	1.133	2.598
25.51	407810	569700	0.0025	2.636	128290	8140800	0.3903	2.562	7200	1.264	2.807
25.51	407970	566400	0.0025	2.616	129590	8140900	0.3928	2.546	2500	0.441	2.676
25.51	405190	568050	0.0025	2.606	129280	8140900	0.3944	2.535	7390	1.301	2.724
25.51	407810	564760	0.0025	2.633	128480	8140700	0.391	2.558	2070	0.367	2.848
26.02	435170	601210	0.0023	2.654	134800	8164100	0.3664	2.729	2100	0.349	-2.826
26.02	430980	596290	0.0023	2.619	135730	8164200	0.3711	2.695	750	0.126	-2.902
26.02	433930	604400	0.0023	2.627	136170	8164300	0.3697	2.705	5320	0.88	-2.969
26.02	434170	592280	0.0023	2.646	135010	8164000	0.3677	2.72	-6000	1.013	-2.797
26.02	428760	596890	0.0023	2.617	135140	8163900	0.3721	2.687	4310	0.722	-2.675
26.02	433430	598840	0.0023	2.641	135090	8164100	0.3682	2.716	1280	0.214	-2.84
26.02	432690	601510	0.0023	2.623	136050	8163900	0.3712	2.694	3850	0.64	-2.707
26.54	478040	647350	0.0021	2.88	133150	8175000	0.3456	2.894	3300	0.51	-0.486
26.54	482150	642600	0.0021	2.917	132100	8175100	0.341	2.933	-4860	0.756	-0.549
26.54	483790	652120	0.0021	2.907	133180	8175300	0.3417	2.927	1890	0.29	-0.688
26.54	484620	646460	0.0021	2.932	131910	8175200	0.339	2.95	-3420	0.529	-0.614
26.54	484570	645910	0.0021	2.913	133030	8175400	0.3407	2.935	-4980	0.771	-0.755
26.54	482540	644030	0.0021	2.924	131790	8175000	0.3402	2.939	-3540	0.55	-0.513
26.54	482150	641720	0.0021	2.911	132440	8175400	0.341	2.933	-6070	0.946	-0.756
27.03	482540	640140	0.0021	2.894	132750	8187700	0.346	2.89	-9110	1.423	0.138
27.03	483790	635410	0.0021	2.92	131540	8187700	0.3431	2.915	-14080	2.216	0.171

T_{Ci} R	QE	QC	1/QE	COP	alpha	beta	1/COP P	COP P	balance	bal%	diffCOP%
[°C]	[W]	[W]	[kW^{-1}]		[W]	[W]			[W]		
27.03	484620	636430	0.0021	2.929	131230	8187600	0.3421	2.923	-13670	2.148	0.205
27.03	479270	640140	0.0021	2.892	131950	8187200	0.3474	2.879	-4870	0.761	0.45
27.03	483380	643020	0.0021	2.898	132750	8187700	0.3456	2.894	-7160	1.113	0.138
27.03	486270	644890	0.0021	2.917	132440	8187700	0.3434	2.912	-8110	1.258	0.171
27.03	485030	638280	0.0021	2.918	132020	8187600	0.3435	2.911	-12980	2.034	0.24
27.42	494950	662230	0.002	2.93	133380	8198800	0.3415	2.928	-1620	0.245	0.068
27.42	499450	667530	0.002	2.961	132770	8198800	0.338	2.959	-580	0.087	0.068
27.42	502390	666090	0.002	2.976	132690	8198700	0.3365	2.972	-5090	0.764	0.134
27.42	503630	668470	0.002	2.994	131970	8198600	0.3348	2.987	-3370	0.504	0.234
27.42	507830	670910	0.002	3.014	131920	8198800	0.332	3.012	-5390	0.803	0.066
27.42	503910	667960	0.002	2.994	132040	8198600	0.3346	2.989	-4250	0.636	0.167
27.42	504870	670420	0.002	2.992	132400	8199000	0.3341	2.993	-3200	0.477	-0.033

APPENDIX G: Experimental Uncertainty Formulae

The Universal Thermodynamic Model predicts the reciprocal of a refrigeration machine's COP according to Equation [3.5]. This formula is reproduced below in Equation [G.1].

$$\frac{1}{COP} = -1 + \frac{T_{Ci}}{T_{Eo}} + \frac{-C_0 + C_1 \cdot T_{Ci} - C_2 \cdot \frac{T_{Ci}}{T_{Eo}}}{Q_E} \qquad [G.1]$$

The difference between measured and predicted COPs was calculated for each recorded data set and these results were discussed in Section 6. One way to relatively ascertain the reliability of the calculated experimental data is to perform a check between the deviations in COP and the inherent experimental uncertainty.

The COP of a machine was defined by Equation [3.7], and it is reproduced in Equation [G.2]. Q_E is the heat transfer at the evaporator and P is the power drawn by the chiller.

$$COP = \frac{Q_E}{P} \qquad [G.2]$$

The corresponding uncertainty for the COP is calculated via Equation [G.3] below.

$$\delta COP = \sqrt{\delta Q_E{}^2 \left(\frac{\partial COP}{\partial Q_E}\right)^2 + \delta P^2 \left(\frac{\partial COP}{\partial P}\right)^2} \qquad [G.3]$$

Where:

$$\frac{\partial COP}{\partial Q_E} = \frac{1}{P}$$

$$\frac{\partial COP}{\partial P} = -\frac{Q_E}{P^2}$$

Therefore Equation [G.3] can be rewritten as Equation [G.4]

$$\delta COP = \sqrt{\delta Q_E{}^2 \left(\frac{1}{P}\right)^2 + \delta P^2 (-\frac{Q_E}{P^2})^2} \qquad [G.4]$$

Since Q_E, the rate of heat transfer at the evaporator was given in Equation [3.6] above as $Q_E = m_{flE}.C_E.\Delta T_E$, which can be rewritten as $Q_E = m_{flE}.C_E.(T_{Ei}-T_{Eo})$ the term δQ_E can be calculated as follows:

$$\delta Q_E = \sqrt{\delta m_{flE}{}^2 \left(\frac{\partial Q_E}{\partial m_{flE}}\right)^2 + \delta T_{Ei}{}^2 (\frac{\partial Q_E}{\partial T_{Ei}})^2 + \delta T_{Eo}{}^2 (\frac{\partial Q_E}{\partial T_{Eo}})^2}$$

Replacing the derivatives in the above results in Equation [G.5]

$$\delta Q_E = \sqrt{\delta m_{flE}{}^2 (C_E\{T_{Ei} - T_{Eo}\})^2 + \delta T_{Ei}{}^2 (m_{flE} C_E)^2 + \delta T_{Eo}{}^2 (-m_{flE} C_E)^2} \qquad [G.5]$$

The term P in Equation [G.4] is the power consumed by the refrigeration machine and was given in Equation [3.8] as $P = \sqrt{3}.V.I.\cos\Theta$. The term δP can then be calculated as follows:

$$\delta P = \sqrt{\delta V^2 \left(\frac{\partial P}{\partial V}\right)^2 + \delta I^2 (\frac{\partial P}{\partial I})^2 + \delta \cos\Theta^2 (\frac{\partial P}{\partial \cos\Theta})^2}$$

Replacing the derivatives results in the above results in Equation [G.6]

$$\delta P = \sqrt{\delta V^2\left(\sqrt{3}I\cos\Theta\right)^2 + \delta I^2(\sqrt{3}V\cos\Theta)^2 + \delta\cos\Theta^2(\sqrt{3}VI)^2} \qquad [G.6]$$

The experimental uncertainty can be calculated by combining Equations [G.4] to [G.6] and the computed results are given in Appendix H.

APPENDIX H: Tabulated Uncertainty Data

The formulae used to obtain the uncertainties for the different experiments have been presented in Appendix G. The tabulated results of the uncertainty analysis are presented below.

The evaporator heat transfer uncertainty values for the centrifugal chiller under normal operation are given in Table H1 below.

Table H1: Evaporator Heat Transfer Uncertainties, Normal Operation for Centrifugal Chiller

$\partial Q_E/\partial m$	$\partial Q_E/\partial T_{Ei}$	$\partial Q_E/\partial Teo$	ΔQ_E
14171	225390	-225400	7769
14423	226230	-226200	7889
14381	224970	-225000	7863
14465	224550	-224500	7899
14465	226650	-226600	7911
14507	225810	-225800	7925
14507	226230	-226200	7928
14465	226650	-226600	7911
14549	224550	-224500	7937
14381	226230	-226200	7870
14549	224970	-225000	7940
14591	226230	-226200	7966
14802	225390	-225400	8058
14549	226650	-226600	7949
14675	224550	-224500	7995
14802	225390	-225400	8058
14675	226650	-226600	8007
14760	224970	-225000	8037
14802	226230	-226200	8063
14844	225390	-225400	8078
14886	223710	-223700	8087
14718	224550	-224500	8015
14718	226230	-226200	8024
14591	225390	-225400	7961
14886	225810	-225800	8099
14928	224970	-225000	8114
15096	226650	-226600	8200
14928	227070	-227100	8126
14844	225390	-225400	8078

$\partial Q_E/\partial m$	$\partial Q_E/\partial T_{Ei}$	$\partial Q_E/\partial Teo$	ΔQ_E
14844	226650	-226600	8084
15138	226650	-226600	8220
15390	226230	-226200	8334
15096	225810	-225800	8196
15432	225390	-225400	8348
15390	223710	-223700	8320
15474	225810	-225800	8370
15264	225390	-225400	8271

The values for the COP uncertainty for the centrifugal machine under normal operation are given below in Table H2.

Table H2: COP Uncertainties, Normal Operation for Centrifugal Chiller

$\partial COP/\partial Q_E$	$\partial COP/\partial P$	ΔPower	ΔCOP	δCOP (%)
5.167E-06	-2.028E-05	14938	0.306	7.798
5.138E-06	-2.048E-05	14998	0.31	7.775
5.133E-06	-2.027E-05	14989	0.307	7.774
5.107E-06	-2.014E-05	14998	0.305	7.731
5.063E-06	-1.998E-05	15059	0.304	7.702
5.062E-06	-1.996E-05	15038	0.303	7.683
5.078E-06	-2.013E-05	15104	0.307	7.745
5.153E-06	-2.07E-05	14978	0.313	7.79
5.16E-06	-2.069E-05	15003	0.313	7.807
5.116E-06	-2.025E-05	14993	0.306	7.731
5.11E-06	-2.033E-05	15079	0.309	7.768
5.076E-06	-2.023E-05	15112	0.308	7.729
5.092E-06	-2.057E-05	15018	0.312	7.723
5.076E-06	-2.021E-05	15087	0.308	7.737
5.168E-06	-2.093E-05	14957	0.316	7.802
5.118E-06	-2.079E-05	15033	0.315	7.757
5.127E-06	-2.079E-05	15031	0.315	7.768
5.1E-06	-2.054E-05	15085	0.313	7.771
5.108E-06	-2.078E-05	14879	0.312	7.67
5.112E-06	-2.079E-05	14846	0.311	7.647
5.111E-06	-2.069E-05	14963	0.312	7.709
5.075E-06	-2.024E-05	15068	0.308	7.721
5.069E-06	-2.034E-05	15110	0.31	7.725
5.087E-06	-2.024E-05	15055	0.307	7.716
5.103E-06	-2.081E-05	15009	0.315	7.722

$\partial COP/\partial Q_E$	$\partial COP/\partial P$	ΔPower	ΔCOP	δCOP (%)
5.076E-06	-2.057E-05	14952	0.31	7.647
5.09E-06	-2.108E-05	14934	0.318	7.679
5.033E-06	-2.042E-05	15192	0.313	7.715
5.049E-06	-2.028E-05	15147	0.31	7.717
5.036E-06	-2.029E-05	15208	0.311	7.719
5.137E-06	-2.153E-05	14818	0.322	7.681
5.147E-06	-2.194E-05	14879	0.329	7.719
5.144E-06	-2.145E-05	15120	0.327	7.842
5.138E-06	-2.184E-05	15161	0.334	7.859
5.143E-06	-2.166E-05	15100	0.33	7.837
5.118E-06	-2.176E-05	15058	0.331	7.783
5.121E-06	-2.146E-05	14977	0.324	7.733

The various uncertainty values involved in obtaining the evaporator heat transfer uncertainty for the centrifugal machine under throttled conditions are given in Table H3 below.

Table H3: Evaporator Heat Transfer Uncertainties, Throttled Operation for Centrifugal Chiller

$\partial Q_E/\partial m$	$\partial Q_E/\partial T_{Ei}$	$\partial Q_E/\partial Teo$	ΔQ_E
15008	242990	-224100	8200
14924	242990	-223200	8159
14756	242990	-223700	8084
15050	242990	-223700	8218
15008	242990	-224500	8201
14966	242990	-222400	8176
15050	242990	-224100	8219
15092	242990	-224500	8239
15134	242990	-224100	8257
15218	242990	-224100	8296
15050	242990	-223700	8218
15176	242990	-224100	8277
15176	242990	-224500	8278
15176	242990	-224500	8278
15471	242990	-224900	8414
15387	242990	-224500	8375
15345	242990	-225300	8357
15471	242990	-224500	8413
15471	242990	-224100	8412
15471	242990	-225300	8415

$\partial Q_E/\partial m$	$\partial Q_E/\partial T_{Ei}$	$\partial Q_E/\partial Teo$	ΔQ_E
15429	242990	-224100	8393
14546	242990	-222800	7985
14714	242990	-223700	8064
14756	242990	-223200	8082
14798	242990	-223700	8103
14588	242990	-223200	8006
14588	242990	-223700	8007

The details of the COP uncertainty calculations for the centrifugal machine operating with the throttling valve tightened are given in Table H4 below.

Table H4: COP Uncertainties, Throttled Operation

$\partial COP/\partial Q_E$	$\partial COP/\partial P$	ΔPower	ΔCOP	δCOP (%)
4.988E-06	-1.99E-05	15789	0.317	7.945
4.988E-06	-1.972E-05	15839	0.315	7.969
4.981E-06	-1.948E-05	15736	0.309	7.903
4.998E-06	-2E-05	15685	0.316	7.896
4.996E-06	-2E-05	15839	0.319	7.967
5.013E-06	-1.99E-05	15735	0.316	7.962
5.008E-06	-2.012E-05	15775	0.32	7.964
5.006E-06	-2.019E-05	15834	0.322	7.982
5.014E-06	-2.028E-05	15758	0.322	7.962
5.004E-06	-2.031E-05	15838	0.324	7.982
5.004E-06	-2.005E-05	15838	0.32	7.986
4.999E-06	-2.022E-05	15929	0.325	8.037
5.016E-06	-2.039E-05	15752	0.324	7.97
4.99E-06	-2.018E-05	15883	0.323	7.987
4.987E-06	-2.058E-05	15867	0.329	7.97
4.987E-06	-2.044E-05	15891	0.327	7.98
4.965E-06	-2.028E-05	15986	0.327	8.007
5.006E-06	-2.07E-05	15884	0.331	8.005
4.975E-06	-2.041E-05	15907	0.327	7.972
4.964E-06	-2.044E-05	15915	0.328	7.967
4.968E-06	-2.03E-05	15927	0.326	7.978
5.106E-06	-2.01E-05	15645	0.317	8.052
5.109E-06	-2.043E-05	15689	0.323	8.077
5.067E-06	-2.011E-05	15844	0.321	8.086
5.1E-06	-2.048E-05	15764	0.325	8.095
5.078E-06	-1.998E-05	15806	0.318	8.083

$\partial COP/\partial Q_E$	$\partial COP/\partial P$	ΔPower	ΔCOP	δCOP (%)
5.074E-06	-1.998E-05	15744	0.317	8.05

The values associated with the evaporator heat transfer uncertainty for the reciprocating chiller are given below in Table H65

Table H5: Evaporator Heat Transfer Uncertainties, Reciprocating Machine

$\partial Q_E/\partial m$	$\partial Q_E/\partial T_{Ei}$	$\partial Q_E/\partial Teo$	ΔQ_E
12194	122790	-122800	6339
12068	123210	-123200	6281
12194	122790	-122800	6339
12068	123210	-123200	6281
12194	123210	-123200	6341
12279	124470	-124500	6387
12279	123630	-123600	6384
13456	124470	-124500	6955
13414	123210	-123200	6930
13372	123210	-123200	6909
13498	122370	-122400	6967
13498	123210	-123200	6970
13330	123630	-123600	6890
14003	123630	-123600	7216
14003	123630	-123600	7216
13919	123210	-123200	7174
13919	123210	-123200	7174
13877	123630	-123600	7155
13877	122790	-122800	7153
13919	123210	-123200	7174
14802	123630	-123600	7605
14760	122790	-122800	7582
14760	123630	-123600	7584
14718	124050	-124000	7565
14633	123210	-123200	7521
14844	122790	-122800	7622
14718	123630	-123600	7564
16315	123210	-123200	8342
16399	123630	-123600	8384
16400	124050	-124000	8385
16484	123630	-123600	8425
16315	124890	-124900	8347

$\partial Q_E/\partial m$	$\partial Q_E/\partial T_{Ei}$	$\partial Q_E/\partial Teo$	ΔQ_E
16357	124050	-124000	8364
16399	123630	-123600	8384
16357	124050	-124000	8364
16399	124050	-124000	8385
16484	123630	-123600	8425
16357	123210	-123200	8362
16442	123630	-123600	8405
16484	124050	-124000	8427
16442	124050	-124000	8406
16778	124050	-124000	8570
16988	123630	-123600	8672
17030	124050	-124000	8694
17072	124050	-124000	8714
17156	124470	-124500	8757
17198	123210	-123200	8774
17114	124050	-124000	8735

Table H6 gives the values for the uncertainty of the measured COP for the reciprocating chiller.

Table H6: COP Uncertainties, Reciprocating Machine

$\partial COP/\partial Q_E$	$\partial COP/\partial P$	ΔPower	ΔCOP	δCOP (%)
6.599E-06	-1.551E-05	9719	0.156	6.638
6.575E-06	-1.529E-05	9631	0.153	6.581
6.579E-06	-1.541E-05	9748	0.156	6.658
6.575E-06	-1.528E-05	9632	0.153	6.581
6.611E-06	-1.561E-05	9703	0.157	6.647
6.562E-06	-1.565E-05	9651	0.157	6.583
6.579E-06	-1.562E-05	9626	0.156	6.568
6.595E-06	-1.733E-05	9602	0.173	6.585
6.577E-06	-1.7E-05	9509	0.168	6.499
6.613E-06	-1.714E-05	9576	0.17	6.561
6.623E-06	-1.723E-05	9562	0.171	6.572
6.6E-06	-1.723E-05	9595	0.172	6.59
6.554E-06	-1.684E-05	9542	0.167	6.501
6.449E-06	-1.712E-05	9698	0.172	6.478
6.449E-06	-1.712E-05	9579	0.17	6.403
6.418E-06	-1.68E-05	9624	0.168	6.42
6.465E-06	-1.704E-05	9674	0.171	6.487

$\partial COP/\partial Q_E$	$\partial COP/\partial P$	ΔPower	ΔCOP	δCOP (%)
6.413E-06	-1.678E-05	9632	0.168	6.422
6.432E-06	-1.676E-05	9723	0.169	6.485
6.457E-06	-1.7E-05	9686	0.171	6.494
6.1E-06	-1.619E-05	10125	0.17	6.405
6.077E-06	-1.592E-05	10291	0.17	6.491
6.055E-06	-1.591E-05	10328	0.171	6.509
6.093E-06	-1.612E-05	10262	0.172	6.5
6.104E-06	-1.598E-05	10118	0.168	6.42
6.093E-06	-1.609E-05	10137	0.17	6.437
6.062E-06	-1.59E-05	10189	0.168	6.405
6.024E-06	-1.735E-05	10253	0.185	6.424
6.049E-06	-1.764E-05	10337	0.189	6.479
6.008E-06	-1.746E-05	10280	0.186	6.398
6.051E-06	-1.774E-05	10335	0.19	6.48
6.013E-06	-1.752E-05	10272	0.187	6.419
6.06E-06	-1.772E-05	10320	0.19	6.498
6.037E-06	-1.757E-05	10230	0.187	6.424
5.998E-06	-1.736E-05	10297	0.186	6.427
6.035E-06	-1.762E-05	10362	0.189	6.473
6.043E-06	-1.77E-05	10348	0.19	6.487
6.034E-06	-1.745E-05	10237	0.186	6.432
5.995E-06	-1.737E-05	10302	0.186	6.418
5.998E-06	-1.749E-05	10173	0.185	6.342
6.016E-06	-1.755E-05	10267	0.187	6.408
5.921E-06	-1.735E-05	10431	0.188	6.416
5.929E-06	-1.756E-05	10417	0.19	6.417
5.925E-06	-1.763E-05	10425	0.191	6.418
5.945E-06	-1.78E-05	10519	0.194	6.48
5.936E-06	-1.789E-05	10535	0.196	6.503
5.942E-06	-1.779E-05	10524	0.194	6.48
5.926E-06	-1.773E-05	10422	0.192	6.417